Response to Reviewer 1 (H. Gordon)
The reviewer comments are in Arial, the responses in Times New Roman

Summary

This manuscript reports on new particle formation at high altitude in the Amazon region. I believe it is an important study and it will surely be highly cited. Addressing my "major" comments should not require substantial revisions to the manuscript.

We thank the reviewer for his/her positive statements and substantive comments and suggestions.

Major comments

Introduction

Given the relatively short length of the introduction the authors do an admirable job of reviewing the relevant literature. However, I think it is necessary to highlight a couple of key papers, which otherwise are a bit lost in the long lists of citations. I didn't read all the references, but from a random selection the Twohy (2002) and Weigel (2011) papers deserve a dedicated couple of summary sentences each somewhere in the introduction to compare them with the current work.

We have added the following sentences: "Twohy et al. (2002) observed particle concentrations up to 45,000 cm^{-3} over North America and suggested that they had been formed in situ from gas-phase precursors brought up by deep convection. Weigel et al. (2011) found similar concentrations in the UT over tropical America, Africa, and Australia, which they attributed to new particle formation from sulfuric acid and possibly organics." The Twohy et al. paper is cited three times in the introduction and four times in the discussion. The Weigel et al. paper is cited six times in the introduction and three times in the discussion. The results from both papers are compared to ours in the discussion.

Methods:

Section 2.10 outlines a sophisticated and valuable treatment of the back trajectories. Some minor clarifications on how the analysis was done, perhaps in the supplementary material, would be useful.

Specifics:

1. I think it may be helpful to show trajectories in longitude-altitude or (better) time-altitude space (e.g. for Figure S1). Would this shed any light on what the model is doing in areas of deep convection? The online HYSPLIT version gives these plots by default.

We have added a longitude-altitude plot to Figure S1. Like the vast majority of the UT trajectories, this one remains in the UT over the time frame considered. The trajectory model does not resolve individual convective elements, but only incorporates a general parameterization of vertical movement. See also the response to comment 3 below.

2. Please can the authors expand on the footnotes in Table 1? Are the maxima and minima that are given the maximum and minimum out of the five trajectories of the five

cluster centres they obtained from FLEXPART? Was the procedure explained in Figure S2 simply repeated for trajectories of each five possible cluster centres each time?

For simplicity, out of the five clusters, we consider only the center cluster given by FLEXPART. Therefore, the minima and maxima values of Table1 correspond only the values of center clusters trajectories within the flight leg time frame traced backwards up to 120 hours. This is now explained in the text. Doing the analysis for all five clusters would require an extraordinary amount of work and is not likely to give any other results, given the high abundance of deep convection in the basin. We have added the following sentence to the text: "For simplicity, out of the five clusters, we consider only the center cluster given by FLEXPART. Therefore, all trajectories mentioned hereafter refer to the center trajectory."

3. After the first contact with deep convection, (though not with the outflow of deep convection) presumably the five cluster centres diverge radically in horizontal and vertical positions as the air mass is vertically redistributed. Could the authors put the trajectories of the other four cluster centres on Figure S2 (or perhaps a copy of Figure S2, to help avoid confusion) as an example? Otherwise it is hard to see where the ranges in Table 1 for the time in gridboxes with deep convection are coming from. Ideally, it would be great to see how these clusters are transported in time-altitude space, as well. I note that Stohl et al (2002), where the clustering is introduced, does not report any validation of the algorithm in regions where deep convective clouds are present. Has this been done elsewhere? Are the five clusters really representative of the underlying distribution and does this affect the ranges for time spent in gridboxes with deep convection in Table 1? Given the huge vertical difference in winds (Figure 4 and line 449) one might speculate that the trajectories can be all over the place after contact with deep convection (though maybe not after contact only with an outflowing air mass).

The reviewer here points to a major problem with this and all other trajectory models. Fundamentally, they rely on the meteorological data from weather models which do not resolve individual convective elements. Convection is only represented in a parameterized way and therefore reflects the general vertical movement of an airmass, but not an individual parcel subject to a convective event. Thus, they cannot trace a parcel backwards through a convective event. The best they can do is show that a parcel came into the vicinity of a convective event, und thus was likely to be affected by the outflow. Coming close to a convective event does not make the parcels diverge, because the trajectory model actually does not see the event. Fundamentally, this is correct behavior, because the air in the outflow joins the general flow in the upper troposphere, and only those subparcels that actually came up through the cloud "should" have backtrajectories that go down through the cloud. Thus, if a back-tracked air parcel is not an outflow parcel, it should track backwards with the mean flow as represented by the model. It is thus legitimate to keep following it backward to perhaps encountering another region of convective outflow. The actual processes can only be resolved by a dedicated mission looking at the development of an individual outflow in a Lagrangian sense, which we hope to do in the future.

The authors do acknowledge this briefly (line 929) and it may not be very important if one contact with outflow is usually enough to produce NPF. However, I think these uncertainties merit a bit more discussion in the text, some kind of demonstration in a supplementary figure as I suggest above, and a brief comment in the caption of Table 1.

We've attempted to clarify this situation as concisely as possible by modifying the text at line 929 (old) by writing:
"Because the model does not "see" the individual convective event that brings up an outflow, it cannot trace a parcel back into this outflow and back down to the boundary layer. On the other hand, an air parcel that passed through the vicinity of the outflow, but is not part of the actual outflow, will keep moving backward along the mean flow in the UT and may then encounter another outflow. Obviously, however, the uncertainty in the trajectory position increases with time going backwards, and is probably enhanced by passage near a region of active convection."
Given that our analysis shows that, in view of the frequency of convection over Amazonia and the generally long residence time of air parcels in the anticyclonic movement over the basin, almost all air parcels will pass near convection over a 72-hour time frame, it does not seem worthwhile to go much further in this analysis. See also our comment below in our response to remark 1 in the results section.

4. The 10-14km altitude range (e.g. line 463) seems quite high compared to many of the NPF bursts observed -one of the examples is at 7km. Some words on what happens at slightly lower altitudes would be useful, if this can be provided without huge extra effort.

Actually, the statement in line 463 was incorrect and, as can be seen in Table 1, the analysis was done for all enriched layers, including those at 7 km.

5. Is there a dependence of the NPF characteristics on trajectory type (A-E in Figure 1)?

We could not identify any obvious relationship.

Is it possible to draw general conclusions in addition to the discussion of specific flights and the statement that only a few daylight hours are needed for the NPF, in Section 3.5?

We don't feel that we can draw further generalizations based on the kind of data we have from this mission. To go further, different flight strategies and instrumentation would be required, which we plan to deploy on a future mission.

Results:
1. I'm reluctant to suggest additions to an already long and comprehensive study. However, I do feel information is lacking on the air masses in the UT in which particle concentrations were low (except for the immediate cloud outflow region, which is already described). Clearly from Fig. 7a quite a few segments with fewer than 2000 particles/cm3 were seen. At line 661 the authors could remind readers of this by changing "two distinct aerosol populations" as "two types of elevated aerosol population".

Done.

If studying the air masses with very low particle concentration shows significant differences in their interaction with deep convection compared to the air masses with high particle concentrations, the authors' conceptual model may become more powerful: it may be possible to suggest contact with deep convection is a necessary condition for particle production in these situations. If no significant differences are found, this would also be interesting, though it would certainly not invalidate the conceptual model, as there are many possible explanations for the absence of NPF. Thus, could the authors consider either adding another (shorter!) Table 1, where at least some of the flight legs where aerosol concentrations in the UT were below 2000 cm-3 are listed?

We felt this was a very valuable suggestion by the reviewer and examined our data for such legs. To our disappointment it was almost impossible to find such segments. Because of the high variability of the CN concentrations in the UT, the times when N_{CN} was below 2000 cm^{-3} were in almost all cases very short, and would not lend themselves to a meaningful analysis of airmass history. To illustrate this, we show a full time series plot of the measurements from Flight AC09 in the supplement:

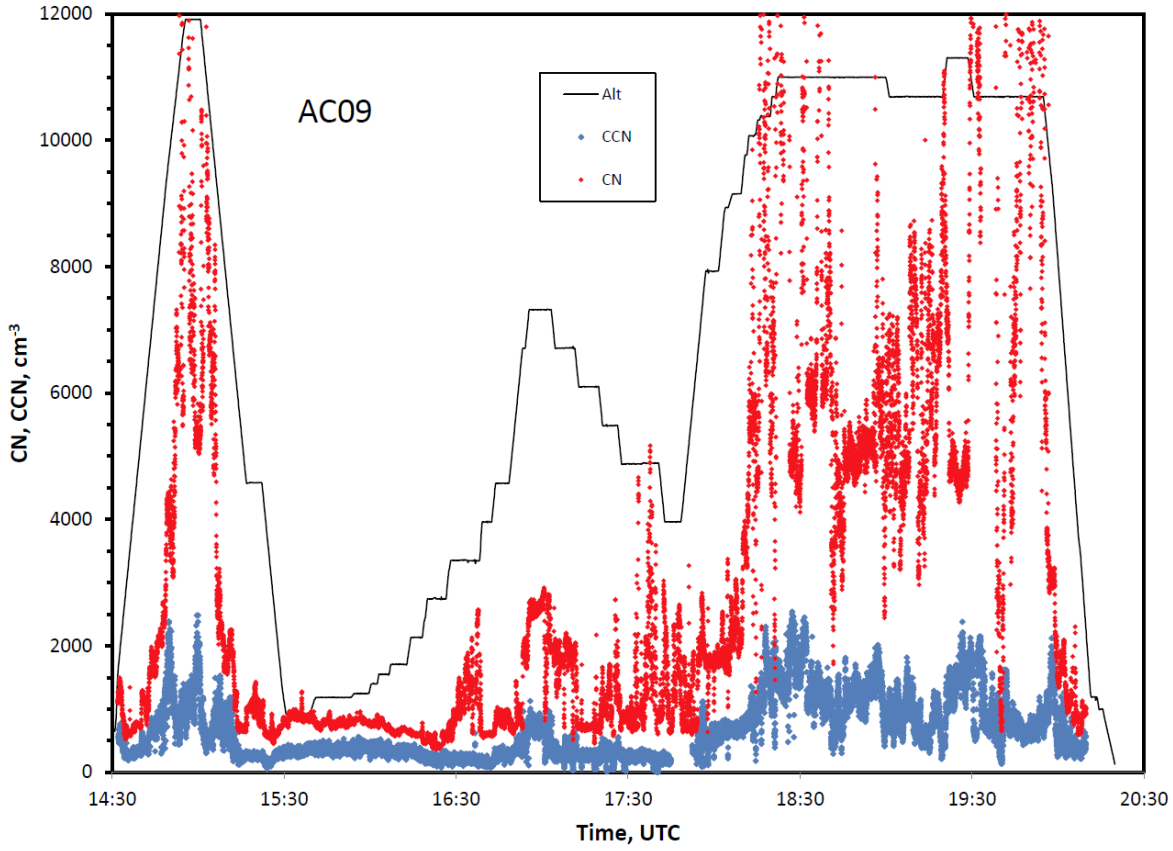

The only exception to this were segments that were within a Cb outflow.

We were able to find only six segments, where N_{CN} was consistently below 3000 cm^{-3}, and which were not identifiably part of an outflow. These are listed in Table S1 in the

supplement. The segments from flights AC16 and AC18 were well away from clouds, whereas those from AC19 and 20 were in the vicinity of Cbs, but not clearly in an outflow. The segment L from AC19 is low in CN, but actually has a relatively high $N_{CCN0.5}$, and may not really be significantly different from the aged enriched segment E2, which follows immediately after it. The airmass trajectory types in these segments do not contain type D, i.e., recirculation within the Amazon basin. Notably, the air in the segments from AC20, which had the lowest particle concentrations, had come in straight from the Pacific within the last 48 hours. We added the following text to section 3.5.2:

"To test whether there was a difference in the airmass histories between segments with high and low N_{CN}, we searched our data for suitable segments with low N_{CN}. However, because of the high variability of the CN concentrations in the UT, the times when N_{CN} was below 3000 cm^{-3} were in almost all cases very short, and would not lend themselves to a meaningful analysis of airmass history. To illustrate this, we show a full time series plot of the measurements from Flight AC09 in the supplement (Fig. S7).

We could find only six segments, where N_{CN} was consistently below 3000 cm^{-3}, and which were not identifiably part of an outflow. These are listed in Table S1 in the supplement. The segments from flights AC16 and AC18 were well away from clouds, whereas those from AC19 and 20 were in the vicinity of Cbs, but not clearly in an outflow. The segment L from AC19 is low in CN, but actually has a relatively high $N_{CCN0.5}$, and may not really be significantly different from the aged enriched segment E2, which follows immediately after it. Consequently, we don't have a data set that would allow a representative analysis of the history of airmasses with low particle concentrations. Notably, however, the airmass trajectory types in these segments do not contain type D, i.e., recirculation within the Amazon basin. The air in the segments from AC20, which had the lowest particle concentrations, had come in straight from the Pacific within the last 48 hours, but may also contain some outflow air."

Is there any systematic difference in the timings at which the air masses with few particles first made contact with deep convection, and at which the air masses with many particles made contact? I appreciate that the authors may prefer to leave this for further work if the analysis has not already been done.

Again, we feel that in view of the complexity of the airmass histories, dedicated campaigns are needed to resolve this question.

2. From Figure 5, the relative humidity at 7-10km altitude is very low – apparently unusually low (line 414 ish). It may be interesting to look for evidence of the RH enhancing or suppressing the particle number concentrations- if there is any effect of RH visible, this might suggest that the new particle formation is not at the kinetic limit for the vapours involved (or that water is important for the chemistry leading to the NPF). However, again I appreciate that this kind of investigation may be more appropriate for future studies with instrumentation better able to measure organic gasphase chemistry.

The discussion in line 414ff (old) refers to the column moisture content and precipitable water, not to the relative humidity in the upper troposphere. However, to follow up on the reviewer's

suggestion, we examined several flights (AC07, AC09, AC13, and AC18) for relationships between RH and N_{CN}. We found a tendency for the layers with high N_{CN} to be associated with moister layers (RH>50%), but also many exceptions. This relationship may simply have to do with the fact that moisture was brought up with the convective clouds, or there may be a relationship with the actual particle formation process, but at this point we have no way to answer these questions. We added a couple of sentences on this in section 3.5.3. We are planning a future campaign dedicated to process-level studies of NPF in the UT.

3. Related to comment #1, can the authors suggest some possible explanations for why the areas of extremely high particle concentration (suggestive of very recent new particle formation) are usually organised in thin layers?

The outflow from convective clouds tends to become stretched into relatively thin layers due to velocity shear and subsidence, especially when transported over considerable distances (for a discussion, see Eastham and Jacob, 2017, and references therein).

Conceptual model:
In general, I find the arguments in this section compelling and I have only minor comments, see below.
Conclusions:
At lines 1230-1238, the authors point out that in pre-industrial times, the mechanism they propose would operate unchanged, while sources of low-altitude particles would be diminished, meaning that upper-troposphere new particle formation may in some cases become the dominant source of CCN in the boundary layer. They further propose that the aerosol profile in polluted continental regions may be flipped in the pre-industrial compared to the present day.
The authors do make it clear that these statements are speculative, and I appreciate the need to be concise. However, at lines 1223-1224 I think they should additionally point out that the pre-industrial atmosphere may not have been particularly pristine in many places, with large marine, volcanic and fire emissions leading to uncertain but possibly high concentrations of boundary layer particles. It would be enough to modify “strongly affected by anthropogenic aerosols” to “strongly affected by anthropogenic or natural primary aerosols”.

Done.

Furthermore, to justify the arguments in the paragraph “The conceptual model proposed here implies…” the authors need to show evidence that in present-day *polluted* areas, concentrations of particles greater than say 3nm in diameter are usually lower at high altitude than they are at low altitude. A very brief look at flight data from INTEX over the eastern USA suggested to me that there is still plenty of particle production in the upper troposphere in polluted regions (in these areas, of course there are more particles in the BL, but also more SO2 making particles in the UT). There is a modification to the gradient of the aerosol profile over the industrial period (modelling studies suggest this is true even as a global average, see for example Fig. 1a of

http://onlinelibrary.wiley.com/doi/10.1002/2017JD026844/abstract) but to say “turned upside down” seems a bit strong.

A climatology of aerosol concentrations in the UT is available from the CARIBIC project. This shows median particle concentrations (> 12 nm) in the region 200-300 hPa to be ~3500 cm^{-3} over North America, ~2500 cm^{-3} over Europe, and ~3000 cm^{-3} over India (Ekman et al., 2012). Of course, there are elevated values at particular place and times, such as those the reviewer refers to, but they appear to be more the exception than the rule. In contrast, the averages measured at ground level at polluted continental sites worldwide range between 3400 and 19,000 cm^{-3} in the compilation by Andreae (2009). This is quite close to being the exact opposite of the distribution measured during ACRIDICON-CHUVA, where the averages (±std.dev.) were 7700±7970 cm^{-3} in the UT and 1650±980 cm^{-3} in the LT. This information has been added into the Conclusions text. But, so as not to over-generalize, we have modified the statement to “… has been turned upside down, at least in many polluted regions”.

Minor comments

The text is well written and logically structured, but as it is long, the introduction of more cross-referencing between sections to relate different parts of the text together would be very helpful. For example, it would be helpful to reference Figures 4 and 6 at the appropriate places in the paragraph starting on line 471.

Done.

Also at line 662 it would be helpful to remind the reader that the two aerosol populations were already introduced at line 547, to confirm the distinctions drawn are the same in the two cases.

Done.

Structurally, the one concern I have is that Section 3.4 and Section 3.5 start with essentially the same question, then Section 3.4 deals with one part of it and then 3.5 introduces another possible source (immediate outflows) and most of the section is then spent dealing with this new issue that was not previously introduced. Can the authors think about whether it is possible to organise these sections more rigidly and flag up the most important messages more strongly?

We have added some introductory sentences at the beginning of section 3.4 that inform the reader what to expect in sections 3.4 and 3.5.

The discussion of the trajectory results (3.5.2,3.5.3) probably merits a new section 3.6.

We prefer to retain the current structure, as we think it is appropriate to the discussion.

Line 93: the authors might cite here only the papers which really focus on UT NPF: the Carslaw (2017) citation seems out of place in this paragraph.

The reference has been deleted.

Line 197 or 218: please state approximate distance between inlet and instrument, to put these flow rates and efficiencies in context. Also for the UHSAS and CCNC.

The length of the line to the CPC was about 2 m, to the CCN about 1.8 m. The flow in the inlets was increased by using a variable flow bypass to reduce particle losses. The UHSAS is mounted in a wing-pod and has no inlet line.

The authors convincingly demonstrate NPF is the only possible source of the particles. However, they should emphasise the sentence at line 843-845 more, where the key reason for why the particles cannot come from long range transport is explained (even though it is fairly obvious). This could be done by forward referencing Section 3.5 from line 553, or restructuring slightly as suggested above.

Done, by the new introductory sentences at the beginning of section 3.4.

Line 806: please label the citation to Schulz as 'submitted', or 'in preparation', here. I couldn't find the paper.

Done.

Line 1087 The authors should specify that the CERN CLOUD chamber studies so far published only provide the temperature dependence of inorganic NPF. NPF involving organic molecules may behave quite differently, though NPF is still obviously expected to increase at lower temperatures (all other things being equal). Similarly, the Yu (2017) study does not fully account for the gas-phase chemistry (as this chemistry is not fully characterised the authors had little choice), so it treats NPF of organics rather similarly to that for H2SO4.

Cautionary sentence added: "Note, however, that these temperature dependencies are based on measurements for inorganic NPF, and that while the trends for organics are expected to be similar, the magnitude of the increase in nucleation rates for organics may be quite different."

Line 1123 The Gordon (2016) modelling study didn't quite suggest "dominant mode of new particle formation in the pre-industrial atmosphere", perhaps replace by "in large parts of the preindustrial atmosphere".

Done.

On page 68, the footnote labels to Table 1 all read "a".

Corrected.

Fig S1 caption: aren't the parcels zoomed in approximately a 6x6 degree box, not 3x3? Despite the valuable efforts of the authors to make things clear with the colour scale of

the trajectories and marking the GOES time on the figure, I found the way this was phrased in the caption a little confusing. If I understand, the snapshots are zoomed in a box centred at the parcel location at the time shown on the top ***of*** the snapshots, ***in parentheses backwards from the parcel start***. Perhaps the authors could add something like the italicised words/phrases to the caption?

The reviewer must be referring to Figure S2 (not S1). Yes, the boxes are 6x6 degrees and we corrected that in the caption. We added the wording on the number of hours in parentheses.

Andreae, M. O., Correlation between cloud condensation nuclei concentration and aerosol optical thickness in remote and polluted regions: Atmos. Chem. Phys., 9, 543–556, 2009.

Eastham, S. D., and Jacob, D. J., Limits on the ability of global Eulerian models to resolve intercontinental transport of chemical plumes: Atmos. Chem. Phys., 17, 2543-2553, doi:10.5194/acp-17-2543-2017, 2017.

Ekman, A. M. L., Hermann, M., Gross, P., Heintzenberg, J., Kim, D., and Wang, C., Sub-micrometer aerosol particles in the upper troposphere/lowermost stratosphere as measured by CARIBIC and modeled using the MIT-CAM3 global climate model: J. Geophys. Res., 117, D11202, doi:10.1029/2011jd016777, 2012.

Twohy, C. H., Clement, C. F., Gandrud, B. W., Weinheimer, A. J., Campos, T. L., Baumgardner, D., Brune, W. H., Faloona, I., Sachse, G. W., Vay, S. A., and Tan, D., Deep convection as a source of new particles in the midlatitude upper troposphere: J. Geophys. Res., 107, 4560, doi:10.1029/2001JD000323, 2002.

Weigel, R., Borrmann, S., Kazil, J., Minikin, A., Stohl, A., Wilson, J. C., Reeves, J. M., Kunkel, D., de Reus, M., Frey, W., Lovejoy, E. R., Volk, C. M., Viciani, S., D'Amato, F., Schiller, C., Peter, T., Schlager, H., Cairo, F., Law, K. S., Shur, G. N., Belyaev, G. V., and Curtius, J., In situ observations of new particle formation in the tropical upper troposphere: the role of clouds and the nucleation mechanism: Atmos. Chem. Phys., 11, 9983-10,010, doi:10.5194/acp-11-9983-2011, 2011.

Response to Reviewer 2

We thank the reviewer for his/her positive and constructive comments and for his/her thorough review. The reviewer comments are in plain font, the responses in *Italics.*

General comments

In this study characteristics of aerosol particles over the Amazon basin are investigated using aircraft measurements. The study focuses on the layers of enhanced particle concentrations observed in the upper troposphere. The particles in these layers were found to differ from particles in the lower troposphere with respect of their concentration, size, and chemical composition. Authors show that in most cases air masses with high particle concentrations have previously been in contact with deep convective outflow. Therefore, they suggest that particles are formed in the upper troposphere from precursors vapors brought up by deep convection. The study is of good scientific quality and certainly worth publishing in the ACP after some minor revisions. First of all, when reading the manuscript, one gets an impression that this is the first time when the conceptual model with the production of particles in the upper troposphere from material brought up by deep convection and the transport of particles back to the boundary layer is suggested (e.g. P2, L52– 60). However, as the authors discuss in Sections 1 and 3.7, this is not an entirely novel idea. Therefore, the authors should make it clearer, what is new in their conceptual model, and what has been suggested before. More specific comments are presented below.

In the introduction, we now write "…where production of new aerosol particles takes place in the UT from ***biogenic volatile organic material*** *brought up by deep convection…" to highlight the fact that our model is based on BVOC, whereas previous authors have mostly considered sulfur compounds or organics from pollution, including biomass burning. We have also added a paragraph to the introduction, making special reference to the work of Clarke and coworkers. See also our response to the first comment by Reviewer 3.*

In section 3.7, we refer extensively to previous work:

"The outflow regions in the UT present an ideal environment for particle nucleation, as had already been suggested in some earlier studies (Twohy et al., 2002; Lee et al., 2004; Kulmala et al., 2006; Weigelt et al., 2009)."

"Over marine regions and polluted continental regions, the particles observed in outflows and in the UT were mostly identified as sulfates (Clarke et al., 1999; Twohy et al., 2002; Kojima et al., 2004; Waddicor et al., 2012), and consequently H_2SO_4 has been proposed as the nucleating species."

We then go on to propose that, in contrast to these studies, organics may be the nucleating species, although a final proof still has to await our next campaign.

We also highlight the difference in the proposed mechanism of downward transport: "Large-scale entrainment of UT and MT air into the boundary layer has been suggested as the major source of new particles in marine regions (Raes, 1995; Katoshevski et al., 1999; Clarke et al., 2013). Over Amazonia with its high degree of convective activity, downdrafts are likely to play a more important role."

We never make the claim that "…this is the first time when the conceptual model with the production of particles in the upper troposphere from material brought up by deep convection and the transport of particles back to the boundary layer is suggested…". *In fact, the reviewer*

says so him/herself: "… as the authors discuss in Sections 1 and 3.7, this is not an entirely novel idea…".

Many more examples could be given. We feel that we have discussed previous work extensively in the introduction, in section 3.7, and in the conclusions. We find it difficult so see what more we could do to put our study in the context of previous work without repeating ourselves.

Specific comments

P4, L113–115: The use of terms is slightly unclear here. The current convention is to use HOMs to generally refer to highly oxygenated organic compounds, while ELVOCs are only those HOMs that have extremely low volatility. In some earlier articles all HOMs were called ELVOCs but this is not preferable.

In the community working on HOMs and ELVOCs there is currently no commonly accepted convention on terminology. Some authors suggest abandoning ELVOCs altogether and calling everything HOMs, while others are not using HOMs at all. In the Introduction we state "Extremely low volatility organic compounds (ELVOCs, which may be at least in part identical to HOMs)…". *In section 3.7 and the conclusions, we either use* "ELVOCs/HOMs*" or use the term that the authors of the papers use in the work that we are referencing.*

P18, L523: Are these values means for different flights?

The values are meant to reflect the range of quartiles above 8 km. This has been clarified in the text.

P18, L535: It would be good if authors presented typical ratios between concentrations in the upper troposphere and lower troposphere for different size ranges.

There is an entire section devoted to this issue, section 3.4.1, which discusses the ratio between ultrafine and accumulation mode particles (expressed as ultrafine fraction, UFF). Averages for the particle concentrations in the different size classes are given in Table 2, to which we now refer to in the first paragraph of section 3.3 by "…, and average concentrations for the particle concentrations in the different size classes and altitude regions are given in Table 2*". We have also added the magnitude of the ratio in the text:* "On average, N_{CN} in the UT were almost five times as high as in the LT." *and* "On average, N_{acc} in the UT was only about half the concentration measured in the LT."

P19, L546: The enhancement of accumulation mode particle concentration as well as high total particle concentrations would be easier to see if particle concentrations were plotted using a logarithmic scale (this also applies to some other plots).

We disagree. We started with log plots and switched to linear ones because they showed the differences much more clearly.

P21, L626: Could higher concentrations of CCN compared to accumulation mode particles be also caused by underestimation of accumulation mode particle concentration due to high losses?

The accumulation mode particles were measured by a UHSAS in a wing pod. There is no evidence for particle losses with this setup, which has been tested thoroughly, see also the paper by Walser et al. (2017) referenced in section 2.4.

P22, L646–647: Why there is a peak in CCN fraction at ~11 km?

The high values of the CCN fraction at this altitude are caused by the inclusion of a large number of measurements from flight AC20 on a horizontal leg at 11 km. This layer has only modest CN concentrations (around 1700 cm^{-3}), but elevated CCN, NO_y, CO, and aerosol nitrate and organics, with similar values to the biomass-burning-polluted boundary layer below. This flight was exceptional in that it was the only flight during the campaign on which we had evidence for transport of biomass smoke to the UT (see section 3.6). We included a short explanation and a forward reference to section 3.6 in the caption to Fig. 12a. We also added the following sentence in section 3.6: "Further evidence for the upward transport of biomass smoke was found in measurements on a horizontal leg at 11 km, which had only modest CN concentrations (around 1700 cm^{-3}), but elevated CCN, NO_y, CO, and aerosol nitrate and organics, with similar vales to the biomass-burning-polluted boundary layer below."

P23, L664: Should UFF be low (instead of high) when discussing these more aged particles?

Corrected.

P23, L668: In Fig. 13 there seems to be AC10-F instead of AC07-F.

We corrected the label in Fig. 13.

P23, L683: For me it is not obvious where this region with high CCN concentrations is in Fig. 11b. In any case, this region could be mentioned already when discussing the vertical distribution of CCN.

The concentrations in this region were not dramatically elevated, only up to about 1500 cm^{-3}. We changed the text to make this clearer. It would not have been appropriate to mention this region earlier, since it is specific to flight AC13, which is discussed in this paragraph as an illustrative example.

P24, L717: It is told here that the average rBC concentration below 5 km is 0.31±0.29 g m-3. It would be good to clarify what 0.29 g m-3 means here (and elsewhere in this section); is it an uncertainty for the average?

Here, and everywhere else, we give averages and standard deviations, unless stated otherwise. To make this clear, we have added this definition of our notation in section 3.2.1, where it is used first.

P31, L915: Please report how large the fraction of the cases where these air masses had encountered deep convection is. Also, would it be possible to perform more statistical analysis of

the connection between enhanced particle concentrations and deep convection, for example by studying correlation between time since contact and particle concentration?

Actually, the fraction was 100%! The "almost" was left over from when we had not yet done the analysis for all cases, and has now been removed. We looked for such correlations, but could not find anything obvious. Unfortunately, since the mission objectives had been focused on aerosol/cloud-microphysics interactions, the flights were not designed to look into this issue. We plan to conduct a dedicated campaign in the future.

P31, L926: Why the flight AC19 was different?

Most of this flight took place outside of the Amazon basin, off the east coast of South America over the Atlantic.

P34, L1009: Please report the correlation coefficient obtained for N_{CN} and O_3.

Because of the great variability in the O_3 concentrations in the UT, there is no general correlation for the entire mission (r^2=0.02). For individual flights, modest but significant correlations emerge, which are still affected by the high variability of both variables. We added the following text:
"Because of the great variability in the O_3 concentrations in the UT, there is no general correlation between N_{CN} and O_3 for the entire mission (r^2=0.02). For individual flights, modest, but statistically significant, negative correlations can be found, e.g., an r^2 value of 0.13 (N=8509) in the UT on flight AC09. The scatter plot in Fig. S08 shows that high O_3 concentrations were always associated with low N_{CN}, but that there were low-O_3 regions in the UT both with and without enhanced particle concentrations."

P35, L1019: Please report the correlation coefficient. Also, adding a plot of NOy vs N_{CN} could be useful.

Again, there is no significant overall correlation. As pointed out in the text, the relationships are very complex because the transformation of NO and the formation of particles both occur on short timescales that cannot be resolved by a general correlation analysis. In the paper, we provide some examples of these interactions, but a full analysis if the nitrogen oxide chemistry and its role in aerosol formation in the UT must await a dedicated mission.

P37, L1078: Check the terminology as VOCs (volatile organic compounds) cannot have low/very low volatilities by definition. Moreover, if low volatile vapors are removed in the cloud outflow, how can there be enough low-volatile vapors to form particles?

We replaced "VOCs" by "organic compounds". However, we remind the reviewer that the terms LVOCs and ELVOCs are very commonly used in the literature. The low-volatile vapors that form the new particles are produced by the oxidation of volatile vapors by photochemistry in the UT, as discussed in the subsequent paragraphs. For a better flow of the discussion we have moved the paragraph with this discussion up, to follow directly after the statement referred to by the reviewer.

P37, L1100 & P38, L1128 & P40, L1194: Instead of “ELVOCs/HOMs” I would suggest using only “HOMs”. See also the comment above.

We responded to this suggestion already above.

P38, L115: Stating that pure organic nucleation is “much more likely” than nucleation including both organic and sulfuric acid appears to be a too strong statement, especially when the authors do not have data on the vapor concentrations. In the summary section, the authors also write that “we propose that BVOCs in the cloud outflow are rapidly oxidized to HOMs/ELVOCs, which because of the low temperatures and low condensation sink can readily nucleate new particles and grow to sizes ≥20 nm within a few hours”. I would suggest modifying this to something like “… oxidized to HOMs, which because of the low temperature and low condensation sink can form new particles, possibly together with sulfuric acid, and condense on particles growing them to sizes >20 nm”

We changed “much more likely” to “likely” and changed the sentence in the summary to include the possible role of H_2SO_4, as suggested by the reviewer.

P39, L1160: The “Summary and conclusions” section is very long and partly seems to repeat some things discussed in the previous section. Therefore, I would suggest making the summary section shorter, especially the end of the section (starting from the line 1205). If needed, some of the text could also be moved to the previous section.

We disagree. This paper describes a very complex data set with a large range of information from many different instruments, from atmospheric transport models, and remote sensing. In the Summary and Conclusions we have tried to pull this information together in a concise way. The summary part must necessarily repeat, to a certain extent, things that have been said before. The end of the section is very important, since it puts the results into a “big picture” perspective.

Technical corrections

P1, L38: Change “September/October” to “September–October”
Done
P2, L47: Change “depleted in aerosol particles” to “depleted of aerosol particles”
Done
P2, L49: Please change hyphen in “5-72” to en dash (–). This should be changed everywhere in the manuscript where ranges of numbers are shown.
Done
P2, L56: Change “biogenic volatile organic carbon” to “biogenic volatile organic compounds”.
Done
P3, L74: Change “are” to “they are”
Done
P3, L81: Rephrase this sentence so that it does not begin with “where”.
Done
P3, L82: Check the use of verb tenses in the whole manuscript. For example, here “was” should be changed to “has been”.

"was" is correct here.
P4, L109: Please rephrase the sentence.
Done
P7, L212: Modify the reference to follow the journal's guidelines.
This reference is a place holder and will be updated when the final files are prepared.
P8, L244: Change to "The DMPS data *were* then analyzed *by* taking into..."
Done
P10, L278: Change "on the S" to "on S".
Done
P10, L284: Change "by M. Pöhlker et al." to "by Pöhlker et al."
Since there are references to two different Pöhlkers as first authors, we use the initial to differentiate them. If the journal does not like this, the copyeditor is free to change it.
P15, L422: Please check that the reference style follows the journal's guidelines.
This can be checked by the copyeditor.
P20, L591–593: The description of ultrafine fraction should be presented in a clearer way.
We can't think of a clearer way. The definition equation is clear and unambiguous. If the editor disagrees, we would appreciate a suggestion for a better expression.
P21, L610: Remove "M." and add this also to the reference list.
Reference deleted.
P23, L662: Please change "at one extreme are" to "at one extreme there are". Also, change "at the other extreme are" to "at the other extreme there are".
Done
P23, L689: The description of volatile fraction is not clear here; it is not explained what Nnonvol stands for.
Definition added.
P25, L722. Change "June/July" to "June–July"
Done
P26, L751: Please use subscripts for chemical compositions (e.g. SO4, NH4…)
These are in fact not chemical formulae, in which case they would have to be written also with the ionic charges, but abbreviations that are commonly used in the AMS literature.
P26, L752: When using abbreviation "BB" for the first time, please write the whole word.
Done
P31, L903: Change "can this be reversed" to "this can be reversed"
Retained as is. Can be changed by copyeditor if necessary.
P34, L1000: Change "close" to for example "strong"
"close correlation" is very common usage. We don't think "strong" would be better.
P34, L1015: Change "2056" to "20:56" etc.
This notation is very common in the meteorological literature.
P36, L1064: "Fig. 20" should be "Fig. 24"
Corrected
P36, L1064: I would suggest using some other term than "classical nucleation events", as a reader may confuse it with the classical nucleation theory. The term is used also elsewhere in the manuscript.
We put "classical" in quotes to distinguish it from other usages.
P37, 1090–1091: Rephrase the sentence "the low particle surface area in the UT presents very little competition to nucleation from a condensation sink", as it is slightly unclear.

Done

P40, L1171: Please make it clear that “UT aerosol was fundamentally different from the aerosol in the LT” is the result of this study.

Done

Table 2: Please state in the table caption what the numbers reported in the table are: means with their uncertainty ranges?

Done

Figure 1: It is difficult to see the difference between normal and “heavier” lines, so I would recommend using some other way to distinguish them.

We increased the thickness contrast between the lines.

Figures 2–4: As the manuscript includes so many figures, I would consider moving these figures (or at least some of them) to the supplementary material.

We disagree. This meteorological information is essential to understand the context of the mission.

Figure 7b: In many of the figures (especially the lower panels) font size and line thickness/dot size should be increased.

The figures were somewhat preliminary. They will be updated for the final submitted files.

Figure 10b: The values in the figure seem to be fractions, not percentage values as indicated by the figure label.

Percentages are one way to express a fraction.

Figure 19a: There seems to be something wrong with the y-axis label.

Fixed.

Response to Reviewer 3

We thank the reviewer for his/her careful review and positive and constructive comments. The reviewer comments are in plain font, the responses in *Italics*

The manuscript is nearly ready for publication, except for several points that I would like the authors to address.

1) The conceptual aerosol life cycle model in which convection lifts boundary layer air with nucleation precursor molecules into the upper troposphere, where nucleation takes place in the detrainment zone, followed by aerosol growth and descent through the troposphere into the boundary layer, has been to the best of my knowledge first formulated by A. D. Clarke (1992) based on observations and supported by subsequent investigations (e.g. Clarke, 1993; Clarke et al., 1998). These measurements were carried out over the oceans and implied sulfuric acid, likely from dimethyl sulfide and sulfur dioxide oxidation, as the molecule driving aerosol nucleation. Clarke and Kapustin (2002) wrote that "the tropics commonly have low aerosol mass but very high number concentrations in the upper free troposphere (FT) that appear to form from sulfuric acid (nucleation) in convective regions and near cloud edges. These age and subside to become effective cloud condensation nuclei (CCN) when mixed into the marine boundary layer." This conceptual model is applied in the present manuscript to a pristine tropical continental region with organic molecules as the likely nucleation precursor. References to works by Clarke et al. and their context do, however, not provide due credit. I would like to ask the authors to add a brief paragraph in which their analysis and findings are placed into the context of this previously developed aerosol life cycle model and which provides credit to A. D. Clarke for its development with the below references.

Clarke, A. D., Atmospheric nuclei in the remote free troposphere, J. Atmos. Chem., 14, 479-488, 1992.

Clarke, A. D., Atmospheric nuclei in the Pacific midtroposphere: Their nature, concentration, and evolution, J. Geophys. Res., 98(D11), 20633-20647, doi:10.1029/93JD00797, 1993.

Clarke, A. D., J. L. Varner, F. Eisele, R. L. Mauldin, D. Tanner, and M. Litchy, Particle production in the remote marine atmosphere: Cloud out-flow and subsidence during ACE 1, J. Geophys. Res., 103, 16,397-16,409, 1998.

Clarke, A. D. and Kapustin, V. N.: A Pacific aerosol survey. Part I: A decade of data on particle production, transport, evolution, and mixing in the troposphere, J. Atmos. Sci., 52, 363-382, doi:10.1175/1520-0469(2002)059<0363:APASPI>2.0.CO;2, 2002.

As submitted, the paper contained 15 references to the work of Clarke and coworkers. In accordance with the reviewer's suggestion, we have added the suggested four new references to Clarke's work and included the following paragraph in the introduction: "Based on observations over the remote Pacific and supported by extensive subsequent investigations, Clarke and coworkers proposed an aerosol life cycle model in which convection lifts boundary layer air with nucleation precursor molecules into the upper troposphere, where nucleation takes place in the detrainment zone, followed by aerosol growth and descent through the troposphere into the boundary layer (Clarke, 1992; Clarke, 1993; Clarke et al., 1998). These measurements were carried out over the oceans and implied sulfuric acid, likely from dimethyl

sulfide and sulfur dioxide oxidation, as the molecule driving aerosol nucleation. Clarke and Kapustin (2002) wrote that "the tropics commonly have low aerosol mass but very high number concentrations in the upper free troposphere (FT) that appear to form from sulfuric acid (nucleation) in convective regions and near cloud edges. These age and subside to become effective cloud condensation nuclei (CCN) when mixed into the marine boundary layer."" In section 3.7, we are contrasting our model to that of Clark and other workers in several important aspects, e.g., the role of organics vs sulfates and the mechanism of downward transport. See also our response to the first comment by Reviewer 2.

2) Line 78-79: " ... or upward into the Tropical Transition Layer (TTL) and the lower stratosphere (Weigel et al., 2011; Randel and Jensen, 2013) ..." Please add a reference to Brock et al. (1995), who identified the role of upper tropospheric aerosol nucleation for stratospheric aerosol concentrations. C. A. Brock, P. Hamill, J. C. Wilson, H. H. Jonsson, K. R. Chan: Particle Formation in the Upper Tropical Troposphere: A Source of Nuclei for the Stratospheric Aerosol, Science, 1650-1653, 1995

Done.

3) Line 719-723: "Interestingly, these concentrations over the Amazon Basin are only slightly higher than the values measured over the tropical Western Atlantic during the Saharan Aerosol Long-range Transport and Aerosol-Cloud-Interaction Experiment (SALTRACE), June/July 2013: ca. 0.2 ug m-3 in the LT and ca. 0.001 ug m-3 in the FT (Schwarz et al., 2017), which suggests that a significant fraction of the rBC is entering the basin by long-range transport from Africa." It is not clear that one can make this statement simply by comparing BC mass concentrations from two campaigns that are more than year apart, without analyzing transport and the contribution of local BC sources. Can you add a supporting discussion or evidence that would corroborate the point, or instead, formulate the statement hypothetically?

We have a considerable amount of evidence for the transport of BC and other aerosol constituents from Africa to the Amazon Basin from several campaigns. Recently, we have published a modeling study on this topic (Wang et al., 2016). We are currently preparing a paper in which we are documenting the transport of biomass smoke from Southern Africa to the Amazon during ACRIDICON-CHUVA. This has also been observed in previous campaigns, e.g., Andreae et al. (1994). We have added the following text to section 3.4.4:

"Transport of biomass smoke containing BC and other constituents from Africa to South America has been documented previously, e.g., from Northern Africa during the wet season (Talbot et al., 1990; Wang et al., 2016) and from Southern Africa during the dry season (Andreae et al., 1994). A detailed study on the transport of Southern African aerosols to the Amazon during ACRIDICON-CHUVA is in preparation and will be published elsewhere."

Clarke, A. D., Atmospheric nuclei in the remote free troposphere: J. Atmos. Chem., 14, 479-488, doi:10.1007/bf00115252, 1992.

Clarke, A. D., Atmospheric nuclei in the Pacific midtroposphere - their nature, concentration, and evolution: J. Geophys. Res., 98, 20,633-20,647, doi:10.1029/93jd00797, 1993.

Clarke, A. D., Varner, J. L., Eisele, F., Mauldin, R. L., Tanner, D., and Litchy, M., Particle production in the remote marine atmosphere: Cloud outflow and subsidence during ACE 1: J. Geophys. Res., 103, 16,397-16,409, doi:10.1029/97jd02987, 1998.

Clarke, A. D., and Kapustin, V. N., A Pacific aerosol survey. Part I: A decade of data on particle production, transport, evolution, and mixing in the troposphere: J. Atmos. Sci., 59, 363-382, 2002.

Wang, Q., Saturno, J., Chi, X., Walter, D., Lavric, J. V., Moran-Zuloaga, D., Ditas, F., Pöhlker, C., Brito, J., Carbone, S., Artaxo, P., and Andreae, M. O., Modeling investigation of light-absorbing aerosols in the Amazon Basin during the wet season: Atmos. Chem. Phys., 16, 14,775-14,794, doi:10.5194/acp-16-14775-2016, 2016.

Andreae, M. O., Anderson, B. E., Blake, D. R., Bradshaw, J. D., Collins, J. E., Gregory, G. L., Sachse, G. W., and Shipham, M. C., Influence of plumes from biomass burning on atmospheric chemistry over the equatorial Atlantic during CITE-3: J. Geophys. Res., 99, 12,793-12,808, 1994.

Aerosol characteristics and particle production in the upper troposphere over the Amazon Basin

Meinrat O. Andreae[1,12], Armin Afchine[2], Rachel Albrecht[3], Bruna Amorim Holanda[1], Paulo Artaxo[4], Henrique M. J. Barbosa[4], Stephan Borrmann[1], Micael A. Cecchini[5,3], Anja Costa[2], Maximilian Dollner[9,13], Daniel Fütterer[6], Emma Järvinen[10], Tina Jurkat[6], Thomas Klimach[1], Tobias Konemann[1], Christoph Knote[9], Martina Krämer[2], Trismono Krisna[8], Luiz A. T. Machado[5], Stephan Mertes[7], Andreas Minikin[6,16], Christopher Pöhlker[1], Mira L. Pöhlker[1], Ulrich Pöschl[1], Daniel Rosenfeld[14], Daniel Sauer[6], Hans Schlager[6], Martin Schnaiter[10], Johannes Schneider[1], Christiane Schulz[1], Antonio Spanu[6,13], Vinicius B. Sperling[5], Christine Voigt[6,15], Adrian Walser[9,6], Jian Wang[1,11], Bernadett Weinzierl[6,13], Manfred Wendisch[8], and Helmut Ziereis[6]

[1]Biogeochemistry, Multiphase Chemistry, and Particle Chemistry Departments, Max Planck Institute for Chemistry, Mainz, Germany
[2]Forschungszentrum Jülich, Jülich, Germany
[3]Instituto de Astronomia, Geofísica e Ciências Atmosféricas, Universidade de São Paulo, São Paulo, Brazil
[4]Institute of Physics, University of São Paulo, São Paulo, Brazil
[5]National Institute for Space Research (INPE), São José dos Campos, Brazil
[6]German Aerospace Center (DLR), Institute of Atmospheric Physics (IPA), Weßling, Germany
[7]Leibniz Institute for Tropospheric Research, 04318 Leipzig, Germany
[8]Leipzig Institute for Meteorology, Leipzig University, Leipzig, Germany
[9]Meteorological Institute, Ludwig Maximilian University, Munich, Germany
[10]Institute for Meteorology and Climate Research, Karlsruhe Institute of Technology, Karlsruhe, Germany
[11]Brookhaven National Laboratory, Upton, New York, USA
[12]Scripps Institution of Oceanography, University of California San Diego, La Jolla, California, USA
[13]University of Vienna, Aerosol Physics and Environmental Physics, Wien, Austria
[14]Institute of Earth Sciences, The Hebrew University of Jerusalem, Israel
[15]Institute of Atmospheric Physics (IPA), Johannes Gutenberg University, Mainz, Germany
[16]German Aerospace Center (DLR), Flight Experiments, Oberpfaffenhofen, Germany

Abstract

Airborne observations over the Amazon Basin showed high aerosol particle concentrations in the upper troposphere (UT) between 8 and 15 km altitude, with number densities (normalized to standard temperature and pressure) often exceeding those in the planetary boundary layer (PBL) by one or two orders of magnitude. The measurements were made during the German-Brazilian cooperative aircraft campaign ACRIDICON–CHUVA on the German High Altitude and Long Range Research Aircraft (HALO). The campaign took place in September–October 2014, with the objective of studying tropical deep convective clouds over the Amazon rainforest and their interactions with atmospheric trace gases, aerosol particles, and atmospheric radiation.

Deleted: ci

Deleted: -

Deleted: /

Aerosol enhancements were observed consistently on all flights during which the UT was probed, using several aerosol metrics, including condensation nuclei (CN) and cloud condensation nuclei (CCN) number concentrations and chemical species mass concentrations. The UT particles differed in their chemical composition and size distribution from those in the PBL, ruling out convective transport of combustion-derived particles from the BL as a source. The air in the immediate outflow of deep convective clouds was depleted ~~of aerosol particles, whereas~~ strongly enhanced number concentrations of small particles (<90 nm diameter) were found in UT regions that had experienced outflow from deep convection in the preceding 5~~-72 hours. We also~~ found elevated concentrations of larger (>90 nm) particles in the UT, which consisted mostly of organic matter and nitrate and were very effective CCN.

Our findings suggest a conceptual model, where production of new aerosol particles takes place in the UT from biogenic volatile organic material brought up by deep convection, which is converted to condensable species in the UT. Subsequently, downward mixing and transport of upper tropospheric aerosol can be a source of particles to the PBL, where they increase in size by the condensation of biogenic volatile organic compound (BVOC) oxidation products. This may be an important source of aerosol particles for the Amazonian PBL, where aerosol nucleation and new particle formation has not been observed. We propose that this may have been the dominant process supplying secondary aerosol particles in the pristine atmosphere, making clouds the dominant control of both removal and production of atmospheric particles.

1. Introduction

Aircraft measurements in the upper troposphere (UT) have consistently shown large regions with very high aerosol particle number concentrations, typically in the tens of thousands of particles per cm^3, with the strongest enhancements reported in tropical and subtropical regions (Clarke et al., 1999; Andreae et al., 2001; de Reus et al., 2001; Krejci et al., 2003; Lee et al., 2003; Young et al., 2007; Ekman et al., 2008; Yu et al., 2008; Froyd et al., 2009; Weigelt et al., 2009; Borrmann et al., 2010; Clarke and Kapustin, 2010; Mirme et al., 2010; Ekman et al., 2012; Waddicor et al., 2012; Reddington et al., 2016; Rose et al., 2017). Twohy et al. (2002) observed particle concentrations up to 45,000 cm^{-3} in the UT over North America and suggested that they had been formed in situ from gas-phase precursors brought up by deep convection. Weigel et al. (2011) found similar concentrations in the UT over tropical America, Africa, and Australia,

Deleted: in

Deleted: -

Deleted: carbon

Deleted: in

Deleted: n

which they attributed to new particle formation from sulfuric acid and possibly organics. Most of these elevated aerosol concentrations are in the nucleation and Aitken mode size ranges, i.e., at particle diameters smaller than about 90 nm, with maxima typically between 20 and 60 nm (e.g., de Reus et al., 2001; Lee et al., 2003; Weigel et al., 2011; Waddicor et al., 2012). They generally occur as layers of a few hundred to thousand meters in thickness, often extending over large horizontal distances, and they are found over continents as well as over the most remote oceanic regions. The high concentrations of these aerosols in the UT are of great significance for the climate system, because they make this region an important reservoir of particles for the transport either downward into the planetary boundary layer (PBL) (Clarke et al., 1999; Clarke et al., 2013; Wang et al., 2016a) or upward into the Tropical Transition Layer (TTL) and the lower stratosphere (Brock et al., 1995; Weigel et al., 2011; Randel and Jensen, 2013), where they can grow into the optically and cloud-microphysically active size range.

Based on observations over the remote Pacific and supported by extensive subsequent investigations, Clarke and coworkers proposed an aerosol life cycle model in which convection lifts boundary layer air with nucleation precursor molecules into the upper troposphere, where nucleation takes place in the detrainment zone, followed by aerosol growth and descent through the troposphere into the boundary layer (Clarke, 1992; Clarke, 1993; Clarke et al., 1998). These measurements were carried out over the oceans and implied sulfuric acid, likely from dimethyl sulfide and sulfur dioxide oxidation, as the molecule driving aerosol nucleation. Clarke and Kapustin (2002) wrote that "the tropics commonly have low aerosol mass but very high number concentrations in the upper free troposphere (FT) that appear to form from sulfuric acid (nucleation) in convective regions and near cloud edges. These age and subside to become effective cloud condensation nuclei (CCN) when mixed into the marine boundary layer."

When enhanced particle concentrations in the accumulation mode (larger than about 90 nm) have been observed, the enrichment was frequently attributed to sources of sulfur dioxide (SO_2) and other combustion emissions, especially biomass burning (BB), based on correlations with combustion tracers, such as carbon monoxide (CO), and airmass trajectories (e.g., Andreae et al., 2001; Clarke and Kapustin, 2010; Weigel et al., 2011; Clarke et al., 2013). After having been lofted to the UT by deep convection, particles in this size range can be transported over hemispheric distances, because removal processes are very inefficient at these altitudes (Andreae et al., 2001; Clarke and Kapustin, 2010).

Deleted: In most cases,

Deleted: were

Deleted: re

The enhanced particle concentrations in the ultrafine (UF) size range (here defined as particles smaller than 90 nm), on the other hand, cannot be explained by transport from the lower troposphere, since they far exceed typical concentrations in the PBL and generally are too short-lived to survive deep convection and long-range transport. Therefore, nucleation and new particle formation (NPF) from gas phase precursors brought into the UT by the outflow from deep convection have been proposed as the source of these enhanced particle concentrations (Clarke et al., 1999; Twohy et al., 2002; Krejci et al., 2003; Lee et al., 2003; Young et al., 2007; Froyd et al., 2009; Merikanto et al., 2009; Weigel et al., 2011; Waddicor et al., 2012). High actinic flux, low preexisting aerosol surface area, and low temperatures make the UT an environment that is highly conducive to nucleation and NPF.

Deleted:

The nature of the gaseous species involved in particle nucleation and growth has been the subject of some debate (Kulmala et al., 2006). Most of the earlier papers attributed the nucleation to H_2SO_4 in combination with H_2O and NH_3, especially in marine and anthropogenically influenced regions, where a sufficient supply of sulfur gases from either DMS oxidation or pollution sources is available (e.g., Clarke et al., 1999; Twohy et al., 2002; Lee et al., 2003; Merikanto et al., 2009). However, there is growing evidence that, in most cases, there is not enough H_2SO_4 available to explain the observed rates of growth. Therefore, the condensation of organics has been proposed to dominate particle growth after nucleation, especially over unpolluted vegetated areas such as the Amazon Basin (Ekman et al., 2008; Weigel et al., 2011; Waddicor et al., 2012; Murphy et al., 2015).

In fact, H_2SO_4 does not even have to be the initially nucleating species in all cases. Recent studies conducted as part of the Cosmics Leaving OUtdoor Droplets (CLOUD) project have shown that organic vapors alone can produce particle nucleation (Kirkby et al., 2016) and that nearly all nucleation throughout the present-day atmosphere involves ammonia or biogenic organic compounds (Dunne et al., 2016). Highly oxygenated multifunctional organic compounds (HOMs) formed by ozonolysis of α-pinene were found to nucleate aerosol particles, especially when aided by ions. Extremely low volatility organic compounds (ELVOCs, which may be at least in part identical to HOMs) are also produced from the O_3- or OH-initiated oxidation of biogenic volatile organic compounds (BVOCs) (Jokinen et al., 2015). Following nucleation by the lowest-volatility species, with increasing particle size the condensation of progressively more volatile compounds is facilitated by the decrease in the Kelvin effect (Tröstl et al., 2016). These

Deleted: may

Deleted: always be required

laboratory studies were confirmed by field observations at a mountain site in the free troposphere, where NPF was found to take place through condensation of HOMs, in this case from anthropogenic precursor VOCs, within 1–2 days after being lofted from the PBL (Bianchi et al., 2016).

The production of particles in the UT may be a key component of the atmospheric budget of optically and cloud-microphysically active aerosols, especially in pristine or relatively unpolluted regions, as was suggested in a modeling study by Merikanto et al. (2009). Studies in the Amazon have shown that NPF almost never takes place under clean conditions in the PBL over the Amazon Forest (Zhou et al., 2001; Martin et al., 2010; Andreae et al., 2015) and rarely occurs over the taiga forest in remote Siberia (Heintzenberg et al., 2011). Over the Amazon, downward transport of aerosols from the free troposphere (FT) has been identified as an important, if not the dominant, source of particles to the lower troposphere (LT) (Zhou et al., 2001; Roberts and Andreae, 2003; Wang et al., 2016a). In turn, the concentrations of aerosols in the PBL have a pronounced influence on the characteristics of convection and thereby influence cloud radiative forcing and atmospheric dynamics (Sherwood, 2002; Rosenfeld et al., 2008; Fan et al., 2012; Rosenfeld et al., 2014; Stolz et al., 2015; Cecchini et al., 2017).

Understanding the processes that control the aerosol burden in the pristine atmosphere is an essential prerequisite for assessing the magnitude of the climate forcing by anthropogenic aerosols, since it forms the baseline from which anthropogenic forcing is derived. Because of the strong non-linearity of the relationship between particle number concentration and cloud-mediated aerosol effects, the uncertainty regarding the aerosol burden of the pristine atmosphere is the largest contributor to the uncertainty in estimates of anthropogenic aerosol climate forcing (Carslaw et al., 2013; Carslaw et al., 2017). For example, model calculations suggest that the inclusion of ion-induced particle formation from biogenic HOMs in the natural atmosphere reduces the cloud-albedo radiative forcing by about one-third because of the higher albedo calculated for the clouds in the pre-industrial atmosphere (Gordon et al., 2016).

In this paper, we present the results of aerosol measurements made in the upper troposphere across the Amazon Basin during the ACRIDICON–CHUVA campaign on the German HALO aircraft during September and October 2014 (Wendisch et al., 2016). ACRIDICON

Deleted: albeit

Deleted: -

Deleted: -

stands for “Aerosol, Cloud, Precipitation, and Radiation Interactions and Dynamics of Convective Cloud Systems”; CHUVA is the acronym for “Cloud Processes of the Main Precipitation Systems in Brazil: A Contribution to Cloud Resolving Modeling and to the GPM (Global Precipitation Measurement)”. We characterize these UT aerosol particles in terms of their microphysical and chemical properties, and contrast them with the LT aerosols. From their spatial distribution and their relationship to deep convection and convective outflow, we derive hypotheses about their mode of formation. Finally, we discuss the role of upper tropospheric aerosol formation in the life cycle of the atmospheric aerosol.

2. Methods

The observations discussed in this paper were collected aboard the HALO aircraft (http://www.halo.dlr.de/), a modified Ultra Long Range Business Jet G 550 (manufactured by Gulfstream, Savannah, USA). Because of its high ceiling altitude (up to 15 km) and long endurance (up to eight hours with a scientific payload), HALO is capable of collecting airborne measurements of cloud microphysical and radiative properties, aerosol characteristics, and chemical tracer compounds in the upper troposphere, in and around tropical deep convective clouds. The aircraft and its instrumentation are described in the ACRIDICON–CHUVA overview paper by Wendisch et al. (2016).

Deleted: -

In-situ meteorological and avionics data were obtained at 1 Hz from the BAsic HALO Measurement And Sensor System (BAHAMAS). This data set includes pressure, temperature, wind direction and speed, humidity, water vapor mixing ratio, aircraft position, and altitude. All concentration data have been normalized to standard temperature and pressure (T = 273.15 K and p =1000 hPa).

2.1. The HALO aerosol submicrometer inlet (HASI)

All aerosol sampling was conducted using the HALO aerosol submicrometer inlet (HASI), designed for HALO by the German Aerospace Center (DLR) in collaboration with enviscope GmbH (Frankfurt, Germany) with the aim of providing up to 30 l min^{-1} sample air flow (divided over four sample lines) to aerosol instruments mounted inside the aircraft cabin. HASI samples the air on top of the fuselage outside of the aircraft boundary layer. The air stream is

aligned in the inlet using a front shroud and decelerated by a factor of approximately 15. Four sample tubes with 6.2 mm outer diameter and frontal diffusors protrude into the decelerated air stream. The design goal is to allow regulating the sample airflow in each of the four sample lines to achieve isokinetic sampling conditions according to the actual speed of the aircraft. Since the automatic adjustment had not been implemented at the time of the field experiment, the flow was fixed to values providing near-isokinetic sampling for typical flight conditions based on geometric considerations and preliminary flow simulations for the initial design of the inlet. The geometric design should prevent large cloud droplets and ice crystals from entering the sample lines directly. The inlet position is located in the shadow zone for larger ice crystals, which precludes artifacts by shattering and break-up of larger ice particles at the inlet tip (Witte, 2008). Judging from the first measurements with HASI, it appears that measurements of interstitial aerosol in liquid clouds are affected by artifacts, while in ice clouds there is no indication for such artifacts. The data selection procedures to exclude artifacts are discussed in section 2.2.

2.2. Condensation nuclei

Condensation nuclei (CN) number concentrations (N_{CN}) were measured using the Aerosol Measurement System (AMETYST). This system was designed to provide an instrument package for HALO to measure basic microphysical properties of the ambient atmospheric aerosol (integral number concentration, sub-micrometer size distribution, fraction of non-volatile particles, and particle absorption coefficient). AMETYST includes four butanol-based condensation particle counters (CPCs, modified Grimm CPC 5.410 by Grimm Aerosol Technik, Ainring, Germany) with flow rates of 0.6 and 0.3 l min^{-1}, configured with different nominal lower cutoff diameters at 4 nm and 10 nm (set via the temperature difference between saturator and condenser). In addition, two differential mobility analyzers (Grimm M-DMA) with a nominal size range between 5.5 and 350 nm using ^{241}Am radioactive sources as aerosol neutralizers are part of the system.

Two of the four CPCs are generally set to measure the integral particle concentrations, while for the two other CPCs the configuration is selectable depending on measurement priorities. They can be used either as detectors for the DMAs or for additional integral concentration measurements. The DMAs can either be set to select specific diameters or operated as a DMPS (differential mobility particle sizer) system scanning the size distribution at predefined diameter

steps. The integration times at each step have to be chosen such that meaningful statistics can be achieved depending on the measurement strategy. AMETYST also includes an optional thermodenuder, which heats a section of the sample line to 250°C for the measurement of the non-volatile particle fraction.

The raw CPC data are corrected using an empirical, pressure-dependent flow correction to account for changes in the volume flow at different flight altitudes (D. Fütterer, PhD thesis, in preparation). Particle losses in the sampling lines have been estimated with the particle loss calculator by von der Weiden et al. (2009). Accounting for these effects leads to an increase of the effective cutoff diameter for all CPCs. The effective cutoffs are calculated as a convolution of the pressure-dependent CPC counting efficiency and the size-dependent transmission efficiency of the sample lines. The data reported here were taken by the CPC operated at 0.6 l min^{-1}, with a nominal cutoff of 4 nm. Due to inlet losses, the effective cutoff diameter increases to 9.2 nm at 1000 hPa, 11.2 nm at 500 hPa, and 18.5 nm at 150 hPa. This implies that the present setup of AMETYST essentially does not detect nucleation mode particles below 10 nm at low altitudes and below 20 nm in the UT. Typical uncertainties of CPC number concentration measurements are estimated to be of the order of 5 to 10% (Petzold et al., 2011).

To eliminate artifacts from cloud hydrometeors and bias from local pollution, we excluded measurements using the following criteria: (1) All cloud passages below 6 km were removed. During passages through water clouds, the CPCs showed erratic, unreasonably high number concentrations that are probably caused by droplet shattering at the probe tip. Cloud passages were identified from the observation of elevated concentrations of particles >3 μm using the hydrometeor probes (see below). (2) In the mixed phase and ice phase regimes, all cloud passages were inspected for possible shattering artifacts, and suspect data were rejected. Cloud passages through pure ice clouds did not show evidence of hydrometeor shattering. (3) The flight segments during departure and approach to Manaus airport were removed to avoid pollution from the airport and its surroundings. (4) Flights segments through the Manaus urban plume, which was sampled during joint flight experiments with the DOE G1 aircraft and in the course of tracer studies in the PBL, were excluded in order to provide a sampling representative of the dry season atmosphere over the Amazon Basin away from local pollution. (5) Fire plumes that were sampled deliberately to study fresh emissions were not analyzed for this paper. (6) Segments where the aircraft passed through its own exhaust were also excluded from the analyzed data set.

2.3. Aitken mode aerosol size spectra

To obtain aerosol size spectra for particle sizes up to 300 nm, the DMAs within AMETYST were connected to two of the CPCs and operated in scanning mode for selected flight sequences (especially during longer flight legs, where relatively homogeneous conditions can be assumed). The size range covered by the scans was typically between 20 and 300 nm diameter in nine steps. To improve the time resolution, the two DMPS were usually set to scan the same sequence in opposite direction. The DMPS data were then analyzed by taking into account a correction for multiple charges following Wiedensohler (1988) after correcting the measured concentrations to standard atmospheric conditions. To derive modal parameters for the particle size distribution, a bi-modal log-normal fit to the data points was computed.

Deleted: are

2.4. Accumulation mode aerosol particles

For the purposes of this paper, we define the accumulation mode as the particle size range from 90 nm to 600 nm and the total number concentration in this size class as the accumulation mode number concentration, N_{acc}. The particle concentrations in this range were measured with an optical particle counter (OPC), the Ultra High Sensitivity Aerosol Spectrometer (UHSAS; Droplet Measurement Technologies, Inc., Longmont, CO) (Cai et al., 2008; Brock et al., 2011). The UHSAS combines a high-power infrared laser (λ=1054 nm) and a large solid angle range in sideways direction for the detection of light scattered by individual particles. Due to the resulting almost monotonic increase of instrument response with particle size, the UHSAS enables high-resolution measurements (100 selectable channels). The high laser intensity enables the detection of particle diameters down to about 60 nm, with the upper limit being approximately 1 µm. Due to changes in the laser and instrument parameter settings during the campaign, only the size range from ~90 nm to ~600 nm is considered here. Particle concentrations of up to 3000 cm^{-3} are recorded without significant counting coincidence losses (Cai et al., 2008). The airborne instrument version is mounted in an under-wing canister and equipped with a forward facing diffusor inlet. The slowed airflow is subsampled by a second inlet at approximately isokinetic conditions. The sample is not actively dried before the measurement, but due to combined heating effects the measured diameters can be assumed to be close to their dry diameters (Chubb et al., 2016). The UHSAS was calibrated with monodisperse polystyrene latex (PSL) spheres of known refractive

Moved (insertion) [1]

index and size. The evaluation of the OPC calibration results and the derivation of realistic uncertainty estimates for the OPC size distributions is outlined in a recent study by Walser et al. (2017).

Moved up [1]: Due to changes in the laser and instrument parameter settings during the campaign, only the size range from ~90 nm to ~600 nm is considered here.

2.5. Cloud condensation nuclei

The number concentration of CCN (N_{CCN}) was measured with a continuous-flow streamwise thermal gradient CCN counter (CCNC, model CCN-200, DMT, Longmont, CO, USA) (Roberts and Nenes, 2005; Rose et al., 2008). The CCN-200 consists of two columns, in which particles with critical supersaturations (S) above a preselected value are activated and form water droplets. Droplets with diameters ≥ 1 µm are detected by an OPC at the exit of the column. The inlet flow rate of the column was 0.5 l min^{-1} with a sheath-to-aerosol flow ratio of 10. The water pump was operated at the CCNC setting of "high" liquid flow. Variations in ambient pressure have a strong influence on S inside the CCNC. For this purpose, a novel constant pressure inlet without significant particle losses was deployed on HALO. The instrument was calibrated before, during, and after the campaign at different pressures and flow rates according to Rose et al. (2008). For the data used in this study, we sampled from the HASI inlet and measured at S = 0.52±0.05% and a time resolution of 1 Hz.

Deleted: optical particle counter (

Deleted:)

Deleted: used

Deleted: L

Deleted: the

Since the flow in the instrument was kept constant for the data used here, the error in *S* was dominated by the calibration uncertainty, as described by M. Pöhlker et al. (2016); it is estimated to be in the range of 10%. According to Krüger et al. (2014), the error in N_{CCN} is based on the counting error of the measured particle number and is 10% of N_{CCN} for large concentrations; given that mostly low concentrations prevailed, the mean error was about 20% of N_{CCN}.

Deleted: resulted from

2.6. Cloud droplet and ice particle measurements

While measurements of liquid water and ice hydrometeor concentrations are not a subject of this paper, they were used to determine whether the aircraft was sampling inside clouds and if so, whether the cloud particles were liquid or frozen. For this purpose, we used data from the Cloud Droplet Probe (CDP) and the Cloud and Aerosol Spectrometer (CAS-DPOL), both of which are based on the principle of forward scattering detection. The CDP detects particles with sizes from 3 µm to 50 µm, and classifies them into size histograms of bin widths between 1 and 2 µm. The CAS-DPOL covers the size range of 0.6–50 µm in 17 bins of varying width. The

Deleted: -

probes are described in Voigt et al. (2017) and probes and data correction techniques in Weigel et al. (2016).

Information regarding the ice particle properties was obtained from the Particle Habit Imaging and Polar Scattering Probe (PHIPS-HALO), a single-particle cloud probe that measures microphysical and angular light scattering properties of individual particles (Abdelmonem et al., 2016). The instrument is composed of a stereoscopic imager that takes two brightfield images from the particles under a viewing angle difference of 120°. Simultaneously to collecting the images, the scattering component of the instrument measures the angular scattering function of the particles from 18° to 170° with an angular resolution of 8°. The optical resolution of the imager is about 2.5 µm.

Deleted: part

2.7. Aerosol mass spectrometer

For in-situ chemical analysis of submicrometer aerosol particles a compact time-of-flight aerosol mass spectrometer (C-ToF-AMS) (Drewnick et al., 2005; Schmale et al., 2010) was operated onboard HALO. The C-ToF-AMS was sampling from the HASI inlet for ambient aerosol measurements. The aerosol particles enter the instrument via a pressure-controlled inlet and are focused into a narrow beam by an aerodynamic lens. In the vacuum chamber, the particles are flash-vaporized and the resulting gas-phase molecules are ionized by electron impact. The ions are guided into the Time-of-Flight mass spectrometer, separated by their mass-to-charge ratio, and detected by a microchannel plate detector. The C-ToF-AMS was operated with a time resolution of 30 seconds, providing mass concentrations of particulate organics, nitrate, sulfate, chloride, and ammonium.

Deleted: through

2.8. Refractory black carbon

An eight-channel Single Particle Soot Photometer (SP2; Max Planck Institute for Chemistry) was used to detect and quantify refractory black carbon (rBC) particles using laser-induced incandescence (Stephens et al., 2003; Schwarz et al., 2006). The instrument measures the time-dependent scattering and incandescence signals produced by individual aerosol particles when crossing a Gaussian-shaped laser beam (Nd:YAG; $\lambda = 1064$ nm). The particles containing rBC cores absorb the laser light and evaporate within the optical chamber emitting thermal radiation

(incandescence). The peak intensity of the incandescence signal, recorded by two photomultiplier tubes over two different wavelength intervals, is linearly proportional to the mass of the rBC in the particle (Laborde et al., 2013). At the detector settings used, the instrument is sensitive to rBC cores in the nominal size range of 70–500 nm mass-equivalent diameter, assuming a density of 1.8 g cm^{-3}. The SP2 also detects the intensity of the light scattered by the particles using an avalanche photo-detector in order to determine the optical size of purely scattering particles in the diameter range of 200–400 nm.

The SP2 incandescence signal was calibrated several times (at the beginning, during, and at the end of the campaign) using size-selected fullerene soot particles. The scattering signal was calibrated using either spherical polystyrene latex size standards (208, 244, and 288 nm) or ammonium sulfate particles of different diameters selected by a differential mobility analyzer (DMA).

2.9. Trace gases

Ozone (O_3) was measured by a dual-cell ultraviolet (UV) absorption detector (TE49C, Thermo Scientific) operating at a wavelength of 254 nm. Signal differences from a cell with the sample air and a parallel cell with ozone-scrubbed air are used to infer the concentration of O_3. Sample air was drawn into the instruments through the standard HALO gas inlet via a Teflon PFA line using an external pump at a nominal flow rate of 1 l min^{-1}. The calibration of the instrument is traceable to the O_3 standard of the Global Atmosphere Watch station at Hohenpeißenberg, Germany. The data output of the instrument is corrected for the temperature and pressure in the absorption cells. The precision of the O_3 measurements is 2% or 1 ppb, whichever is larger, the accuracy is 5%. Details on the use of this instrument can be found in Huntrieser et al. (2016).

Carbon monoxide (CO) was detected with a fast-response fluorescence instrument (AL5002, Aerolaser, Garmisch, Germany) (Gerbig et al., 1999). The detection of CO is based on the excitation of CO at 150 nm using a CO_2 resonance UV lamp. The fluorescence light is detected by a UV-sensitive photomultiplier. The CO detector was calibrated in-flight using onboard calibration and zero gas sources. Data are recorded at 1 Hz. The precision and accuracy are 3 ppb and 5%, respectively.

Deleted: -
Deleted:
Deleted: -
Deleted:

Nitrogen monoxide (NO) and total reactive nitrogen (NO_y) were measured by a dual-channel chemiluminescence detector (CLD-SR, Eco Physics). For the NO_y channel, the chemiluminescence detector is combined with a custom-built Au converter which reduces all oxidized reactive nitrogen species to NO (Ziereis et al., 2000). Detection of ambient NO is performed via reaction with O_3 in a chamber and the luminescence signal of the excited NO_2 produced by this reaction. Both detector channels are equipped with a pre-reaction chamber for determination of cross-reactions of O_3 with interfering species. Sampling of ambient air is conducted via a standard HALO gas inlet using a Teflon line. The precision and accuracy of the measurements depend on the ambient concentrations, typical values are 5% and 7% (NO) and 10% and 15% (NO_y), respectively.

2.10. Trajectories and air mass history analysis

Backtrajectories were calculated for each minute, starting at the location of the HALO aircraft and using the FLEXPART ("FLEXible PARTicle") Lagrangian Particle Dispersion Model version 9.02 (Stohl et al., 1998; Stohl and Thomson, 1999; Seibert and Frank, 2004; Stohl et al., 2005). Trajectories were driven by six-hourly analyses, interlaced with the three-hour forecasts, from the Global Forecast System (GFS) of the National Centers for Environmental Prediction (NCEP), provided on a 0.5 x 0.5 degree horizontal grid (http://www.nco.ncep.noaa.gov/pmb/products/gfs/, last accessed 8 Sep 2016). For each trajectory, 10,000 'particles' (infinitesimally small air parcels) are released and followed back in time for 10 days. Sub-grid-scale processes like convection and turbulence act stochastically on each 'particle', resulting in a trajectory location probability distribution at each point in time. For convenience, the location probability distribution is simplified using a clustering algorithm, calculating five cluster centers of most probable trajectory locations (Stohl et al., 2002). Additional trajectory calculations were performed using the HYSPLIT model (Stein et al., 2015) with NCEP GDAS1 data and model vertical velocities. For simplicity, out of the five clusters, we consider only the center cluster given by FLEXPART. Therefore, all trajectories mentioned hereafter refer to the center trajectory.

We examined the history of the sampled airmasses for interactions with deep convection using the FLEXPART trajectories and GOES (Geostationary Operational Environmental Satellite) imagery. Every one-minute flight position was traced back in time in one-hour steps up to

120 hours. Each position was then matched in time to the closest GOES-13 (Geostationary Operational Environmental Satellite) infrared brightness temperature (T_b). As a proxy for deep convection, we searched for cloud top T_b below –30 ºC and looked up the minimum T_b in a 1ºx1º box around the center of the back-traced parcel. An example of this procedure is available in the Supplement (Figs. S1-S3). From these data, we recorded the time difference between the moment that HALO was sampling the airmass and its encounter with deep convection, possibly including multiple contacts with deep convection. We also noted the "deepest convection" (minimum T_b) encountered by the parcels and their height at the time of the encounter, as well as the number of hours that the parcel was within boxes with deep convection (T_b < –30 ºC).

3. Results and Discussion

3.1. The ACRIDICON–CHUVA campaign

The ACRIDICON–CHUVA flights covered most of the Amazon Basin, reaching from the Atlantic coastal waters in the east to near the Colombian border in the west, and from the Guyanas border in the north to the arc of deforestation in the south. The flight tracks of the flights analyzed in this paper are shown in Fig. 1, where the flight segments at altitudes >8 km are shown as heavier lines. The dates of the flights and other supporting information are given in the overview paper by Wendisch et al. (2016)

3.2. Synoptic situation and chemical context

3.2.1. Meteorological overview

During boreal summer, the Intertropical Convergence Zone (ITCZ) undergoes a seasonal northward shift towards the northernmost part of South America, so that almost all of the Amazon Basin is in the meteorological Southern Hemisphere. Examination of cloud top height and precipitation images showed that the ITCZ was located between about 4 and 12 °N during the campaign (6 Sep to 1 Oct 2014), but was often not very well defined over South America (worldview.earthdata.nasa.gov, last accessed 13 Jan 2017). This seasonal shift establishes the large-scale thermodynamic conditions that define the dry season over the Amazon Basin, characterized by synoptic-scale subsidence, a relatively dry planetary boundary layer (PBL) and mid-troposphere, and warm temperatures at the top of the PBL, resulting in elevated convective inhibition energy (CINE) (Fu et al., 1999; Wang and Fu, 2007; Collow et al., 2016). During the dry

Deleted: -

Deleted: -

Deleted: is

season, there is less shallow convection, cloud cover, and rainfall than in the wet season, but the convection that does occur is more organized with pronounced vertical development because of the simultaneous presence of high convective available potential energy (CAPE) and high CINE (Machado et al., 2004; Collow et al., 2016; Giangrande et al., 2017; Zhuang et al., 2017). The deep convective cloud fraction peaks in the late afternoon and evening (1600LT to 2400LT) with a cloud fraction maximum between 9 and 13 km altitude and a minimum near and above the freezing level between 4 and 7 km (Collow et al., 2016; Zhuang et al., 2017).

During the ACRIDICON–CHUVA campaign, the intense warm sea-surface temperature (SST) anomaly that had earlier prevailed in the southern South Atlantic and a less intense cold SST anomaly in the northern South Atlantic and near the Equator were strongly reduced, and a warm SST anomaly in the equatorial Pacific was building to form the 2015 El Nino (see also Martin et al., 2016). Consequently, the pattern of wind and omega (vertical motion) field anomalies decreased to nearly normal conditions. However, during the campaign there was a clear northeast-southwest contrast with drier conditions in the northeast and wetter ones in the southwest, as seen in the columnar precipitable water anomaly data from the NCEP Climate Forecast System Version 2 Reanalysis (Fig. 2) (Saha et al., accessed 20 March 2017). The majority of HALO flights were over the drier anomaly or the neutral region. As a consequence of this drier anomaly, these regions presented warmer temperatures and lower relative humidity than the normal climatology. The synoptic pattern during the campaign resulted in a spatial rainfall distribution with a meridional pattern, with more intense rainfall in the west, around 300 mm in September, and less than 100 mm in the eastern Amazon (Fig. 3). Nine cold fronts penetrated into Brazil during September, however, only two moved northward and they had little interaction with Amazon convection. Only the cold front on 20 to 23 September was able to organize convection in the south of the Amazon Basin.

Figures 4a and 4b show the low (850 hPa) and high (200 hPa) level wind fields during September 2014. The mean low-level flow at 850 hPa shows the typical easterly winds throughout the Amazon Basin (Fig. 4a), decelerating near the Andes and curving to the subtropics. At high levels (Fig. 4b), there is a weak anticyclonic circulation over the southern basin, featuring the initial increased deep convection in the transition from the dry to the wet season (September) and the development of the Bolivian High during the onset of the wet season (December to March) (Virji, 1981; Zhou and Lau, 1998).

Deleted: -

During the research flights, HALO reached maximum altitudes of 12.6 to 14.4 km a.s.l., corresponding to potential temperatures between 352 and 360 K (Fig. 5), i.e., the bottom of the tropical tropopause layer (TTL). The vertical profiles of temperature and potential temperature were remarkably consistent between the flights, showing a fairly stable stratification up to about 8 km and a slightly weaker gradient in potential temperature above this altitude. Relative humidity shows a broad minimum in the region between 6 and 10 km. For comparison, the data from radiosonde soundings at Manacapuru (a site southwest of Manaus) are provided in the supplement (Fig. S4).

Based on the soundings, the mean height of the thermal tropopause during the campaign was 16.9±0.6 km (unless mentioned otherwise, we use the notation "arithmetic average±standard deviation" to indicate mean and variance in this paper), corresponding to a potential temperature of about 380 K. During September 2014, the mean CAPE was 1536 J kg^{-1} and the mean CINE value was 37 J kg^{-1}, the precipitable water was 42 mm, the lifting condensation level 919 hPa, and the bulk shear 4.8 m s^{-1} (difference between the mean wind speed in the first 6 km and 500 meters). These values give a clear idea about the typical cloud base expected, the high instability, the need of a forcing due to the CINE, the high shear, and the amount of integrated water vapor.

In this paper, we use the following terminology to describe the different layers of the tropical atmosphere: The region from the surface to the convective cloud base (typically about 1.2 to 1.7 km during mid-day) is the planetary boundary layer (PBL), above which is the convective cloud layer (CCL), which typically reached to altitudes of about 4–5 km during our campaign. The region between the CCL and the TTL is the free troposphere (FT), which we subdivide into the middle troposphere (MT) between about 5 km and 9 km and the and the upper troposphere (UT) above ca. 9 km.

Deleted: -

3.2.2. Airmass origins and history

For an overview of airmass movement in the UT over the central Amazon during the campaign, we obtained trajectory frequency statistics for airmasses arriving at altitudes between 7 and 14 km over the central Amazon Basin. The frequency analysis indicated that airmass movement in the upper troposphere was generally relatively slow and tended to follow anticyclonic patterns (Fig. 6), consistent with the 200 hPa streamlines shown in Fig. 4b. The frequency diagram for the 72-h trajectories initialized at 12 km altitude (Fig. 6a) shows that most airmasses

Deleted: 10

had remained over the basin for the preceding three days (only about 1% of the endpoints fall outside of the basin), and therefore had a high probability of encountering deep convection outflow. The 10 and 14 km statistics show essentially the same patterns (Supplement Figs. S5–S6), as do the individual trajectories calculated from the aircraft positions along the flight tracks (not shown).

The 120-h trajectory statistics (Fig. 6b) and the examination of the individual trajectories along the flight tracks indicate that the air sampled in the UT had followed a number of different general flow patterns before being sampled by HALO: 1) flow from the Pacific with an anticyclonic loop of variable extent over the basin, ranging from almost zonal west-to-east flow (type A in Table 1) to a huge loop going as far south as Argentina and as far east as the Atlantic, and then returning to the basin (type B, the southernmost trajectories in Fig. 6b), 2) flow from the Atlantic, often almost zonal (type C), 3) internal circulation within the basin, usually along anticyclonic loops, but sometimes erratic (type D), and 4) flow from the Caribbean, often following an anticyclonic pattern (type E, the northernmost trajectories in Fig. 6b). These flow patterns are also evident in the streamlines shown in Fig. 4. Inflow from the Pacific is evident south of 10º S, which can merge with the dominant anticyclone centered at about 8º S, 62º W, whereas inflow from the Atlantic and Caribbean is important mostly north of the Equator. The flow pattern types of the UT airmasses that were enriched in aerosol particles are given in Table 1.

3.2.3. Atmospheric chemical environment

The atmospheric chemical environment over the Amazon Basin shows a pronounced seasonal variation (Talbot et al., 1988; Andreae et al., 1990b; Talbot et al., 1990; Andreae et al., 2002; Artaxo et al., 2002; Martin et al., 2010; Andreae et al., 2012; Artaxo et al., 2013; Andreae et al., 2015). During the rainy season, regional biomass burning is at a minimum and biological sources dominate trace gas and aerosol emissions in the basin, resulting in often near-pristine conditions. The most significant pollution input during this season is long-range transport from North and West Africa, which brings in a mixture of mineral dust and emissions from biomass and fossil fuel burning (Talbot et al., 1990; Wang et al., 2016b). In contrast, ACRIDICON–CHUVA took place during the dry season, when the Amazon Basin is impacted by a mixture of pollution from regional and remote sources (Andreae et al., 1988; Talbot et al., 1988; Artaxo et al., 2013). Deforestation and pasture-maintenance burning occurs throughout the basin, with the

Deleted: -

Deleted: s

Deleted: A and

Deleted: in Table 1

Deleted: s

Deleted: -

highest intensity along the southern periphery, the so called "arc of deforestation". This creates a steep gradient of pollutant concentrations from the relatively moist and less densely developed northern and western basin to the drier and highly deforested and developed southern basin (Andreae et al., 2012).

Long-range transport from Africa affects pollution levels over the Amazon, in addition to regional sources. In the northern part of the basin, part of the 10-day backtrajectories arriving at the aircraft positions in the lower troposphere come from West Africa, where biomass burning and fossil-fuel emissions are prevalent, while other trajectories follow the northeastern coast of Brazil, which is densely populated. As one moves south, the influence of long-range transport from Southern Africa becomes more prevalent. This was clearly observed during flight AC19, much of which took place over the Atlantic Ocean east of the Brazilian coast. On this flight, an extended, 300-m thick layer of pollution at 4 km altitude was identified over the Atlantic with elevated rBC concentrations up to 2 μg m^{-3} (see section 3.4.4). The backtrajectories from the Amazon south of the Equator very frequently end in the central and eastern tropical Atlantic (see Fig. 3 in Andreae et al., 2015), where high levels of ozone, aerosols, and other pollutants from biomass burning have been documented by in-situ and satellite observations, starting in the 1980s (Watson et al., 1990; Fishman et al., 1991; Andreae et al., 1994; Browell et al., 1996; Fishman et al., 1996).

Deleted: reach

Deleted: extended

3.3. Vertical distribution of aerosol particle number concentrations over the Amazon Basin

Figure 7a shows a statistical summary of all CN number concentrations (N_{CN}) observed during the campaign. Data affected by local pollution and cloud artifacts have been removed as discussed in section 2.2. (Additional information about the flight segments on which elevated N_{CN} were encountered is provided in Table 1, and average concentrations for the particle concentrations in the different size classes and altitude regions are given in Table 2.) In the PBL, which typically reached heights of 1.4 to 1.8 km during the afternoon, mean N_{CN} ranged from ~750 cm^{-3} on the least polluted flights to ~4500 cm^{-3} in the most polluted regions over the southern part of the basin. Above the PBL, CN concentrations typically remained relatively high within the lower troposphere up to about 3–4 km, and then declined with altitude. N_{CN} reached a minimum of ~700 cm^{-3} at about 4–5 km altitude everywhere over the basin. This aerosol minimum coincides with the minimum in cloud cover that has been observed at and above the freezing

Deleted: -

Deleted: -

Deleted: -

level, which has been suggested to be associated with rain development by the Wegener-Findeisen-Bergeron process at this level (Collow et al., 2016).

Above this level, we found a general increase in particle concentrations, such that above 8 km, N_{CN} were typically in the range of 2000 to 19,000 cm^{-3} (i.e., the range of quartiles above 8 km in Fig. 7a). On average, N_{CN} in the UT were almost five times as high as in the LT. The 8-km altitude level corresponds approximately to the 340 K potential temperature level, above which elevated CN concentrations had also been found in previous studies (Borrmann et al., 2010; Weigel et al., 2011).

While the statistical plot in Fig. 7a shows a general particle enrichment in the UT, individual vertical profiles show more complex structures (Fig. 7b). The highest N_{CN}, sometimes reaching up to 65,000 cm^{-3}, were encountered in thin layers often only a few hundreds of meters thick. A typical example for such a layer is seen in the descent profile (segment A2) from flight AC09 (Fig. 4b), with peak CN concentrations of ca. 35,000 cm^{-3}. Other profiles, e.g., the descent profile from flight AC07 (segment G), show enhancements over a layer about 3 km thick, with N_{CN} of 10,000 – 20,000 cm^{-3}.

The CN enrichments in the UT consist predominantly of ultrafine particles in the size range below 90 nm. In contrast to N_{CN}, the enhancement of accumulation mode particles (N_{acc}, defined here as the particles in the size range 90 to 600 nm) in the UT is much less pronounced. The concentration of accumulation mode particles in the LT typically ranged from ~500 to ~3000 cm^{-3}, depending on the level of pollution (Fig. 8a). Like the vertical profile of N_{CN}, the profile of N_{acc} also shows a decrease above the LT to a minimum around 4–5 km, followed by an increase towards the upper troposphere. Over the more polluted regions in the southern basin, N_{acc} in the UT was often considerably lower than in the LT. On average, N_{acc} in the UT was only about half the concentration measured in the LT.

Figure 8b illustrates the different behavior of CN and accumulation mode particle number concentrations at the example of a sounding in the central Amazon Basin from flight AC19. In the LT, N_{CN} and N_{acc} have similar values and decline to a minimum at about 4.7 km. Above this altitude, N_{CN} shows several sharp concentration peaks, with one at about 7.4 km reaching concentrations around 65,000 cm^{-3}. These peaks are only weakly, if at all, reflected in N_{acc}, which shows a broad enhancement in the UT to values around 1000 cm^{-3}. Consequently, we find two

Deleted: 0
Deleted: .
Deleted: is
Deleted: distinct
Deleted: -

types of aerosol enrichments in the UT: at one extreme, thin layers with extremely high N_{CN} values but no significant increase in particles larger than 90 nm, at the other, broad overall particle enrichments with modest values of both N_{CN} and N_{acc}.

3.4. Differences between UT and LT aerosols

The high concentrations of particles in the UT over the Amazon Basin beg the question of their origin. Three different mechanisms can be considered: vertical transport of particles from the PBL by deep convection, horizontal long-range transport from remote source regions, and in-situ new particle formation in the outflow from deep convection. To assess these possibilities, we discuss in the following sections the chemical and physical properties of the UT aerosols and contrast them with the LT aerosol. In section 3.4, we will compare the physical and chemical properties of the aerosols in the LT and UT to examine the role that vertical transport may have played as a source for the UT aerosol enrichments. Long-range transport and new particle formation in the UT will be discussed in section 3.5.

A first argument against vertical transport as the dominant source mechanism for the large particle concentrations in the UT comes simply from the observed CN concentrations. Since we are using concentrations normalized to standard temperature and pressure, N_{CN} should not change with vertical transport alone, and the values measured in the UT should not exceed those measured in the PBL. The fact that CN concentrations in the UT across the entire Amazon Basin are higher than the PBL values we measured anywhere in the basin, often by very large factors, rules out vertical transport of particles from the Amazon PBL as the dominant source of UT particles.

3.4.1. Particle size

The particles in the UT have a very different size distribution from those in the LT, which confirms that they could not have originated from upward transport of PBL aerosols by deep convection. Unfortunately, a detailed analysis of the size distribution of the particles in the UT is hampered by the significant losses of small particles in our inlet system. As discussed in section 2.2, the particle losses increase with altitude such that in the UT most of the particles below ca. 20 nm are lost in the inlet system before reaching the CPC. Because of a longer inlet tubing con-

Deleted: also shows

nection and lower sample flow, the losses were even more significant for the DMPS, and as a result of this and other operational limitations, valid particle size distributions are only available from the LT.

The DMPS measurements in the LT showed that the aerosol size distribution was dominated by an accumulation mode centered at about 190 nm, flanked by an Aitken mode with a maximum at about 80 nm (Fig. 9), in good agreement with the size distributions measured previously at ground level in the Amazon (Zhou et al., 2002; Rissler et al., 2006; Andreae et al., 2015; Pöhlker et al., 2016) and those obtained over the Amazon on the G1 aircraft during the GoAmazon 2014 campaign (Martin et al., 2016; Wang et al., 2016a). For comparison, we show size spectra from GoAmazon 2014 from Wang et al. (2016a), the only published size spectra from the FT over central Amazonia. Unfortunately, these data reach only up to 5.8 km, the ceiling altitude of the G1 aircraft. In the PBL, the spectra were similar to our measurements from the LT. With increasing altitude, total particle concentrations increased and the size spectrum became dominated by an Aitken mode at ca. 50 nm (Wang et al., 2016a). A previous study over the northern Amazon in Suriname had also found a decrease in the modal diameter of the Aitken mode from ~70 nm in the LT to ~ 30 nm in the UT above 10 km (Krejci et al., 2003). Assuming that similar size distributions prevailed in the UT during ACRIDICON–CHUVA, and given the fact that inlet losses limited our measurements to particle diameters >20–30 nm, it seems justified to conclude that our N_{CN} concentrations in the UT are actually lower limits and that the true concentrations might have been significantly higher.

In the absence of full size spectra, we use the ultrafine fraction [UFF, defined as the fraction of particles with diameters between 90 nm (the lower cutoff of the UHSAS) and ~20 nm (the lower cutoff of the CPC), i.e., UFF = $(N_{CN}-N_{acc})/N_{CN}$] as a metric for the contribution of the Aitken and nucleation modes to the total observed particle concentration. The summary profile plot (Fig. 10a) shows the dramatic difference between the UFF in the LT and UT: In the LT, the mean UFF is about 0.2±0.1, showing the dominance of the accumulation mode. The share of ultrafine particles increases throughout the middle troposphere, and in the UT they account for the vast majority of particles, with UFF values around 0.7 in regions where both N_{acc} and N_{CN} are moderately enriched, and values approaching 1.0 in the layers with very high N_{CN}. This shows up even more clearly in individual profiles, e.g., the soundings from flight AC18 shown in Fig 10b. The highly enriched layers are represented by UFF peaks in the range of 0.7 to 1.0, whereas

Deleted: even

Deleted: se

Deleted: -

Deleted: -

Deleted: 0.05 to

Deleted: in Fig 10b

the background UT enrichment exhibits UFF values of 0.5 to 0.8. The highest UFF values were measured in the very young aerosol layer in segment E2 at 13.5 km (Fig. 10b), which had an estimated particle age of about 1–5 hours (more on this layer in section 3.5.2).

3.4.2. Cloud nucleating properties

The cloud nucleating ability of aerosol particles depends both on their size and their chemical composition. Here we focus on CCN concentrations at 0.52% supersaturation ($N_{CCN0.5}$), which are dominated by the particles in the accumulation mode size range, but also include a fraction of the Aitken mode. A full discussion of the CCN measurements during ACRIDICON–CHUVA will be presented elsewhere.

Figure 11a shows the vertical distribution of CCN for the entire campaign, indicating strong variability in the LT, a minimum at ca. 5 km, and elevated concentrations in the UT. The $N_{CCN0.5}$ variability in the LT is related to the variable levels of regional pollution, mostly from biomass burning, which were much higher in the southern part of the basin than in the north. In contrast, there was no systematic difference between the CCN concentrations in the UT above polluted and relatively clean regions. Therefore, depending on the level of pollution in the lower troposphere, the $N_{CCN0.5}$ in the UT during our campaign were higher or lower than those in the LT. This is illustrated at the example of the $N_{CCN0.5}$ profiles from a clean region (AC09) and from one polluted by biomass burning emissions (AC12+13), respectively (Fig. 11b). While there was a large difference in the CCN concentrations in the LT, the values in the UT were very similar between these flights, indicating that the CCN enrichments in the UT are independent of the pollution levels in the LT.

The $N_{CCN0.5}$ in the UT were consistently greater than the corresponding accumulation particle number concentrations, N_{acc}, resulting in a median $N_{CCN0.5}/N_{acc}$ ratio of 1.66 (quartile range 1.32 – 2.32, N=53,382) above 8 km. This implies that some of the particles smaller than 90 nm are also able to nucleate cloud drops at S=0.52%. Because size-selective CCN measurements were not performed during ACRIDICON–CHUVA, it was not possible to derive the actual critical diameters and hygroscopicity factors (κ, Petters and Kreidenweis, 2007) for the CCN on this campaign. However, a consistency check can be made using the measured chemical composition. As will be discussed in detail in section 3.4.4, the UT particles consist predominantly of or-

Deleted: with
Deleted: -
Deleted: -
Deleted: (M. Pöhlker et al., 2017, in preparation)
Deleted: was
Deleted: was
Deleted: Flights AC09 and AC12+13, from
Deleted: CCN concentrations at a supersaturation S=0.52%
Deleted: values of
Deleted: -

ganic material, with minor amounts of nitrate and very small fractions of sulfate. The hygroscopicity of particles consisting completely of organic matter can vary greatly, with κ between near 0 and about 0.3 (Engelhart et al., 2008; Jimenez et al., 2009; Engelhart et al., 2011). Our AMS measurements (see section 3.4.4) showed that the UT secondary organic aerosol (SOA) contains a substantial fraction of organics derived from the oxidation of isoprene (IEPOX-SOA) (Schulz et al., 2017), which has relatively high hygroscopicity (κ≥0.12) (Engelhart et al., 2011; Thalman et al., 2017). Assuming a conservative value of $\kappa_{org} \cong 0.1$, which had been found previously for the Amazon PBL (Gunthe et al., 2009; Pöhlker et al., 2016), pure SOA particles would have to have diameters of ≥80 nm to act as CCN at 0.52% supersaturation, whereas for pure ammonium sulfate particles ($\kappa \cong 0.6$), the critical diameter would be ca. 45 nm (Petters and Kreidenweis, 2007). At a typical organic mass fraction of 0.8 for the UT aerosol (see section 3.4.4), an effective κ of ca. 0.2, corresponding to a critical diameter of ~65 nm, is likely. Given the expected steep increase in particle concentration between the N_{acc} cutoff of 90 nm and the estimated critical diameter of 65 nm, a $N_{CCN0.5}/N_{acc}$ ratio of the observed magnitude appears thus quite reasonable.

The vertical distribution of the CCN fraction, i.e., the ratio $N_{CCN0.5}/N_{CN}$, shows a pronounced decrease with altitude (Fig. 12a), reflecting the smaller particle size in the UT. It also exhibits a strong inverse relation to the total particle concentration, N_{CN}. This is illustrated at the example of flight AC18 (Fig. 12b), where data from the different flight segments are plotted. Segments A and F (yellow and orange) are from soundings in the somewhat more polluted central part of the Amazon Basin, whereas B and C (green) are from the cleaner westernmost part and show the lowest CCN concentrations and the highest CCN fractions. Both soundings have high-CN layers at altitudes between 7 and 13 km, with N_{CN} up to almost 23,000 cm^{-3}, and correspondingly low $N_{CCN0.5}/N_{CN}$. Segment E2 (red) is from a layer that was intercepted downwind of a massive convective complex, with a transport time of only 1–5 hours between the anvil and the aircraft (see section 3.5.2). This layer had N_{CN} values up to 45,000 cm^{-3}, CCN fractions down to 0.01, and UFF ≅ 0.98, suggesting that these recently formed particles were too small to act as CCN. This layer was embedded in a region of moderately elevated CN (segment E1 at 13–14 km; lilac), which had much higher $N_{CCN0.5}/N_{CN}$ (0.2–0.5) and lower UFF (0.6–0.8), indicating larger particle sizes and likely a more aged aerosol. Segment D (blue), at 11–12 km altitude, had

Deleted: the

Deleted: while

Deleted: -

Deleted: -

Deleted: -

Deleted: -

Deleted: -

similar properties to E1. These observations confirm the presence of the two distinct types of elevated aerosol populations in the UT, introduced in section 3.3. At one extreme, there are aerosols with very high N_{CN} and ultrafine fractions and low CCN fractions (e.g., E2), presumably representing newly formed particles with sizes too small to act as CCN. At the other extreme, there are populations with modest N_{CN}, but low UFF and high CCN fractions, indicating a more aged aerosol with larger particles (e.g., E1 and D).

The existence of these two populations is confirmed in plots of $N_{CCN0.5}$ and $N_{CCN0.5}/N_{CN}$ against supersaturation. Examples are shown in Figs. 13a and 13b, with AC18-DD representing a segment dominated by larger and aged particles, AC07-F a region with high concentrations of small and younger particles, and AC09-AA a mixed case with short periods of very high N_{CN} over a background of moderately elevated particle concentrations. Even though the mean CN concentration exceeds 8900 cm^{-3} in AC07-F, the mean $N_{CCN0.5}$ in the same region is only 13 cm^{-3} and therefore the $N_{CCN0.5}/N_{CN}$ vs. S plot falls essentially on the baseline. In contrast, AC18-DD presents a fairly "classical" supersaturation spectrum, and AC09-AA is a mixed case with the measurements made during the N_{CN} peaks showing very low $N_{CCN0.5}/N_{CN}$.

In Figs. 13c and 13d, we compare the mean supersaturation spectra from the lower, middle, and upper troposphere obtained on flights AC12 and AC13, which were taken on successive days over the same region and where the LT was influenced by biomass burning pollution. In the LT, the CCN fraction is in the range observed at ground level at the Amazon Tall Tower Observatory (ATTO) site (Pöhlker et al., 2016) and in close agreement with measurements in the southern Amazon during the biomass burning season (Vestin et al., 2007). In the UT, we observed low CCN fractions representing the regions with high N_{CN} and UFF, mostly at altitudes of 10–11 km, and higher CCN fractions at 12 km and above corresponding to a region with somewhat elevated CCN (1000–1500 cm^{-3}; cf. Fig. 11b, which shows the CCN concentrations from these flights). In the middle troposphere (5–8 km) we found intermediate CCN fractions, consistent with a mixture of LT and UT aerosols.

3.4.3. Volatility

On several flights (AC16, 18, 19, and 20), a second CPC was operated behind a thermodenuder at a temperature of 250 °C, in parallel to the regular CPC, providing the concentration of non-volatile particles, N_{nonvol}. The results of these measurements are shown in Fig. 14a in

Deleted: point
Deleted: to
Deleted: high
Deleted: -
Deleted: -
Formatted: Subscript

the form of the volatile fraction (VF=[N_{CN} - N_{nonvol}]/N_{CN}) plotted against altitude. In the LT, most particles are nonvolatile and the VF is typically between 10 and 20%. This is consistent with the behavior described by Clarke and Kapustin (2010) and Thornberry et al. (2010), who found that aged combustion aerosols (from biomass or fossil-fuel burning) are non-volatile and mostly in the accumulation mode size fraction. With increasing altitude, the VF increases, closely resembling the profile of the UFF. In the UT, the mean VF reaches about 80%, and approaches 100% in the most highly enriched layers (e.g., segment E2). In previous campaigns, high volatile fractions had also been observed in the tropical UT and TTL, with the highest VF in the region between 340 and 360 K potential temperature, corresponding to about 9–15 km (Borrmann et al., 2010; Weigel et al., 2011).

More detail can be seen when looking at data from an individual flight. In Fig. 14b we show the profiles from AC18, which we had already discussed in the context of CCN concentrations in the previous section. The profiles (segments A, B, C, and F) show the overall increase in VF with height, with peak values at embedded high-CN layers. The freshest layer (E2), which had the highest UFF, also has the highest VF. In contrast, segments D and E1, representing larger UT regions with moderate CN enrichments, larger particles, and higher CCN fraction also have lower VFs, between 0.4 and 0.7. A contribution from aged combustion aerosols can be ruled out as source for the non-volatile particles in these layers, because the rBC concentrations are close to zero (see below). As we will show in the next section, it appears that these low-volatility particles represent a more aged organic aerosol.

3.4.4. Chemical composition

As discussed above, the LT aerosol over the Amazon during the dry season is dominated by the products of biomass burning, with increasing concentrations from north to south. This is clearly reflected in its chemical composition, which is dominated by carbonaceous matter (organic and elemental carbon) and only contains minor fractions of inorganic species, such as potassium, sulfate, and nitrate. Elemental or black carbon is a unique tracer of combustion emissions and was measured on HALO in the form of refractory black carbon (rBC).

The vertical profile of rBC shows a sharp separation between LT and FT (Fig. 15). The average rBC concentration in the region below 5 km was 0.25±0.21 µg m^{-3}, whereas in the FT above 6 km it was 0.002±0.006 µg m^{-3} in terms of mass concentrations, and 99±92 cm^{-3} vs.

Deleted:), i.e.,
Deleted: (
Deleted:)
Deleted: ,
Deleted: f
Deleted: -
Deleted: 31
Deleted: 9
Deleted: 6
Deleted: 9

1.5±2.5 cm^{-3} in number concentrations of rBC particles. Interestingly, these concentrations over the Amazon Basin are only slightly higher than the values measured over the tropical Western Atlantic during the Saharan Aerosol Long-range Transport and Aerosol-Cloud-Interaction Experiment (SALTRACE; Weinzierl et al., 2017), June–July 2013: ca. 0.2 μg m^{-3} in the LT and ca. 0.001 μg m^{-3} in the FT (Schwarz et al., 2017), which suggests that a significant fraction of the rBC is entering the basin by long-range transport from Africa. Transport of biomass smoke containing BC and other constituents from Africa to South America has been documented previously, e.g., from Northern Africa during the wet season (Talbot et al., 1990; Wang et al., 2016b) and from Southern Africa during the dry season (Andreae et al., 1994). A detailed study on the transport of Southern African aerosols to the Amazon during ACRIDICON-CHUVA is in preparation and will be published elsewhere.

In 14 instances, elevated rBC concentrations were seen for short durations (usually less than 30 sec) in the UT. Most of the time, they occurred during cloud penetrations in the course of vertical cloud microphysics profiling. In the case of the flights over the northern half of the Amazon Basin, they could likely be attributed to sampling of HALO's own exhaust, based on the flight track and the presence of associated NO enhancements in the absence of strong enhancements of CO and other aerosol species (CCN, N_{acc}, N_{CN}). On flights over the southern Amazon (AC07, AC12, AC13, and AC20), where the PBL was more polluted and active fires were present, there were a few instances when elevated rBC coincided with peaks in CO and accumulation mode particles, which suggests upward transport of biomass smoke aerosols. In view of the scarcity of such events during our campaign and their modest rBC concentrations, it is clear that they do not represent a major source of combustion aerosol for the UT during our campaign. No elevated rBC concentrations were observed during the extensive outflow sampling legs on any of the flights. A detailed discussion of the rBC measurements during the campaign will be presented in a companion paper (Holanda et al., 2017).

The drop in rBC concentration by two orders of magnitude between LT and FT implies that rBC, and by extension other aerosols (which are likely even more prone to being removed by nucleation scavenging), are efficiently removed during deep convection and consequently that there is little transport of LT aerosols into the FT. This provides further evidence that enrichments in N_{CN} and N_{acc} in the FT cannot be explained by vertical transport of particles from the FT.

Deleted: (SALTRACE)

Deleted: /

Deleted: Consequently,

The AMS measurements also show pronounced differences in the composition of the LT and UT aerosols (Fig. 16). In Table 2 we present a detailed analysis of the results from three flights, AC07 from a polluted region in the southern Amazon, and AC09 and AC18 from relatively clean regions in the northern and northwestern parts of the Basin, respectively. Organic aerosol (OA) is the dominant aerosol species in all three regions at all altitudes, as expected in an area where biomass burning and secondary organic aerosol (SOA) production are the dominant sources.

In the LT, (ammonium) sulfates (SO4) are together with rBC the next most important species. Here, we see a clear difference between the BB-dominated region in the south (with high OA, ammonium [NH4], and rBC, and relatively low SO4) versus the northern basin, where SO4, likely from long-range transport, plays a more important role. The ratio OA/rBC in the LT is in the range 3–11, consistent with values from BB aerosols. The biomass burning marker, f_{60} (Schneider et al., 2006; Alfarra et al., 2007), is present in all the measurements from the LT, but always mixed with oxidized secondary organics. It should also be noted that the f_{60} marker is not an inert tracer but decays with time, and a typical observed background level of the f_{60} tracer is 0.3% of OA (Cubison et al., 2011).

Deleted: -

Deleted: n

In the UT, SO4 shows lower concentrations than in the LT, with the most pronounced difference on flights AC07 and AC18. The latter flights also show a large difference in the OA/SO4 ratio, which is around 10 in the UT and around 2 in the LT. Because of the high BB component in flight AC07, this ratio is also relatively high in the LT on this flight. The most pronounced differences between UT and LT are seen in the nitrogen species. Ammonium is usually present in the BL, sometimes at considerable levels (e.g., on AC07), but always below the detection limit in the UT. In contrast, nitrate (NO3) is a minor species in the LT, whereas in the UT it is comparable or greater than SO4, so that the ratio NO3/SO4 is about an order of magnitude higher in the UT than in the LT. High concentrations of organics, especially oxidized organics, and nitrate had been seen previously in the UT by Froyd et al. (2009).

The nature of the nitrate signal in the UT cannot be definitely identified from our data. The absence of NH4 and the ratio of the peaks associated with ammonium nitrate make it unlikely that the NO3 signal represents ammonium nitrate (Fry et al., 2009; Bruns et al., 2010). It may be, at least to a large part, indicative of organonitrates, which have been shown to account

for 15–40% of SOA mass in laboratory experiments (Berkemeier et al., 2016) and whose formation is enhanced at low temperatures (Lee et al., 2014).

A closer look at the aerosol-enriched layers in the UT from these flights reinforces these conclusions (Table 2). In these layers, the ratios OA/SO4 and NO3/SO4 can reach very high values, especially in the SO4-poor UT of flight AC07. On flights AC09 and AC18, we encountered extended periods when N_{acc} and $N_{CCN0.5}$ were elevated, while N_{CN} did not show extremely high values (AC09-AA, AC18-AA, and AC18-DD). The AMS data from these segments were generally similar to the UT averages, suggesting that they are representative of the ambient UT aerosols. The layers with very high N_{CN} on these flights (AC09-BB, AC09-EE, AC09-A1+A2, and AC18-A1, AC18-A2, AC18-E2, AC18-F) also did not show significant differences from the UT means on these flights, likely because the numerous, but very small CN in these layers did not contain enough mass to influence the AMS measurements in a detectable way.

We attempted to examine this hypothesis further by investigating the size dependence of the AMS signals, but because of the small aerosol mass concentrations in the UT, size information from the AMS data required extended integration periods, which precluded obtaining size data from the relatively short segments with very high N_{CN}. The most robust size data were from the segments where relative high N_{acc} concentrations prevailed over extended periods of time, e.g., segment DD (Table 2) on flight AC18. Here, the organic aerosol (OA) showed a broad mode between 80 and 250 nm, with a modal diameter at 150 nm. This confirms that the AMS compositional data are dominated by the accumulation mode, while the particles that make up most of the UF fraction in the UT do not have enough mass to provide a clear AMS signal. An exception may be some segments on AC09 (BB and EE), where OA and NO3 data suggest a mass mode between 60 and 120 nm. Here, the UFF is quite high (0.85 and 0.92, compared to segment DD on flight AC18, where it was 0.61) suggesting a smaller and therefore younger aerosol population.

More detailed information on the origin of the organics in the UT aerosol can be obtained from specific markers. In the UT, the BB marker f_{60} is typically not detectable, which in combination with the fact that the ratio OA/rBC is of the order of 1000, precludes a significant contribution of aerosols from biomass burning or other primary combustion aerosols to the OA in the UT. In contrast, the marker f_{82}, which is indicative of IEPOX-SOA formed by the photooxidation

Deleted: -

of isoprene (Robinson et al., 2011; Hu et al., 2015), is found in the aerosol-enriched layers in the UT, suggesting oxidation of isoprene and other biogenic volatile organic compounds (BVOC) as source of the OA. The f_{82} marker is not correlated with sulfate, which suggests that sulfate may not have been participating in the formation of the IEPOX-SOA. Furthermore, in all cases with high f_{82}, the aerosol is not neutralized by NH_4^+. These issues will be discussed in detail in a forthcoming paper by Schulz et al. (2017)

The plot f_{43} vs. f_{44} is frequently used to represent the aging of organic aerosols (Ng et al., 2011). In Fig. 17, we show the median locations of the LT and UT aerosol in this plot, which indicates that both are fairly well aged and oxidized, with the UT data plotting slightly towards less oxidized and younger values. This may reflect an overall younger aerosol, or the admixture of recent material either by condensation on the accumulation mode particles or in the form of an external mixture of larger aged particles with small younger ones. The individual segments from flight AC18, which had the lowest OA/SO4 and NO3/SO4 ratios, also plot in this region, showing that they are dominated by a relatively well-aged aerosol. In contrast, segments AC09-AA, and AC07-AA1, AC07-AA2, and AC07-GG, which have the highest OA/SO4 and NO3/SO4 ratios and much higher N_{CN}, plot much further to the lower right indicating a less oxidized, fresher aerosol. On this flight, the concentrations of accumulation mode aerosols in the UT were relatively low, so that freshly formed aerosol could be more evident because of a lower background of aged aerosol.

Deleted: –

In summary, the chemical composition data show that, while both LT and UT aerosols are dominated by aged organics, their sources must be different because the UT aerosol is essentially devoid of the combustion tracers, rBC and f_{60}, whereas the OA/rBC ratios in the LT are consistent with combustion aerosols. Nitrate is strongly elevated in the UT, and may consist to a large extent of organonitrates. NH4 is a significant component in the LT, whereas it is below the detection limit in the UT. Size-selective chemical analysis is difficult because of the low aerosol mass concentrations, but the available data suggest that the AMS measurements are dominated by the accumulation mode, and the strong N_{CN} enhancements are not distinctly seen in the AMS data. Chemical marker analysis shows the general absence of BB tracers in the UT, while the marker f_{82} indicates production of IEPOX-SOA from isoprene. Most of the UT organics are aged

and oxidized, but in some of the CN-enriched layers, younger and less oxidized OA was evidenced by much lower f_{44}/f_{43} ratios. A detailed discussion of the AMS measurements during ACRIDICON–CHUVA will be presented in Schulz et al. (2017).

3.5. The roles of long-range transport and deep convection

In the preceding sections, we have documented the differences between the aerosols in the LT and the UT, which rule out the possibility that convective transport of PBL aerosols can be an important source for the UT aerosols. This opens the question about the other potential sources of these particles: are they the result of long-range transport from remote sources or do they originate over the Amazon Basin? In the latter case, are they directly released in the outflow from the convective clouds or are they produced by subsequent nucleation and growth in the UT?

For the larger particles in the accumulation mode, represented by elevated N_{acc} and $N_{CCN0.5}$ in the UT, long-range transport cannot be excluded, because such particles can have long lifetimes in the upper troposphere (Williams et al., 2002). While the absence of detectable rBC still rules out an origin from pollution aerosols lofted from the LT, they may have formed days or weeks ago by gas-to-particle formation mechanisms anywhere in the free troposphere. In contrast, the high concentrations of small UF particles that we observed with high frequency in the UT cannot come from distant sources, as they persist only for hours to a few days before growing to larger sizes and decreasing in concentration due to coagulation and dilution processes (Williams et al., 2002; Krejci et al., 2003; Ekman et al., 2006).

3.5.1. Aerosols in cloud tops, anvils and outflows

First, we consider the possibility of these particles having been produced already inside the clouds and released by outflow into the UT. In earlier studies, NPF had been shown to occur in ice clouds in the tropical/subtropical UT, especially in conditions where the available surface area of ice particles was relatively low (e.g., Lee et al., 2004; Frey et al., 2011). To look for this phenomenon, we examined the particle concentrations during passages through the upper levels of deep convective clouds and in the anvils directly attached to active cumulonimbus clouds (Cb). Our measurements during these passages consistently show lower CN and CCN concentra-

Deleted: -

Deleted: Relationship to

Deleted: D

Deleted: C

Deleted: the

tions than in the surrounding UT air, as exemplified in Fig. 18a by data from flight AC18. During this flight segment, we performed multiple penetrations of the tops of growing Cb at altitudes between 10.7 and 12.0 km and temperatures in the range of 225 to 236 K. During each cloud passage (indicated in Fig. 18a by the ice particle concentrations) the aerosol concentrations decreased sharply, to values of N_{CN} around 800 cm^{-3} and $N_{CCN0.5}$ around 250 cm^{-3} during the longer cloud passages. (Here, we use $N_{CCN0.5}$ as proxy for the accumulation mode particles, since the N_{acc} measurements in clouds were perturbed by shattering at the probe tip, whereas the N_{CN} and $N_{CCN0.5}$ measurements showed no artifacts in ice clouds.) In the case of N_{CN}, the values in the cloud tops are about the same as the PBL concentrations measured in the same region, while for $N_{CCN0.5}$ they are significantly lower than the PBL values of around 400 cm^{-3}.

The same behavior was found for all cloud penetrations in the UT during the campaign. In particular, extensive cloud top and outflow sampling on AC09, AC15, and AC16 showed $N_{CCN0.5}$ values down to 160–250 cm^{-3} and N_{CN} values down to 600–1000 cm^{-3}. The lowest particle concentrations were seen in a large outflow sampled on AC13 (20:08–20:30 UTC), when both N_{CN} and $N_{CCN0.5}$ reached values below 50 cm^{-3} (Fig. 18b). In this airmass, NO and NO_y were strongly elevated indicating recent NO production by lightning in the large Cb from which this outflow originated.

Given that the air sampled during the cloud passages had already mixed in by lateral entrainment some of the surrounding air with much higher particle concentrations (Bertram et al., 2007; Yang et al., 2015), these low particle concentrations in the cloud tops and outflows are clear evidence that in-cloud processes were a sink and not a source of particles in the size class measureable with our instrumentation. A rough estimate of the scavenging efficiency of the convective process can be gained by using CO as a conservative tracer. For example, on flight AC18 the PBL concentrations of CO and N_{CN} averaged ~120 ppb and 780 cm^{-3}, and the UT during the cloud penetrations around 1900 UTC had CO ~95 ppb and N_{CN} ~1500 cm^{-3}. In the cloud, CO rose to 108 ppb and N_{CN} dropped to 750 cm^{-3}. Following the approach of Bertram et al. (2007), we can estimate that the fraction of PBL air in the center of the cloud was ca. 0.52, and that without scavenging, $N_{CCN0.5}$ would be ca. 1130 cm^{-3}. From these values, a scavenging loss of 90% or more of CCN can be estimated, in good agreement with previous studies (e.g., Andreae et al., 2001; Yang et al., 2015), and consistent with the absence of detectable rBC.

Deleted: also

Deleted: -

Deleted: -

Deleted: -

Flight AC20 was the only exception to this behavior. Here, CN were strongly enhanced during cloud passages and even CCN were slightly elevated in some passages. The cloud that was sampled on this flight appears to have been a pyrocumulus that had been ingesting fresh biomass smoke, as suggested by the strongly elevated CO during the cloud passages. This flight will be discussed as a separate case study below (section 3.6.).

While these results show that the high particle concentrations we observed in the UT were not directly released from the cloud tops, they do not rule out the possibility that new particle formation had already started in the clouds or anvils. This is because the newly formed particles observed in the earlier studies were almost exclusively in the size range below 20 nm (Lee et al., 2004; Frey et al., 2011). Since our measurements are limited to particle sizes >20 nm, we would not have been able to detect such freshly nucleated particles, and therefore the earliest phases of particle nucleation and NPF over Amazonia will have to be addressed in future studies. Our data do show, however, that release of particles by hydrometeor evaporation following deep convection is not a net source of particles to the UT over Amazonia, in contrast to what was observed over the Indian Ocean region by Engström et al. (2008). Because the N_{CN} and $N_{CCN0.5}$ concentrations in the ambient air in the UT are actually higher than in the air detrained by the Cb clouds, the detrainment leads at least initially to a reduction in UT particle concentrations in the size class >20 nm. Only through subsequent NPF can this be reversed and deep convection then become a net source of UT aerosols.

3.5.2. Relationship between aerosol enhancements and airmass history

Connections between the presence of aerosol enhancements and the outflow from convective systems had been observed in some previous studies (de Reus et al., 2001; Twohy et al., 2002; Benson et al., 2008; Weigelt et al., 2009). We examined the connection between deep convection (DC) and the presence of high CN concentrations by a combination of backtrajectory calculations and the analysis of cloud-top temperatures from GOES-13 weather satellite images, similar to the approach used in some previous studies (de Reus et al., 2001; Froyd et al., 2009; Weigelt et al., 2009). We analyzed backtrajectories initialized at the aircraft locations where we had observed elevated aerosol concentrations, as listed in Table 1. Then we checked for each hour along the backtrajectories whether the airmass had crossed a region with DC (cloud top

temperatures below -30 ºC). The results show that in all cases, the aerosol enriched airmasses had encountered deep convection within the last 120 hours.

In Fig. 19 we present the results from two flights (AC09 and AC18) as examples. We find that for all flight segments that showed high aerosol concentrations in the UT (dark shading), the airmasses had made contact with DC with cloud tops typically reaching about -80 ºC. Of course, given the abundance of convection over Amazonia, it is to be expected that most airmasses would have interacted with convection within 120 hours (such as the example shown in the Supplement Fig. S2). For comparison, over the northeastern United States during summertime, Bertram et al. (2007) had found that more than 50% of UT air had encountered DC within the previous 2 days.

The cumulative plot of the time since the most recent DC contact (Fig. 20a) shows that on all flights (except AC19, the flight over the Atlantic) almost all aerosol-enhanced air masses had seen DC within the last 30–40 hours. The cloud tops during these encounters typically reached -70 to -80 ºC (Fig. 20b). In many cases, the airmass history analysis shows multiple contacts with deep convection within the preceding 72 hours. It must be noted, however, that the physical interaction between an UT airmass and a specific deep convective event is not represented in the trajectory model. Because the model does not "see" the individual convective event that brings up an outflow, it cannot trace a parcel back into this outflow and back down to the boundary layer. On the other hand, an air parcel trajectory that passed through the vicinity of the outflow, but is not part of the actual outflow, will keep moving backward along the mean flow in the UT and may then encounter another outflow. Obviously, however, the uncertainty in the trajectory position increases with time going backwards, and is probably enhanced by passage near a region of active convection.

In some cases, the airmasses could be tracked back to regions where the cold cloud encountered by the tracked airmass looked more like cirrus than identifiable deep convective outflow. The same favorable conditions for nucleation (low temperature, low pre-existing aerosol surface) as in the outflow regions prevail also in native cirrus, and Lee et al. (2004) had reported NPF in cirrus without immediate connection to DC. This might also have occurred in our campaign, but it is usually difficult to distinguish cirrus and very aged outflow.

Deleted: almost

Deleted: -

Deleted: -

Deleted: and that the trajectory history preceding the most recent such encounter becomes much more uncertain.

To test whether there was a difference in the airmass histories between segments with high and low N_{CN}, we searched our data for suitable segments with low N_{CN}. However, because of the high variability of the CN concentrations in the UT, the times when N_{CN} was below 3000 cm^{-3} were in almost all cases very short, and would not lend themselves to a meaningful analysis of airmass history. To illustrate this, we show a full time series plot of the measurements from Flight AC09 in the supplement (Fig. S7).

We were only able to find a total of six segments, where N_{CN} was consistently below 3000 cm^{-3}, and which were not identifiably part of an outflow. These are listed in Table S1 in the supplement. The segments from flights AC16 and AC18 were well away from clouds, whereas those from AC19 and 20 were in the vicinity of Cbs, but not clearly in an outflow. The segment L from AC19 is low in CN, but actually has a relatively high $N_{CCN0.5}$, and may not really be significantly different from the aged enriched segment E2, which was sampled immediately after it. Consequently, we don't have a data set that would allow a representative analysis of the history of airmasses with low particle concentrations. Notably, however, the airmass trajectory types in these segments do not contain type D, i.e., recirculation within the Amazon basin. The air in the segments from AC20, which had the lowest particle concentrations, had come in straight from the Pacific within the last 48 hours, but may also contain some outflow air.

Information about the time required for particle production and the evolution of the aerosol populations in the UT can be derived from a close examination of the trajectories for individual flight segments. Flight AC18 provides some illustrative examples. The trajectories of the first particle plumes encountered (A1 and A2, Table 1) had passed close to areas of intense deep convection (-30 to -60 ºC) about 17–21 hours before sampling. Because it is likely that the aerosol precursor substances are formed by photochemical reactions, we also looked at the amount of time that the airmass was exposed to sunlight (Lee et al., 2003). Since the convective encounters occurred between 16LT and 00LT and the measurements were taken at about 11LT, the airmass had only about 5–7 h of sun exposure. Assuming that the formation of the particles required photochemical processes, this implies that about 5–7 h were sufficient to produce particle concentrations above 20,000 cm^{-3} with sizes >20 nm. The enrichment in this case occurred only in the particles size range <90 nm, with a UFF of about 0.98, while N_{acc} remained at the same levels as in the surrounding background FT. Segment F, near the end of the flight, was sampling a similar region as A1, with a similar airmass trajectory. Since this segment was taken near the end of the

Deleted: ¶
More specific i

Deleted: -

Deleted: -

Deleted: -

Deleted: occured

Deleted: s

day, the airmass had experienced about 11 hours of sunlight. There is somewhat of a shift towards larger particles, but this might also be coincidental.

The air in segments B and C had traveled along similar trajectories as A1 and A2, but unfortunately there are no GOES images available for the time when they crossed the convective region encountered by A1 and A2, and so no conclusions can be drawn for these segments. Segments D and E1 represent airmasses that had made multiple and extended convection encounters over the central and western Amazon during the past three days. Here, we find only weak enhancements in N_{CN}, but significantly elevated $N_{CCN0.5}$ and N_{acc}, with a UFF of 0.73 and 0.82, respectively, suggesting that coagulation and growth had taken place over this time period.

Some of the highest N_{CN} (up to ca. 45,000 cm^{-3}) and UFF (0.98) were found in Segment AC18-E2, which was sampling the air just a few hours downwind of a massive convective system that reached well above our flight altitude of almost 14 km. The air sampled here had traveled for about one hour after leaving the convective complex before being encountered by HALO and had been interacting with this complex for up to 5 h, all of them in daylight. As in A1, A2, and F, there was no detectable enhancement in aerosol mass, as represented by N_{acc} and $N_{CCN0.5}$. In contrast to this very fresh aerosol with high number concentrations, the strongest enhancement in aerosol mass was seen in the early part of segment E1, which didn't show a strong increase in number concentration. The air during this segment had made its last contact with a convective system about 65–72 hours before sampling.

Another illustrative case is flight AC09 over a clean region in the northern Amazon. Segments A1-A3 sampled clear air that had DC contact about 16 and 60 hours ago and the UFF around 0.94 indicated a moderately aged aerosol. Segments B1 and B2 were taken in air immediately surrounding a Cb anvil, with previous DC contacts at about 14, 80, and 120 hours before. Here, the relatively low UFF of ~0.92 signaled no influence from the freshly outflowing air. Segments C, D, and E were in air close to a Cb, within its anvil, and in a large anvil/outflow, respectively. Otherwise, they had a DC contact history similar to B. Here also, the UFF remains fairly low, and there is no evidence of particle production directly in the anvil/outflow.

To summarize, our observations indicate that, while there is no evidence of immediate production of detectable particles (i.e., >20 nm) in the actual anvil or outflow, a small number of daylight hours are sufficient to produce very large concentrations of particles with sizes larger

Deleted: 3

Deleted: T

Deleted: , on the other hand,

Deleted: -

than about 20 nm in the FT. This is consistent with the observations made in the outflow of a convective complex off Darwin, Australia, where maximum Aitken concentrations were reported after ca. 3 hours since the outflow (Waddicor et al., 2012). During NPF events in the FT on the Jungfraujoch, high concentrations of particles >20 nm were observed about 4–6 hours after sunrise (Bianchi et al., 2016). In the FT over other regions, growth may be considerably slower; for example the measurements over oceanic regions by Weigelt et al. (2009) showed that it took about 12 hours for particles >12 nm to reach their maximum concentrations.

Deleted: -

Considerably longer times (a few days) are required, however, before increases are detectable in the size class >90 nm. The development of significant amounts of particles in the accumulation mode appears to take two days or more, in agreement with the observations of Froyd et al. (2009), who had found enhanced aerosol organic mass concentrations over the Caribbean in UT air originating from Amazonia after 2–4 days in the atmosphere. Since many, if not most of our trajectories remain over Amazonia for this amount of time, there is enough time available in the UT over the Amazon Basin to produce CCN-sized aerosols within the region, which can subsequently be transported downward or be exported to other regions.

Deleted: -

3.5.3. Aerosol enhancements and chemical tracers

The relationship between new particle production and the input of boundary layer air is also reflected in a correlation between N_{CN} and CO. When taking all data above 8 km, this correlation is highly significant given the large number of data points (N=68,360) but not very close (r^2=0.52) because of the large variability of CO concentrations in the PBL and UT background between flights (Fig. 21). Closer relationships are obtained when looking at individual flights and especially at individual profiles within flights.

Weigel et al. (2011) had seen a strong correlation between CO and nucleation mode particles over West Africa and interpreted it as indication of anthropogenic inputs. In contrast, over Amazonia we have not seen any evidence that UT aerosol production shows any relationship to boundary layer pollution, and we interpret the correlation between N_{CN} and CO simply as reflecting the input of air from the PBL, which generally has higher CO concentrations that the UT, by the cloud outflow.

An opposite relationship is generally seen between N_{CN} and O_3, which tends to be lower in the particle-enriched layer. We also see this as an indication of injection of air from the PBL,

which generally has lower O_3 concentrations than the UT. Because of the great variability in the O_3 concentrations in the UT, there is no general correlation between N_{CN} and O_3 for the entire mission (r^2=0.02). For individual flights, modest, but statistically significant, negative correlations can be found, e.g., an r^2 value of 0.13 (N=8509) in the UT on flight AC09. The scatter plot in Fig. S08 shows that high O_3 concentrations were always associated with low N_{CN}, but that there were low-O_3 regions in the UT both with and without enhanced particle concentrations.

To look for a possible relationship between water vapor concentration and NPF, we examined several flights (AC07, AC09, AC13, and AC18) for relationships between RH and N_{CN}. We found a tendency for the layers with high N_{CN} to be associated with moister layers (RH>50%), but also many exceptions. This relationship may simply have to do with the fact that moisture was brought up with the convective clouds, or there may be a relationship with the actual particle formation process, but at this point we do not have the data needed to answer these questions.

The nitrogen oxides show a complex relationship with the particle enhancements in the UT, as illustrated at the example of a flight segment from AC07 (Fig. 22). The highest NO concentrations are found in the Cb anvils or freshest outflows, as identified by significant concentrations of ice particles (e.g., at 2056, 2119, and 2154 UTC). In these regions, we typically observed particle minima, as discussed above. In these airmasses, NO has been formed very recently by lightning, and the NO to NO_y ratios are usually still very high. Here, the particles are still depleted by convection scavenging and there has not been enough time for new particles to form, at least not in the size range detectable by our instrumentation. On the other hand, there is a strong positive relationship between NO_y and N_{CN}, as seen in Fig. 22 during the entire period from 2051 to 2210 UTC. Regions with high concentrations of new particles generally show elevated NO_y, typically in the range of 1 to 3 ppb, indicating that photochemical reactions had taken place that both produced new particles and converted NO to NO_y.

Deleted: have

3.6. Flight AC20: A special case with NPF from biomass smoke

On flight AC20, HALO performed detailed sampling of the anvil and outflow of a large Cb over northern Rondonia, a state with a high incidence of deforestation burning. Numerous outflow penetrations around this Cb were made, and the ice particles sampled here could be clearly identified as freshly produced in the Cb top. The CN concentrations in the UT away from

the outflow were unimpressive, typically in the range 2000 to 10,000 cm^{-3}. However, in sharp contrast to the other flights, where the air in the outflow always had been depleted in aerosol particles, on this flight the outflow often showed much higher CN concentrations, between 10,000 and 20,000 cm^{-3} (Fig. 23a). The concentrations of CCN and nonvolatile CN in the outflow were either the same as in the surrounding air or slightly higher, also contrasting with the observations on the other flights, where they had been depleted. Since the N_{CN} in the outflow were also much higher than in the PBL (~2000 cm^{-3}), entrainment of PBL air cannot explain the CN enrichment.

The mixing ratios of CO, NO, and NO_y were also elevated in the outflow (Fig. 23b), which in the case of CO and NO_y might be explained by inputs from the PBL, where CO and NO_y levels were around 120–200 ppb and 2–3 ppb, respectively. The NO values in the PBL, on the other hand, were only about 0.13 ppb, similar to the UT values, requiring an additional NO source for the outflow.

The explanation for this unusual behavior may be found in the layer between 11.5 and 12.5 km that was penetrated during both ascent and descent (Fig. 23c). In this layer, N_{CN} reached 30,000 cm^{-3}, CO was elevated to ~140 ppb, N_{acc} to 850 cm^{-3}, and NO_y to ~1.6 ppb. The data also suggest a slight enrichment in rBC, but this is close to the limit of detection. These values suggest that this is a detrainment layer polluted with biomass smoke, as we have often seen on previous campaigns over the burning regions in southern Amazonia (Andreae et al., 2004). An urban origin of this pollution is unlikely, since the only town in the region, Porto Velho, lies about 50–100 km downwind of the sampling area.

For a comparison with biomass smoke, we computed the enhancement ratios, $\Delta N_{acc}/\Delta CO$ and $\Delta CCN0.5/\Delta CO$, as the slopes of the bivariate regression between these variables for the time period between 16:53 and 16:58 UTC. The enhancement ratios in this layer differ clearly from fresh biomass smoke. The ratio $\Delta N_{acc}/\Delta CO$ is ~6–12 cm^{-3} ppb^{-1} and the ratio $\Delta CCN/\Delta CO$ about 2.5 cm^{-3} ppb^{-1}, much lower than the typical ratios in fresh smoke, which are about 20–40 cm^{-3} ppb^{-1} (Janhäll et al., 2010), indicating removal of CCN-sized particles during the upward transport. In contrast, the ratio $\Delta CN/\Delta CO$ was about 350 cm^{-3} ppb^{-1}, almost an order of magnitude above the values typical of fresh smoke. These results suggest that biomass smoke was brought to the UT either from the strongly smoke-polluted PBL in this region or actually by a pyro-Cb over an active fire, and that the concentration of the larger primary smoke particles was

Deleted: -
Deleted: -
Deleted: -
Deleted: , however,
Deleted: -
Deleted: -

strongly reduced by scavenging, which allowed new particle formation in this smoke layer. The enrichments seen in the outflow penetrations at altitudes above the 12-km layer may be the result of entrainment of air from this layer or of rapid particle formation in situ. Further evidence for the upward transport of pyrogenic emissions was found in measurements on a horizontal leg at 11 km, which had only modest CN concentrations (around 1700 cm^{-3}), but elevated CCN, NO_y, CO, and aerosol nitrate and organics, with similar vales to the biomass-burning polluted boundary layer below. While we have this kind of observations from only one flight, which took place over the most polluted region sampled during this campaign, they are suggestive of the potential of rapid particle formation and growth in smoke detrainment layers, an issue that merits further study in future campaigns.

3.7. Conceptual model and role in aerosol life cycle

The discussion in the preceding sections can be summarized in a conceptual model of the aerosol life cycle over the Amazon Basin (Fig. 24). Cloud updrafts in deep convection bring air from the PBL into the middle and upper troposphere, where it is released in the convective outflow (Krejci et al., 2003). During this process, most pre-existing aerosols are removed by precipitation scavenging, especially the larger particles that account for most of the condensation sink (Ekman et al., 2006). Most likely, organic compounds with low and very low volatilities are also removed by deposition on hydrometeors, which provide a considerable amount of surface area inside the clouds (Murphy et al., 2015).

On the other hand, the rapid transport of PBL air to the UT inside deep convective clouds facilitates lofting of the more volatile reactive BVOCs from the Amazon boundary layer (Colomb et al., 2006; Apel et al., 2012). Here, the initially O_3- and NO_x-poor boundary layer air is supplied with O_3 by mixing with UT air and addition of NO from lightning, creating a highly reactive chemical environment. This mixture is exposed to an extremely high actinic flux due to the high altitude and multiple scattering by ice particles. Because of the low airmass at UT altitudes, the actinic flux is already very high shortly after sunrise. In this environment, rapid photooxidation of BVOCs and formation of ELVOCs/HOMs is to be expected. In laboratory studies, ELVOCs/HOMs have been shown to be rapidly produced at fairly high yields both by ozonolysis of terpenes and by reactions with OH radicals (Ehn et al., 2014; Jokinen et al., 2015; Berndt et al., 2016; Dunne et al., 2016).

Deleted: 0

Deleted: In the Amazon PBL, the classical nucleation events characterized by the rapid appearance of large numbers of particles <10 nm and subsequent growth into an Aitken mode (e.g., Kulmala and Kerminen, 2008) has never been reported, in spite of several years of observations by several teams (Martin et al., 2010; Rizzo et al., 2013; Andreae et al., 2015). This has been attributed to the low emissions of gaseous sulfur species in the basin (Andreae and Andreae, 1988; Andreae et al., 1990a), which result in H_2SO_4 vapor concentrations that are too low to induce nucleation (Martin et al., 2010). Nucleation of particles from organic vapors alone is not favored in the Amazonian PBL because of high temperatures and humidity as well as the competition by the condensation sink on pre-existing particles, which results in organic coatings on almost all primary and secondary particles in the Amazonian PBL (Pöschl et al., 2010; Pöhlker et al., 2012).¶

Deleted: VOCs

The outflow regions in the UT present an ideal environment for particle nucleation, as had already been suggested in some earlier studies (Twohy et al., 2002; Lee et al., 2004; Kulmala et al., 2006; Weigelt et al., 2009). The temperatures are some 60 ~~- 80 K lower than in the PBL,~~ which decreases the equilibrium vapor pressure of gaseous species (Murphy et al., 2015) and increases the nucleation rate. Based on classical nucleation theory and molecular dynamics calculations, Yu et al. (2017) have estimated an increase in nucleation rate by one order of magnitude per 10 K. Nucleation rate measurements in the CERN CLOUD chamber indicate a similar temperature dependence (Dunne et al., 2016). Note, however, that these temperature dependencies are based on measurements for inorganic NPF, and that while the trends for organics are expected to be similar, the magnitude of the increase in nucleation rates for organics may be quite different. Because the preexisting aerosol has been depleted during the passage through convective clouds before being released into the UT from the cloud outflow, the low particle surface area in the UT presents only a small condensation sink and thus very little competition to nucleation ~~(Twohy et al., 2002; Lee et al., 2003; Lee et al., 2004; Young et al., 2007; Benson et al., 2008).~~

In the absence of measurements of the relevant gaseous sulfur species and the composition of the nucleating clusters, we cannot make firm conclusions about the actual nucleation mechanism. Over marine regions and polluted continental regions, the particles observed in outflows and in the UT were mostly identified as sulfates (Clarke et al., 1999; Twohy et al., 2002; Kojima et al., 2004; Waddicor et al., 2012), and consequently H_2SO_4 has been proposed as the nucleating species. However, since in some cases this identification was based only on the volatility of the particles, they could have also consisted of organics or mixtures of organics and H_2SO_4. Over the Amazon, nucleation by H_2SO_4 cannot be excluded based on our observations, especially if there was already some SO_2 or H_2SO_4 present in the UT before the injection of the organic-rich PBL air. However, since the Amazonian BL contains very little SO_2, the sulfur species would have had to come from outside the region and thus they would have had the opportunity to be oxidized to H_2SO_4 and nucleate into particles during its travel in the UT well before entering Amazonia. It is therefore likely that the particles in the Amazon UT formed by homogeneous nucleation of organics, as has been suggested by several authors (Kulmala et al., 2006; Ekman et al., 2008; Murphy et al., 2015). Nucleation by formation of clusters containing both H_2SO_4 and oxidized organic molecules is of course also a possibility that we cannot exclude

Deleted: -

Deleted: from a condensation sink

Deleted: The rapid transport of PBL air to the UT inside deep convective clouds facilitates lofting of reactive BVOCs from the Amazon boundary layer (Colomb et al., 2006; Apel et al., 2012). Here, the initially O_3- and NO_x-poor boundary layer air is supplied with O_3 by mixing with UT air and addition of NO from lightning, creating a highly reactive chemical environment. This mixture is exposed to an extremely high actinic flux due to the high altitude and multiple scattering by ice particles. Because of the low airmass at UT altitudes, the actinic flux is already very high shortly after sunrise. In this environment, rapid photooxidation of BVOCs and formation of ELVOCs/HOMs is to be expected. In laboratory studies, HOMs have been shown to be rapidly produced at fairly high yields both by ozonolysis of terpenes and by reactions with OH radicals (Ehn et al., 2014; Jokinen et al., 2015; Berndt et al., 2016; Dunne et al., 2016).¶

Deleted: much more

(Metzger et al., 2010; Riccobono et al., 2014). However, recent studies have shown that HOM compounds can nucleate to form particles even in the absence of H_2SO_4, especially in the UT (Bianchi et al., 2016; Kirkby et al., 2016), and nucleation of HOMs without involvement of H_2SO_4 has been suggested to be the dominant mode of new particle formation in large parts of the pre-industrial atmosphere by the modeling study of Gordon et al. (2016). The importance of ions produced from cosmic radiation in this nucleation process is still controversial (Lee et al., 2003; Yu et al., 2008; Bianchi et al., 2016; Kirkby et al., 2016).

Regardless of the actual nucleating species, H_2SO_4 or HOMs/ELVOCs, the growth of the particles observed in our campaign must have been dominated by organics, as shown by the composition of the aerosol measured by the AMS. The dominance of organics in the growth of aerosols in pristine environments has also been suggested on the basis of measurements and modeling studies, both for the lower troposphere (Laaksonen et al., 2008; Riipinen et al., 2011; Riipinen et al., 2012; Öström et al., 2017) and the UT (Ekman et al., 2008; Murphy et al., 2015). In particular, isoprene-derived SOA has been suggested to be important in the growth of sub-CCN-size particles to CCN (Ekman et al., 2008; Jokinen et al., 2015), which would be consistent with the prevalence of isoprene in the Amazonian PBL and our observations of IEPOX-SOA in the UT aerosol. As the particles grow, the decrease of the Kelvin (curvature) effect with increasing size of the growing particles implies that subsequently relatively more volatile organics can condense (Tröstl et al., 2016), in agreement with the observed high volatile fraction we observed in the upper tropospheric CN.

While in general the volatile fraction of the particles in the UT was very high, there were also regions with a significant fraction of particles that did not evaporate at 250 ºC (see section 3.4.3). These were dominated by relatively aged organics, which, based on the absence on detectable rBC, must also be of secondary origin. Such thermally refractory organics may explain the presence of non-volatile particles in the tropical UTLS, which had been observed in previous campaigns especially in the region above 360 K (Borrmann et al., 2010).

Once particles have nucleated in the UT and grown into the Aitken mode and in some cases even into the accumulation mode size ranges, they can be transported downward towards the lower troposphere both by general subsidence under the prevailing high pressure system over Amazonia and by downdrafts associated with deep convective activity. Large-scale entrainment

of UT and MT air into the boundary layer has been suggested as the major source of new particles in marine regions (Raes, 1995; Katoshevski et al., 1999; Clarke et al., 2013). Over Amazonia with its high degree of convective activity, downdrafts are likely to play a more important role. Downward transport of UT air by downdrafts associated with deep convective activity has been shown to inject air with lower moisture content, lower equivalent potential temperature, and elevated O_3 into the PBL (Zipser, 1977; Betts et al., 2002; Sahu and Lal, 2006; Grant et al., 2008; Hu et al., 2010; Gerken et al., 2016). It would follow that the same mechanism also brings down aerosol-rich air from the UT into the PBL. Indeed, in a recent aircraft study over the central Amazon, this mechanism was shown to be an important source of atmospheric aerosols, predominantly in the Aitken mode, to the Amazonian PBL (Wang et al., 2016a). Here, they can continue to grow by condensation of BVOC-derived organics into the accumulation mode and become available as CCN, closing the aerosol cycle over Amazonia.

This mechanism provides an explanation for the origin of secondary aerosol particles in the clean Amazon PBL, where the occurrence of "classical" nucleation events, characterized by the rapid appearance of large numbers of particles <10 nm and subsequent growth into an Aitken mode (e.g., Kulmala and Kerminen, 2008), has never been reported, in spite of several years of observations by several teams (Martin et al., 2010; Rizzo et al., 2013; Andreae et al., 2015). This has been attributed to the low emissions of gaseous sulfur species in the basin (Andreae and Andreae, 1988; Andreae et al., 1990a), which result in H_2SO_4 vapor concentrations that are too low to induce nucleation (Martin et al., 2010). Nucleation of particles from organic vapors alone is not favored in the Amazonian PBL because of high temperatures and humidity as well as the competition by the condensation sink on pre-existing particles, which results in organic coatings on almost all primary and secondary particles in the Amazonian PBL (Pöschl et al., 2010; Pöhlker et al., 2012).

4. Summary and Conclusions

As part of the ACRIDICON-CHUVA 2014 aircraft campaign, we investigated the characteristics and sources of aerosols in the upper troposphere over the Amazon Basin. We observed regions with high number concentrations of aerosol particles (tens of thousands per cm^3 STP) in the UT on all flights that reached above 8 km. The aerosol enhancements were commonly in the

form of distinct layers with thicknesses of a few hundreds to a few thousands of meters. Such layer structures are a common feature of the free troposphere and have been related to detrainment from deep convection and large-scale subsidence (Newell et al., 1999).

In other regions, upward transport of aerosols from the PBL had been suggested to be an important source of UT aerosols, based on the abundance of low-volatility particles (Clarke and Kapustin, 2010), TEM analysis of individual particles (Kojima et al., 2004), or modeling of cloud processes (Yin et al., 2005). Over Amazonia, however, our study showed that the UT aerosol was fundamentally different from the aerosol in the LT, indicating that upward transport of PBL aerosols, especially combustion aerosols from BB, is not an important source of aerosols to the Amazonian UT.

The number concentrations of particles in the UT were often several orders of magnitude higher than in the LT, and their size distribution was dominated by the Aitken rather than the accumulation mode. In contrast to the LT, the particles in the UT were predominantly volatile at 250 ºC and had much higher organics and nitrate contents. The extremely low concentrations of rBC in the MT and UT show that the aerosols above the LT are not combustion-derived and indicate that the low-volatility fraction must be representing secondary organics of extremely low volatility (ELVOCs/HOMs). Regarding the size class large enough to act as CCN (i.e., larger than 60–80 nm), we can conclude based on the absence of rBC and the lack of BB indicators in the AMS measurements that the enhanced CCN in the UT are not related to upward transport of combustion products, in contrast to most previous studies (e.g., Krejci et al., 2003; Engström et al., 2008; Clarke et al., 2013).

By analyzing the history of the particle-enriched airmasses and comparing the transport paths to GOES infrared imagery, we could show in all cases that these airmasses had been in contact with deep convective outflow. Measurements inside the cloud tops and the outflow anvils close to the clouds showed that the pre-existing aerosols in the ascending air had been almost completely scavenged by in-cloud processes, making the clouds initially a net aerosol sink. The near-complete scavenging is consistent with the hypothesized large water vapor supersaturation in pristine tropical deep convective clouds, which can nucleate particles that are much smaller than the commonly defined CCN (Khain et al., 2012).

Deleted: by

Deleted: -

Deleted: almost

Based on our measurements, we propose that BVOCs in the cloud outflow are rapidly oxidized to HOMs/ELVOCs, which because of the low temperatures and low condensation sink can ~~form new particles, possibly together with H_2SO_4, and grow to sizes ≥20 nm within a few~~ hours, making deep convective clouds an indirect aerosol source. This had also been concluded based on a large statistical sampling of UT air in the Northern Hemisphere by the CARIBIC aircraft measurement program (Weigelt et al., 2009). The importance of NPF in the UT for the budget of CN and CCN had been proposed previously on the basis of modeling studies (Yu et al., 2008; Merikanto et al., 2009; Carslaw et al., 2017), and is evident in the global enhancement of CN in the UT, especially in tropical regions, seen in compilations of data from numerous aircraft campaigns (Yu et al., 2008; Reddington et al., 2016). In this way, aerosol production by BVOC oxidation in the UT can provide the "missing source" of FT organic aerosol, which had been deduced from a mismatch between models and observations (Heald et al., 2005).

The high aerosol concentrations in the UT provide a reservoir of particles that are available for downward transport into the PBL both by large-scale downward motion and by convective downdrafts. In a recent study, we have shown that transport of aerosols by downdrafts from the free troposphere is an important, if not the dominant, source of particles to the lower troposphere (LT) over the Amazon (Wang et al., 2016a). The particles that are produced by this mechanism in the UT over the Amazon (and probably other tropical continents as well) can be transported globally due to their long lifetime in the UT (Williams et al., 2002; Clarke et al., 2013) and affect the microstructure of low-level clouds after they eventually descend into the PBL, possibly at very large distances from the source areas of their precursors.

Our study and the results of some previous studies (Lee et al., 2003; Froyd et al., 2009) suggest that UT aerosol production is especially important in the tropics because of the high rate of BVOC production and the abundance of deep convection, but its relevance may also extend to temperate and boreal regions. Our measurements both in the Amazon and at a remote site in central Siberia, distant from SO_2 emission sources and thus experiencing very low H_2SO_4 concentrations, show that "classical" nucleation events are very rare to absent at such sites and may not provide a strong source of new particles (Heintzenberg et al., 2011; Andreae et al., 2015; Wiedensohler et al., 2017). Consequently, the UT may be an important, possibly even the dominant source of tropospheric aerosol particles in regions that are not strongly affected by anthropogenic or natural primary aerosols. This would assign clouds a central role in the aerosol life

Deleted: readily nucleate

Deleted: classical

cycle, controlling both source and sink of aerosol particles, at least in regions of low anthropogenic pollution. Furthermore, the relevance of UT aerosol production may not be limited to the troposphere, because the UT and the TTL are also important reservoirs for the transport of particles into the lower stratosphere (Fueglistaler et al., 2009; Borrmann et al., 2010; Randel and Jensen, 2013). Organic aerosols in the lower stratosphere have been shown to have significant radiative effects (Yu et al., 2016).

The conceptual model proposed here implies a profound difference between the present-day polluted atmosphere and the pristine pre-industrial situation, especially over the continents. In the pristine atmosphere, the gradient of particle number concentrations may have been from high values in the UT to low values in the PBL, as we have found in Amazonia. In polluted continental regions, on the other hand, nucleation and NPF occur predominantly in the lower troposphere, where they add to primary emitted particles (Spracklen et al., 2006), and which thus has become the dominant source region of atmospheric aerosols in today's atmosphere over much of the world. Average N_{CN} measured at ground level at polluted continental sites worldwide range between 3400 and 19,000 cm^{-3} in the compilation by Andreae (2009). In the UT, on the other hand, the median particle concentrations (> 12 nm) measured in the CARIBIC program over polluted continents are ~3500 cm^{-3} over North America, ~2500 cm^{-3} over Europe, and ~3000 cm^{-3} over India (Ekman et al., 2012). Of course, there are elevated values in the UT at particular places and times over polluted continents, such as those reported by Twohy et al. (2002), but they appear to be more the exception than the rule. This vertical structure is quite close to being the exact opposite of the distribution measured over Amazonia during ACRIDICON–CHUVA, where the averages (±std.dev.) were 7700±7970 cm^{-3} in the UT and 1650±980 cm^{-3} in the LT. Consequently, in the anthropocene the aerosol concentration profile has been turned upside down, at least in many polluted regions, since now the highest concentrations are found in the PBL.

This has important consequences for the Earth's climate system. The aerosol concentrations in the PBL influence cloud microphysical properties and radiative energy fluxes, which affect the characteristics of convection and thereby influence cloud radiative forcing, atmospheric stability, precipitation, and atmospheric dynamics at all scales (Jiang et al., 2008; Koren et al., 2008; Rosenfeld et al., 2008; Koren et al., 2010; Fan et al., 2012; Rosenfeld et al., 2014;

Gonçalves et al., 2015; Stolz et al., 2015; Dagan et al., 2016; Braga et al., 2017). By their radiative and microphysical effects on convection dynamics, aerosols are also able to increase upper tropospheric humidity, which plays an important role in the Earth's radiation budget (Sherwood, 2002; Kottayil and Satheesan, 2015; Riuttanen et al., 2016) and may also affect the potential for aerosol nucleation in the UT, thus providing an additional feedback.

5. Acknowledgments

We thank the entire ACRIDICON–CHUVA team for the great cooperation that made this study possible. Our thanks go especially to the HALO pilots, Steffen Gemsa, Michael Grossrubatscher, and Stefan Grillenbeck, who always worked hard to put the aircraft at the right place for our measurements, even under sometimes difficult conditions. We appreciate the support of the colleagues from enviscope GmbH for their valuable help in certifying and installing the numerous instruments for HALO and thank the HALO team of the DLR for their cooperation. We acknowledge the generous support of the ACRIDICON–CHUVA campaign by the Max Planck Society, the German Aerospace Center (DLR), FAPESP (São Paulo Research Foundation), and the German Science Foundation (Deutsche Forschungsgemeinschaft, DFG) within the DFG Priority Program (SPP 1294) "Atmospheric and Earth System Research with the Research Aircraft HALO (High Altitude and Long Range Research Aircraft)" by contract no VO1504/4-1, SCHN1138/1-2, MI 583/4-1 and JU 3059/1-1, WE 1900/22-1, WE 1900/24-1, WE 1900/36-1. This study was also supported by EU Project HAIC under FP7-AAT-2012-3.5.1-1 and by the German Federal Ministry of Education and Research (BMBF, grant No. 01LG1205E). C. Voigt acknowledges financing by the Helmholtz Association under contract no. W2/W3-60. M. A. Cecchini was funded by FAPESP grants number 2014/08615-7 and 2014/21189-7. The participation of D. Rosenfeld was supported by project BACCHUS, European Commission FP7-603445. B. Weinzierl, M. Dollner, D. Sauer, and A. Walser received funding from the Helmholtz Association under Grant VH-NG-606 (Helmholtz-Hochschul-Nachwuchsforschergruppe AerCARE) and from the European Research Council under the European Community's Horizon 2020 research and innovation framework program/ERC Grant Agreement 640458 (A-LIFE). A. Spanu was funded through the Marie Curie Initial Training Network VERTIGO (grant agreement number 607905).

Deleted: -

Formatted: Indent: First line: 0.49", Space Before: 6 pt, After: 0 pt, Line spacing: 1.5 lines

Deleted: -

Deleted: by the German Science Foundation within DFG SPP 1294 HALO by contract no VO1504/4-1 and contract no JU 3059/1-1

Deleted: This study was also supported by the German Federal Ministry of Education and Research (BMBF, grant No. 01LG1205E), and by the German Science Foundation within DFG SPP 1294 HALO by contract no VO1504/4-1, SCHN1138/1-2, and contract no JU 3059/1-1.

Deleted: ¶

6. Figure Captions

Figure 1: Tracks of the flights on which measurements at high altitude were made during ACRIDICON-CHUVA. The flight segments at altitudes >8 km are shown as heavier lines.

Figure 2: Columnar precipitable water anomaly for September 2014 (based on the 1981-2010 average NCEP/NCAR Reanalysis).

Figure 3: Total rainfall (mm per month, 1º resolution) for September 2014. Data from the Global Precipitation Climatology Centre (GPCC).

Figure 4: Mean wind speeds during September 2014 at a) 850 hPa and b) 200 hPa (Data from NCEP/NCAR).

Figure 5: Vertical profiles of potential temperature, static air temperature, and relative humidity measured on HALO during the ACRIDICON-CHUVA flights over the Amazon Basin.

Figure 6: Trajectory statistics based on (a) 72-hour and (b) 120-hour backtrajectory calculations for September 2014, initialized at Manaus at an elevation of 12 km.

Figure 7: Vertical profiles of CN concentrations, N_{CN}; a) overall statistics from all flights, b) examples from individual profiles on flight AC07 (segment G) and AC09 (segments A1 and A2).

Figure 8: Vertical profiles of accumulation mode particle concentrations, N_{acc}; a) 1-min averaged data from all flights, b) N_{acc} profile from flight AC19 together with the profile of N_{CN} from the same flight (1-sec data).

Figure 9: Size spectra: The black line shows the mean boundary layer DMPS size spectrum from a segment in the PBL on flight AC13 (16:55 to 17:18 UTC). The square black symbols represent the mean, the grey shaded area the standard deviation of the measurements. The line is a logarithmic fit with modal diameters of 74 and 175 nm. The colored lines represent size distributions from 0.65 to 5.8 km from a G1 flight during GoAmazon (Wang et al., 2016a).

Figure 10: Vertical profiles of the ultrafine fraction (UFF); a) overall statistics from all flights, b) examples from individual profiles on flight AC18.

Figure 11: Vertical profiles of CCN concentrations at 0.52% supersaturation; a) overall statistics from all flights (1-min averages), b) examples from individual profiles on flights AC09 (green)

and AC12+13 (red). Flights AC12 and AC13 were conducted over the same region on successive days.

Figure 12: a) CCN fraction ($N_{CCN0.5}/N_{CN}$) vs altitude, all data. The peak at 11 km is caused by the inclusion of a large number of measurements from flight AC20 on a horizontal leg at 11 km, which was influenced by biomass burning (see section 3.6). b) CCN fraction vs. CN concentration for specific segments from flight AC18 (see text for discussion).

Figure 13: a) CCN fractions ($N_{CCN0.5}/N_{CN}$) and b) CCN concentrations ($N_{CCN0.5}$) vs. supersaturation from selected legs from flights AC07, AC09, and AC10; c,d) data from flights AC12 and AC13 for the LT, MT, and UT.

Figure 14: Volatile fraction. a) statistics from all flights; b) individual segments from flight AC18 (see text for discussion).

Figure 15: Refractory black carbon vs altitude, all flights, 30-second averages.

Figure 16: Aerosol chemical composition as determined by AMS and SP2 measurements in the lower, middle, and upper troposphere.

Figure 17: Plot of the AMS factors f_{44} vs. f_{43}, indicating the median values for the LT and UT and values for some UT flight segments with elevated aerosol concentrations. With increasing degree of oxidation, the measurements move to the upper left of the triangle

Figure 18: Measurements during passages through cumulonimbus cloud tops and outflow anvils: a) Several cloud top penetrations at 10.7 to 12 km altitude on flight AC18 showing reduced N_{CN} and $N_{CCN0.5}$ inside the cloud top; b) Outflow from a large active cumulonimbus, showing strong aerosol depletion and NO production by lightning.

Fig. 19: Airmass contacts with deep convection. The colors indicate the cloud top temperature of the convective system with which the trajectory had the most recent contact. The aircraft altitude at which the airmass was sampled is indicated by the red line. The colored dots are plotted at the altitude at which the airmass crossed the grid cell with the convective system. The dots are only plotted if this altitude is greater than 6 km and if it encountered a DC region (i.e., $T_b < -30$ ºC). The shaded areas correspond to the flight segments with elevated CN concentrations. a) flight AC09, b) flight AC18.

Formatted: Font: Not Italic

Formatted: Font: Not Italic

Deleted: , and AC18

Figure 20: a) Number of hours since last contact with deep convection for flight segments with elevated aerosol concentrations (cumulative frequency, all flights); b) frequency distribution of minimum GOES brightness temperature (T_b) for selected flights legs (within 5-day backward trajectories).

Figure 21: CN vs CO concentrations in the upper troposphere above 8 km (15-second averages).

Figure 22: CN, NO, and NO_y concentrations in a flight segment in the upper troposphere on flight AC07.

Figure 23: a) Measurements of $N_{CCN0.5}$, N_{CN}, N_{nonvol}, and ice particles during cloud top penetrations on flight AC20 at altitudes between 12.3 and 13.5 km. b) Concentrations of CO, NO, and NO_y on the same flight segments. c) Measurements of N_{acc}, N_{CN}, rBC, CO, and O_3 during the climb from 11.0 to 13.5 km.

Figure 24: Conceptual model of the aerosol life cycle over the Amazon Basin.

7. References

Abdelmonem, A., Järvinen, E., Duft, D., Hirst, E., Vogt, S., Leisner, T., and Schnaiter, M., PHIPS–HALO: the airborne Particle Habit Imaging and Polar Scattering probe – Part 1: Design and operation: Atmos. Meas. Tech., 9, 3131-3144, doi:10.5194/amt-9-3131-2016, 2016.

Alfarra, M. R., Prevot, A. S. H., Szidat, S., Sandradewi, J., Weimer, S., Lanz, V. A., Schreiber, D., Mohr, M., and Baltensperger, U., Identification of the mass spectral signature of organic aerosols from wood burning emissions: Environ. Sci. Technol., 41, 5770-5777, doi:10.1021/es062289b, 2007.

Andreae, M. O., and Andreae, T. W., The cycle of biogenic sulfur compounds over the Amazon Basin. I. Dry season: J. Geophys. Res., 93, 1487-1497, 1988.

Andreae, M. O., Browell, E. V., Garstang, M., Gregory, G. L., Harriss, R. C., Hill, G. F., Jacob, D. J., Pereira, M. C., Sachse, G. W., Setzer, A. W., Dias, P. L. S., Talbot, R. W., Torres, A. L., and Wofsy, S. C., Biomass-burning emissions and associated haze layers over Amazonia: J. Geophys. Res., 93, 1509-1527, 1988.

Andreae, M. O., Berresheim, H., Bingemer, H., Jacob, D. J., Lewis, B. L., Li, S.-M., and Talbot, R. W., The atmospheric sulfur cycle over the Amazon Basin, 2. Wet Season: J. Geophys. Res., 95, 16,813-16,824, 1990a.

Andreae, M. O., Talbot, R. W., Berresheim, H., and Beecher, K. M., Precipitation chemistry in central Amazonia: J. Geophys. Res., 95, 16,987-16,999, 1990b.

Andreae, M. O., Anderson, B. E., Blake, D. R., Bradshaw, J. D., Collins, J. E., Gregory, G. L., Sachse, G. W., and Shipham, M. C., Influence of plumes from biomass burning on atmospheric chemistry over the equatorial Atlantic during CITE-3: J. Geophys. Res., 99, 12,793-12,808, 1994.

Andreae, M. O., Artaxo, P., Fischer, H., Freitas, S. R., Gregoire, J. M., Hansel, A., Hoor, P., Kormann, R., Krejci, R., Lange, L., Lelieveld, J., Lindinger, W., Longo, K., Peters, W., Reus, M. d., Scheeren, B., Silva Dias, M. A. F., Ström, J., van Velthoven, P. F. J., and Williams, J., Transport of biomass burning smoke to the upper troposphere by deep convection in the equatorial region: Geophys. Res. Lett., 28, 951-954, 2001.

Andreae, M. O., Artaxo, P., Brandão, C., Carswell, F. E., Ciccioli, P., da Costa, A. L., Culf, A. D., Esteves, J. L., Gash, J. H. C., Grace, J., Kabat, P., Lelieveld, J., Malhi, Y., Manzi, A. O., Meixner, F. X., Nobre, A. D., Nobre, C., Ruivo, M. d. L. P., Silva-Dias, M. A., Stefani, P., Valentini, R., von Jouanne, J., and Waterloo, M. J., Biogeochemical cycling of carbon, water, energy, trace gases and aerosols in Amazonia: The LBA-EUSTACH experiments: J. Geophys. Res., 107, 8066, doi:10.1029/2001JD000524, 2002.

Andreae, M. O., Rosenfeld, D., Artaxo, P., Costa, A. A., Frank, G. P., Longo, K. M., and Silva-Dias, M. A. F., Smoking rain clouds over the Amazon: Science, 303, 1337-1342, 2004.

Andreae, M. O., Correlation between cloud condensation nuclei concentration and aerosol optical thickness in remote and polluted regions: Atmos. Chem. Phys., 9, 543–556, 2009.

1695 Andreae, M. O., Artaxo, P., Beck, V., M. Bela, Gerbig, C., Longo, K., Munger, J. W.,
1696 Wiedemann, K. T., and Wofsy, S. C., Carbon monoxide and related trace gases and
1697 aerosols over the Amazon Basin during the wet and dry seasons: Atmos. Chem. Phys.,
1698 12, 6041–6065, 2012.

1699 Andreae, M. O., Acevedo, O. C., Araùjo, A., Artaxo, P., Barbosa, C. G. G., Barbosa, H. M. J.,
1700 Brito, J., Carbone, S., Chi, X., Cintra, B. B. L., da Silva, N. F., Dias, N. L., Dias-Júnior,
1701 C. Q., Ditas, F., Ditz, R., Godoi, A. F. L., Godoi, R. H. M., Heimann, M., Hoffmann, T.,
1702 Kesselmeier, J., Könemann, T., Krüger, M. L., Lavric, J. V., Manzi, A. O., Lopes, A. P.,
1703 Martins, D. L., Mikhailov, E. F., Moran-Zuloaga, D., Nelson, B. W., Nölscher, A. C.,
1704 Santos Nogueira, D., Piedade, M. T. F., Pöhlker, C., Pöschl, U., Quesada, C. A., Rizzo,
1705 L. V., Ro, C. U., Ruckteschler, N., Sá, L. D. A., de Oliveira Sá, M., Sales, C. B., dos
1706 Santos, R. M. N., Saturno, J., Schöngart, J., Sörgel, M., de Souza, C. M., de Souza, R. A.
1707 F., Su, H., Targhetta, N., Tóta, J., Trebs, I., Trumbore, S., van Eijck, A., Walter, D.,
1708 Wang, Z., Weber, B., Williams, J., Winderlich, J., Wittmann, F., Wolff, S., and Yáñez-
1709 Serrano, A. M., The Amazon Tall Tower Observatory (ATTO): overview of pilot
1710 measurements on ecosystem ecology, meteorology, trace gases, and aerosols: Atmos.
1711 Chem. Phys., 15, 10,723-10,776, doi:10.5194/acp-15-10723-2015, 2015.

1712 Apel, E. C., Olson, J. R., Crawford, J. H., Hornbrook, R. S., Hills, A. J., Cantrell, C. A.,
1713 Emmons, L. K., Knapp, D. J., Hall, S., Mauldin, R. L., Weinheimer, A. J., Fried, A.,
1714 Blake, D. R., Crounse, J. D., St Clair, J. M., Wennberg, P. O., Diskin, G. S., Fuelberg, H.
1715 E., Wisthaler, A., Mikoviny, T., Brune, W., and Riemer, D. D., Impact of the deep
1716 convection of isoprene and other reactive trace species on radicals and ozone in the upper
1717 troposphere: Atmos. Chem. Phys., 12, 1135-1150, doi:10.5194/acp-12-1135-2012, 2012.

1718 Artaxo, P., Martins, J. V., Yamasoe, M. A., Procópio, A. S., Pauliquevis, T. M., Andreae, M. O.,
1719 Guyon, P., Gatti, L. V., and Leal, A. M. C., Physical and chemical properties of aerosols
1720 in the wet and dry season in Rondonia, Amazonia: J. Geophys. Res., 107, 8081,
1721 doi:10.1029/2001JD000666, 2002.

1722 Artaxo, P., Rizzo, L. V., Brito, J. F., Barbosa, H. M. J., Arana, A., Sena, E. T., Cirino, G. G.,
1723 Bastos, W., Martin, S. T., and Andreae, M. O., Atmospheric aerosols in Amazonia and
1724 land use change: from natural biogenic to biomass burning conditions: Faraday
1725 Discussions, 165, 203-235, doi:10.1039/C3FD00052D, 2013.

1726 Benson, D. R., Young, L. H., Lee, S. H., Campos, T. L., Rogers, D. C., and Jensen, J., The
1727 effects of airmass history on new particle formation in the free troposphere: case studies:
1728 Atmos. Chem. Phys., 8, 3015-3024, 2008.

1729 Berkemeier, T., Ammann, M., Mentel, T. F., Poschl, U., and Shiraiwa, M., Organic nitrate
1730 contribution to new particle formation and growth in secondary organic aerosols from
1731 alpha-pinene ozonolysis: Environ. Sci. Technol., 50, 6334-6342,
1732 doi:10.1021/acs.est.6b00961, 2016.

1733 Berndt, T., Richters, S., Jokinen, T., Hyttinen, N., Kurten, T., Otkjaer, R. V., Kjaergaard, H. G.,
1734 Stratmann, F., Herrmann, H., Sipila, M., Kulmala, M., and Ehn, M., Hydroxyl radical-
1735 induced formation of highly oxidized organic compounds: Nature Communications, 7,
1736 13677, doi:10.1038/ncomms13677, 2016.

1737 Bertram, T. H., Perring, A. E., Wooldridge, P. J., Crounse, J. D., Kwan, A. J., Wennberg, P. O.,
1738 Scheuer, E., Dibb, J., Avery, M., Sachse, G., Vay, S. A., Crawford, J. H., McNaughton,
1739 C. S., Clarke, A., Pickering, K. E., Fuelberg, H., Huey, G., Blake, D. R., Singh, H. B.,
1740 Hall, S. R., Shetter, R. E., Fried, A., Heikes, B. G., and Cohen, R. C., Direct
1741 measurements of the convective recycling of the upper troposphere: Science 315, 816-
1742 820, 2007.

1743 Betts, A. K., Gatti, L. V., Cordova, A. M., Dias, M. A. F. S., and Fuentes, J. D., Transport of
1744 ozone to the surface by convective downdrafts at night: J. Geophys. Res., 107, 8046,
1745 doi:10.1029/2000JD000158, 2002.

1746 Bianchi, F., Tröstl, J., Junninen, H., Frege, C., Henne, S., Hoyle, C. R., Molteni, U., Herrmann,
1747 E., Adamov, A., Bukowiecki, N., Chen, X., Duplissy, J., Gysel, M., Hutterli, M.,
1748 Kangasluoma, J., Kontkanen, J., Kürten, A., Manninen, H. E., Münch, S., Peräkylä, O.,
1749 Petäjä, T., Rondo, L., Williamson, C., Weingartner, E., Curtius, J., Worsnop, D. R.,
1750 Kulmala, M., Dommen, J., and Baltensperger, U., New particle formation in the free
1751 troposphere: A question of chemistry and timing: Science, 352, 1109-1112,
1752 doi:10.1126/science.aad5456, 2016.

1753 Borrmann, S., Kunkel, D., Weigel, R., Minikin, A., Deshler, T., Wilson, J. C., Curtius, J., Volk,
1754 C. M., Homan, C. D., Ulanovsky, A., Ravegnani, F., Viciani, S., Shur, G. N., Belyaev, G.
1755 V., Law, K. S., and Cairo, F., Aerosols in the tropical and subtropical UT/LS: in-situ
1756 measurements of submicron particle abundance and volatility: Atmos. Chem. Phys., 10,
1757 5573-5592, doi:10.5194/acp-10-5573-2010, 2010.

1758 Braga, R. C., Rosenfeld, D., Weigel, R., Jurkat, T., Andreae, M. O., Wendisch, M., Pöschl, U.,
1759 Voigt, C., Mahnke, C., Borrmann, S., Albrecht, R. I., Molleker, S., Vila, D. A., Machado,
1760 L. A. T., and Grulich, L., Aerosol concentrations determine the height of warm rain and
1761 ice initiation in convective clouds over the Amazon basin: Atmos. Chem. Phys. Discuss.,
1762 2017, 1-44, doi:10.5194/acp-2016-1155, 2017.

1763 Brock, C. A., Hamill, P., Wilson, J. C., Jonsson, H. H., and Chan, K. R., Particle formation in the
1764 upper tropical troposphere - a source of nuclei for the stratospheric aerosol: Science, 270,
1765 1650-1653, doi:10.1126/science.270.5242.1650, 1995.

1766 Brock, C. A., Cozic, J., Bahreini, R., Froyd, K. D., Middlebrook, A. M., McComiskey, A.,
1767 Brioude, J., Cooper, O. R., Stohl, A., Aikin, K. C., de Gouw, J. A., Fahey, D. W., Ferrare,
1768 R. A., Gao, R. S., Gore, W., Holloway, J. S., Hubler, G., Jefferson, A., Lack, D. A.,
1769 Lance, S., Moore, R. H., Murphy, D. M., Nenes, A., Novelli, P. C., Nowak, J. B., Ogren,
1770 J. A., Peischl, J., Pierce, R. B., Pilewskie, P., Quinn, P. K., Ryerson, T. B., Schmidt, K.
1771 S., Schwarz, J. P., Sodemann, H., Spackman, J. R., Stark, H., Thomson, D. S.,
1772 Thornberry, T., Veres, P., Watts, L. A., Warneke, C., and Wollny, A. G., Characteristics,
1773 sources, and transport of aerosols measured in spring 2008 during the aerosol, radiation,
1774 and cloud processes affecting Arctic Climate (ARCPAC) Project: Atmos. Chem. Phys.,
1775 11, 2423-2453, doi:10.5194/acp-11-2423-2011, 2011.

1776 Browell, E. V., Fenn, M. A., Butler, C. F., Grant, W. B., Clayton, M. E., Fishman, J., Bachmeier,
1777 A. S., Anderson, B. E., Gregory, G. L., Fuelberg, H. E., Bradshaw, J. D., Sandholm, S.
1778 T., Blake, D. R., Heikes, B. G., Sachse, G. W., Singh, H. B., and Talbot, R. W., Ozone

and aerosol distributions and air mass characteristics over the South Atlantic basin during the burning season: J. Geophys. Res., 101, 24,043-24,068, 1996.

Bruns, E. A., Perraud, V., Zelenyuk, A., Ezell, M. J., Johnson, S. N., Yu, Y., Imre, D., Finlayson-Pitts, B. J., and Alexander, M. L., Comparison of FTIR and particle mass spectrometry for the measurement of particulate organic nitrates: Environ. Sci. Technol., 44, 1056-1061, doi:10.1021/es9029864, 2010.

Cai, Y., Montague, D. C., Mooiweer-Bryan, W., and Deshler, T., Performance characteristics of the ultra high sensitivity aerosol spectrometer for particles between 55 and 800 nm: Laboratory and field studies: J. Aerosol Sci., 39, 759-769, doi:10.1016/j.jaerosci.2008.04.007, 2008.

Carslaw, K. S., Lee, L. A., Reddington, C. L., Pringle, K. J., Rap, A., Forster, P. M., Mann, G. W., Spracklen, D. V., Woodhouse, M. T., Regayre, L. A., and Pierce, J. R., Large contribution of natural aerosols to uncertainty in indirect forcing: Nature, 503, 67-71, doi:10.1038/nature12674, 2013.

Carslaw, K. S., Gordon, H., Hamilton, D. S., Johnson, J. S., Regayre, L. A., Yoshioka, M., and Pringle, K. J., Aerosols in the pre-industrial atmosphere: Current Climate Change Reports, 3, 1-15, doi:10.1007/s40641-017-0061-2, 2017.

Cecchini, M. A., Machado, L. A. T., Andreae, M. O., Martin, S. T., Albrecht, R. I., Artaxo, P., Barbosa, H. M. J., Borrmann, S., Fütterer, D., Jurkat, T., Mahnke, C., Minikin, A., Molleker, S., Pöhlker, M. L., Pöschl, U., Rosenfeld, D., Voigt, C., Weinzierl, B., and Wendisch, M., Sensitivities of Amazonian clouds to aerosols and updraft speed: Atmos. Chem. Phys., 17, 10,037-10,050, doi:10.5194/acp-17-10037-2017, 2017.

Chubb, T., Huang, Y., Jensen, J., Campos, T., Siems, S., and Manton, M., Observations of high droplet number concentrations in Southern Ocean boundary layer clouds: Atmos. Chem. Phys., 16, 971-987, doi:10.5194/acp-16-971-2016, 2016.

Clarke, A., and Kapustin, V., Hemispheric aerosol vertical profiles: Anthropogenic impacts on optical depth and cloud nuclei: Science, 329, 1488-1492, 2010.

Clarke, A. D., Atmospheric nuclei in the remote free troposphere: J. Atmos. Chem., 14, 479-488, doi:10.1007/bf00115252, 1992.

Clarke, A. D., Atmospheric nuclei in the Pacific midtroposphere - their nature, concentration, and evolution: J. Geophys. Res., 98, 20,633-20,647, doi:10.1029/93jd00797, 1993.

Clarke, A. D., Varner, J. L., Eisele, F., Mauldin, R. L., Tanner, D., and Litchy, M., Particle production in the remote marine atmosphere: Cloud outflow and subsidence during ACE 1: J. Geophys. Res., 103, 16,397-16,409, doi:10.1029/97jd02987, 1998.

Clarke, A. D., Eisele, F., Kapustin, V. N., Moore, K., Tanner, D., Mauldin, L., Litchy, M., Lienert, B., Carroll, M. A., and Albercook, G., Nucleation in the equatorial free troposphere: Favorable environments during PEM-Tropics: J. Geophys. Res., 104, 5735-5744, doi:10.1029/98JD02303, 1999.

Clarke, A. D., and Kapustin, V. N., A Pacific aerosol survey. Part I: A decade of data on particle production, transport, evolution, and mixing in the troposphere: J. Atmos. Sci., 59, 363-382, 2002.

1820 Clarke, A. D., Freitag, S., Simpson, R. M. C., Hudson, J. G., Howell, S. G., Brekhovskikh, V. L.,
1821 Campos, T., Kapustin, V. N., and Zhou, J., Free troposphere as a major source of CCN
1822 for the Equatorial Pacific boundary layer: long-range transport and teleconnections:
1823 Atmos. Chem. Phys., 13, 7511-7529, doi:10.5194/acp-13-7511-2013, 2013.

1824 Collow, A. B. M., Miller, M. A., and Trabachino, L. C., Cloudiness over the Amazon rainforest:
1825 Meteorology and thermodynamics: J. Geophys. Res., 121, 7990-8005,
1826 doi:10.1002/2016JD024848, 2016.

1827 Colomb, A., Williams, J., Crowley, J., Gros, V., Hofmann, R., Salisbury, G., Klupfel, T.,
1828 Kormann, R., Stickler, A., Forster, C., and Lelieveld, J., Airborne measurements of trace
1829 organic species in the upper troposphere over Europe: the impact of deep convection:
1830 Environmental Chemistry, 3, 244-259, doi:10.1071/en06020, 2006.

1831 Cubison, M. J., Ortega, A. M., Hayes, P. L., Farmer, D. K., Day, D., Lechner, M. J., Brune, W.
1832 H., Apel, E., Diskin, G. S., Fisher, J. A., Fuelberg, H. E., Hecobian, A., Knapp, D. J.,
1833 Mikoviny, T., Riemer, D., Sachse, G. W., Sessions, W., Weber, R. J., Weinheimer, A. J.,
1834 Wisthaler, A., and Jimenez, J. L., Effects of aging on organic aerosol from open biomass
1835 burning smoke in aircraft and laboratory studies: Atmos. Chem. Phys., 11, 12,049-
1836 12,064, doi:10.5194/acp-11-12049-2011, 2011.

1837 Dagan, G., Koren, I., Altaratz, O., and Heiblum, R. H., Aerosol effect on the evolution of the
1838 thermodynamic properties of warm convective cloud fields: Scientific Reports, 6, 38769,
1839 doi:10.1038/srep38769, 2016.

1840 de Reus, M., Krejci, R., Williams, J., Fischer, H., Scheele, R., and Strom, J., Vertical and
1841 horizontal distributions of the aerosol number concentration and size distribution over the
1842 northern Indian Ocean: J. Geophys. Res., 106, 28,629-28,641, 2001.

1843 Drewnick, F., Hings, S. S., DeCarlo, P., Jayne, J. T., Gonin, M., Fuhrer, K., Weimer, S.,
1844 Jimenez, J. L., Demerjian, K. L., Borrmann, S., and Worsnop, D. R., A new time-of-
1845 flight aerosol mass spectrometer (TOF-AMS) - Instrument description and first field
1846 deployment: Aerosol Sci. Tech., 39, 637-658, 2005.

1847 Dunne, E. M., Gordon, H., Kürten, A., Almeida, J., Duplissy, J., Williamson, C., Ortega, I. K.,
1848 Pringle, K. J., Adamov, A., Baltensperger, U., Barmet, P., Benduhn, F., Bianchi, F.,
1849 Breitenlechner, M., Clarke, A., Curtius, J., Dommen, J., Donahue, N. M., Ehrhart, S.,
1850 Flagan, R. C., Franchin, A., Guida, R., Hakala, J., Hansel, A., Heinritzi, M., Jokinen, T.,
1851 Kangasluoma, J., Kirkby, J., Kulmala, M., Kupc, A., Lawler, M. J., Lehtipalo, K.,
1852 Makhmutov, V., Mann, G., Mathot, S., Merikanto, J., Miettinen, P., Nenes, A., Onnela,
1853 A., Rap, A., Reddington, C. L. S., Riccobono, F., Richards, N. A. D., Rissanen, M. P.,
1854 Rondo, L., Sarnela, N., Schobesberger, S., Sengupta, K., Simon, M., Sipilä, M., Smith, J.
1855 N., Stozkhov, Y., Tomé, A., Tröstl, J., Wagner, P. E., Wimmer, D., Winkler, P. M.,
1856 Worsnop, D. R., and Carslaw, K. S., Global atmospheric particle formation from CERN
1857 CLOUD measurements: Science, 354, 1119-1124, doi:10.1126/science.aaf2649, 2016.

1858 Ehn, M., Thornton, J. A., Kleist, E., Sipila, M., Junninen, H., Pullinen, I., Springer, M., Rubach,
1859 F., Tillmann, R., Lee, B., Lopez-Hilfiker, F., Andres, S., Acir, I. H., Rissanen, M.,
1860 Jokinen, T., Schobesberger, S., Kangasluoma, J., Kontkanen, J., Nieminen, T., Kurten,
1861 T., Nielsen, L. B., Jorgensen, S., Kjaergaard, H. G., Canagaratna, M., Dal Maso, M.,
1862 Berndt, T., Petaja, T., Wahner, A., Kerminen, V. M., Kulmala, M., Worsnop, D. R.,

Wildt, J., and Mentel, T. F., A large source of low-volatility secondary organic aerosol: Nature, 506, 476-479, doi:10.1038/nature13032, 2014.

Ekman, A. M. L., Wang, C., Strom, J., and Krejci, R., Explicit simulation of aerosol physics in a cloud-resolving model: Aerosol transport and processing in the free troposphere: J. Atmos. Sci., 63, 682-696, 2006.

Ekman, A. M. L., Krejci, R., Engström, A., Ström, J., de Reus, M., Williams, J., and Andreae, M. O., Do organics contribute to small particle formation in the Amazonian upper troposphere?: Geophys. Res. Lett., 35, L17810, doi:10.1029/2008GL034970, 2008.

Ekman, A. M. L., Hermann, M., Gross, P., Heintzenberg, J., Kim, D., and Wang, C., Sub-micrometer aerosol particles in the upper troposphere/lowermost stratosphere as measured by CARIBIC and modeled using the MIT-CAM3 global climate model: J. Geophys. Res., 117, D11202, doi:10.1029/2011jd016777, 2012.

Engelhart, G. J., Asa-Awuku, A., Nenes, A., and Pandis, S. N., CCN activity and droplet growth kinetics of fresh and aged monoterpene secondary organic aerosol: Atmos. Chem. Phys., 8, 3937-3949, 2008.

Engelhart, G. J., Moore, R. H., Nenes, A., and Pandis, S. N., Cloud condensation nuclei activity of isoprene secondary organic aerosol: J. Geophys. Res., 116, D02207, doi:10.1029/2010jd014706, 2011.

Engström, A., Ekman, A. M. L., Krejci, R., Strom, J., de Reus, M., and Wang, C., Observational and modelling evidence of tropical deep convective clouds as a source of mid-tropospheric accumulation mode aerosols: Geophys. Res. Lett., 35, L23813, doi:10.1029/2008gl035817, 2008.

Fan, J. W., Rosenfeld, D., Ding, Y. N., Leung, L. R., and Li, Z. Q., Potential aerosol indirect effects on atmospheric circulation and radiative forcing through deep convection: Geophys. Res. Lett., 39, L09806, doi:10.1029/2012gl051851, 2012.

Fishman, J., Fakhruzzaman, K., Cros, B., and Nganga, D., Identification of widespread pollution in the southern hemisphere deduced from satellite analyses: Science, 252, 1693-1696, 1991.

Fishman, J., Brackett, V. G., Browell, E. V., and Grant, W. B., Tropospheric ozone derived from TOMS/SBUV measurements during TRACE-A: J. Geophys. Res., 101, 24,069-24,082, 1996.

Frey, W., Borrmann, S., Kunkel, D., Weigel, R., de Reus, M., Schlager, H., Roiger, A., Voigt, C., Hoor, P., Curtius, J., Kraemer, M., Schiller, C., Volk, C. M., Homan, C. D., Fierli, F., Di Donfrancesco, G., Ulanovsky, A., Ravegnani, F., Sitnikov, N. M., Viciani, S., D'Amato, F., Shur, G. N., Belyaev, G. V., Law, K. S., and Cairo, F., In situ measurements of tropical cloud properties in the West African Monsoon: upper tropospheric ice clouds, Mesoscale Convective System outflow, and subvisual cirrus: Atmos. Chem. Phys., 11, 5569-5590, doi:10.5194/acp-11-5569-2011, 2011.

Froyd, K. D., Murphy, D. M., Sanford, T. J., Thomson, D. S., Wilson, J. C., Pfister, L., and Lait, L., Aerosol composition of the tropical upper troposphere: Atmos. Chem. Phys., 9, 4363-4385, 2009.

Fry, J. L., Kiendler-Scharr, A., Rollins, A. W., Wooldridge, P. J., Brown, S. S., Fuchs, H., Dube, W., Mensah, A., dal Maso, M., Tillmann, R., Dorn, H. P., Brauers, T., and Cohen, R. C., Organic nitrate and secondary organic aerosol yield from NO_3 oxidation of beta-pinene evaluated using a gas-phase kinetics/aerosol partitioning model: Atmos. Chem. Phys., 9, 1431-1449, 2009.

Fu, R., Zhu, B., and Dickinson, R. E., How do atmosphere and land surface influence seasonal changes of convection in the tropical Amazon?: J. Clim., 12, 1306-1321, 1999.

Fueglistaler, S., Dessler, A. E., Dunkerton, T. J., Folkins, I., Fu, Q., and Mote, P. W., Tropical tropopause layer: Rev. Geophys., 47, RG1004, doi:10.1029/2008rg000267, 2009.

Gerbig, C., Schmitgen, S., Kley, D., Volz-Thomas, A., Dewey, K., and Haaks, D., An improved fast-response vacuum-UV resonance fluorescence CO instrument: J. Geophys. Res., 104, 1699-1704, doi:10.1029/1998jd100031, 1999.

Gerken, T., Wei, D., Chase, R. J., Fuentes, J. D., Schumacher, C., Machado, L. A. T., Andreoli, R. V., Chamecki, M., Ferreira de Souza, R. A., Freire, L. S., Jardine, A. B., Manzi, A. O., Nascimento dos Santos, R. M., von Randow, C., dos Santos Costa, P., Stoy, P. C., Tóta, J., and Trowbridge, A. M., Downward transport of ozone rich air and implications for atmospheric chemistry in the Amazon rainforest: Atmospheric Environment, 124, 64-76, doi:10.1016/j.atmosenv.2015.11.014, 2016.

Giangrande, S. E., Feng, Z., Jensen, M. P., Comstock, J., Johnson, K. L., Toto, T., Wang, M., Burleyson, C., Mei, F., Machado, L. A. T., Manzi, A., Xie, S., Tang, S., Silva Dias, M. A. F., de Souza, R. A. F., Schumacher, C., and Martin, S. T., Cloud Characteristics, Thermodynamic Controls and Radiative Impacts During the Observations and Modeling of the Green Ocean Amazon (GoAmazon2014/5) Experiment: Atmos. Chem. Phys. Discuss., 2017, 1-41, doi:10.5194/acp-2017-452, 2017.

Gonçalves, W. A., Machado, L. A. T., and Kirstetter, P. E., Influence of biomass aerosol on precipitation over the Central Amazon: an observational study: Atmos. Chem. Phys., 15, 6789-6800, doi:10.5194/acp-15-6789-2015, 2015.

Gordon, H., Sengupta, K., Rap, A., Duplissy, J., Frege, C., Williamson, C., Heinritzi, M., Simon, M., Yan, C., Almeida, J., Tröstl, J., Nieminen, T., Ortega, I. K., Wagner, R., Dunne, E. M., Adamov, A., Amorim, A., Bernhammer, A.-K., Bianchi, F., Breitenlechner, M., Brilke, S., Chen, X., Craven, J. S., Dias, A., Ehrhart, S., Fischer, L., Flagan, R. C., Franchin, A., Fuchs, C., Guida, R., Hakala, J., Hoyle, C. R., Jokinen, T., Junninen, H., Kangasluoma, J., Kim, J., Kirkby, J., Krapf, M., Kürten, A., Laaksonen, A., Lehtipalo, K., Makhmutov, V., Mathot, S., Molteni, U., Monks, S. A., Onnela, A., Peräkylä, O., Piel, F., Petäjä, T., Praplan, A. P., Pringle, K. J., Richards, N. A. D., Rissanen, M. P., Rondo, L., Sarnela, N., Schobesberger, S., Scott, C. E., Seinfeld, J. H., Sharma, S., Sipilä, M., Steiner, G., Stozhkov, Y., Stratmann, F., Tomé, A., Virtanen, A., Vogel, A. L., Wagner, A. C., Wagner, P. E., Weingartner, E., Wimmer, D., Winkler, P. M., Ye, P., Zhang, X., Hansel, A., Dommen, J., Donahue, N. M., Worsnop, D. R., Baltensperger, U., Kulmala, M., Curtius, J., and Carslaw, K. S., Reduced anthropogenic aerosol radiative forcing caused by biogenic new particle formation: Proc. Natl. Acad. Sci., 113, 12,053-12,058, doi:10.1073/pnas.1602360113, 2016.

Grant, D. D., Fuentes, J. D., DeLonge, M. S., Chan, S., Joseph, E., Kucera, P., Ndiaye, S. A., and Gaye, A. T., Ozone transport by mesoscale convective storms in western Senegal: Atmospheric Environment, 42, 7104-7114, doi:10.1016/j.atmosenv.2008.05.044, 2008.

Gunthe, S. S., King, S. M., Rose, D., Chen, Q., Roldin, P., Farmer, D. K., Jimenez, J. L., Artaxo, P., Andreae, M. O., Martin, S. T., and Pöschl, U., Cloud condensation nuclei in pristine tropical rainforest air of Amazonia: size-resolved measurements and modeling of atmospheric aerosol composition and CCN activity: Atmos. Chem. Phys., 9, 7551–7575, 2009.

Heald, C. L., Jacob, D. J., Park, R. J., Russell, L. M., Huebert, B. J., Seinfeld, J. H., Liao, H., and Weber, R. J., A large organic aerosol source in the free troposphere missing from current models: Geophys. Res. Lett., 32, L18809, doi:10.1029/2005GL023831, 2005.

Heintzenberg, J., Birmili, W., Otto, R., Andreae, M. O., Mayer, J.-C., Chi, X., and Panov, A., Aerosol particle number size distributions and particulate light absorption at the ZOTTO tall tower (Siberia), 2006-2009: Atmos. Chem. Phys., 11, 8703-8719, 2011.

Holanda, B. A., Wang, Q., Saturno, J., Ditas, F., Ditas, J., Pöhlker, M., Klimach, T., Moran, D., Schulz, C., Ming, J., Cheng, Y., Su, H., Wendisch, M., Machado, L. A. T., Schneider, J., Pöhlker, C., Artaxo, P., Pöschl, U., and Andreae, M., Transatlantic transport of pollution aerosol from Africa to the Amazon rain forest - Aircraft observations in the context of the ACRIDICON-CHUVA campaign: Atmos. Chem. Phys. Discuss., 2017, in preparation.

Hu, W. W., Campuzano-Jost, P., Palm, B. B., Day, D. A., Ortega, A. M., Hayes, P. L., Krechmer, J. E., Chen, Q., Kuwata, M., Liu, Y. J., de Sa, S. S., McKinney, K., Martin, S. T., Hu, M., Budisulistiorini, S. H., Riva, M., Surratt, J. D., St Clair, J. M., Isaacman-Van Wertz, G., Yee, L. D., Goldstein, A. H., Carbone, S., Brito, J., Artaxo, P., de Gouw, J. A., Koss, A., Wisthaler, A., Mikoviny, T., Karl, T., Kaser, L., Jud, W., Hansel, A., Docherty, K. S., Alexander, M. L., Robinson, N. H., Coe, H., Allan, J. D., Canagaratna, M. R., Paulot, F., and Jimenez, J. L., Characterization of a real-time tracer for isoprene epoxydiols-derived secondary organic aerosol (IEPOX-SOA) from aerosol mass spectrometer measurements: Atmos. Chem. Phys., 15, 11,807-11,833, doi:10.5194/acp-15-11807-2015, 2015.

Hu, X. M., Fuentes, J. D., and Zhang, F. Q., Downward transport and modification of tropospheric ozone through moist convection: J. Atmos. Chem., 65, 13-35, doi:10.1007/s10874-010-9179-5, 2010.

Huntrieser, H., Lichtenstern, M., Scheibe, M., Aufmhoff, H., Schlager, H., Pucik, T., Minikin, A., Weinzierl, B., Heimerl, K., Futterer, D., Rappengluck, B., Ackermann, L., Pickering, K. E., Cummings, K. A., Biggerstaff, M. I., Betten, D. P., Honomichl, S., and Barth, M. C., On the origin of pronounced O_3 gradients in the thunderstorm outflow region during DC3: J. Geophys. Res., 121, 6600-6637, doi:10.1002/2015jd024279, 2016.

Janhäll, S., Andreae, M. O., and Pöschl, U., Biomass burning aerosol emissions from vegetation fires: particle number and mass emission factors and size distributions: Atmos. Chem. Phys., 10, 1427-1439, 2010.

Jiang, J. H., Su, H., Schoeberl, M. R., Massie, S. T., Colarco, P., Platnick, S., and Livesey, N. J., Clean and polluted clouds: Relationships among pollution, ice clouds, and precipitation in South America: Geophys. Res. Lett., 35, L14804, doi:10.1029/2008GL034631, 2008.

Jimenez, J. L., Canagaratna, M. R., Donahue, N. M., Prevot, A. S. H., Zhang, Q., Kroll, J. H., DeCarlo, P. F., Allan, J. D., Coe, H., Ng, N. L., Aiken, A. C., Docherty, K. D., Ulbrich, I. M., Grieshop, A. P., Robinson, A. L., Duplissy, J., Smith, J. D., Wilson, K. R., Lanz, V. A., Hueglin, C., Sun, Y. L., Tian, J., Laaksonen, A., Raatikainen, T., Rautiainen, J., Vaattovaara, P., Ehn, M., Kulmala, M., Tomlinson, J. M., Collins, D. R., Cubison, M. J., Dunlea, E. J., Huffman, J. A., Onasch, T. B., Alfarra, M. R., Williams, P. I., Bower, K., Kondo, Y., Schneider, J., Drewnick, F., Borrmann, S., Weimer, S., Demerjian, K., Salcedo, D., Cottrell, L., Griffin, R., Takami, A., Miyoshi, T., Hatakeyama, S., Shimono, A., Sun, J. Y., Zhang, Y. M., Dzepina, K., Kimmel, J. R., Sueper, D., Jayne, J. T., Herndon, S. C., Trimborn, A. M., Williams, L. R., Wood, E. C., Kolb, C. E., Baltensperger, U., and Worsnop, D. R., Evolution of organic aerosols in the atmosphere: Science, 326, 1525-529, doi:10.1126/science.1180353, 2009.

Jokinen, T., Berndt, T., Makkonen, R., Kerminen, V.-M., Junninen, H., Paasonen, P., Stratmann, F., Herrmann, H., Guenther, A. B., Worsnop, D. R., Kulmala, M., Ehn, M., and Sipilä, M., Production of extremely low volatile organic compounds from biogenic emissions: Measured yields and atmospheric implications: Proc. Natl. Acad. Sci., 112, 7123-7128, doi:10.1073/pnas.1423977112, 2015.

Katoshevski, D., Nenes, A., and Seinfeld, J. H., A study of processes that govern the maintenance of aerosols in the marine boundary layer: J. Aerosol Sci., 30, 503-532, 1999.

Khain, A. P., Phillips, V., Benmoshe, N., and Pokrovsky, A., The role of small soluble aerosols in the microphysics of deep maritime clouds: J. Atmos. Sci., 69, 2787-2807, doi:10.1175/2011jas3649.1, 2012.

Kirkby, J., Duplissy, J., Sengupta, K., Frege, C., Gordon, H., Williamson, C., Heinritzi, M., Simon, M., Yan, C., Almeida, J., Tröstl, J., Nieminen, T., Ortega, I. K., Wagner, R., Adamov, A., Amorim, A., Bernhammer, A.-K., Bianchi, F., Breitenlechner, M., Brilke, S., Chen, X., Craven, J., Dias, A., Ehrhart, S., Flagan, R. C., Franchin, A., Fuchs, C., Guida, R., Hakala, J., Hoyle, C. R., Jokinen, T., Junninen, H., Kangasluoma, J., Kim, J., Krapf, M., Kürten, A., Laaksonen, A., Lehtipalo, K., Makhmutov, V., Mathot, S., Molteni, U., Onnela, A., Peräkylä, O., Piel, F., Petäjä, T., Praplan, A. P., Pringle, K., Rap, A., Richards, N. A. D., Riipinen, I., Rissanen, M. P., Rondo, L., Sarnela, N., Schobesberger, S., Scott, C. E., Seinfeld, J. H., Sipilä, M., Steiner, G., Stozhkov, Y., Stratmann, F., Tomé, A., Virtanen, A., Vogel, A. L., Wagner, A. C., Wagner, P. E., Weingartner, E., Wimmer, D., Winkler, P. M., Ye, P., Zhang, X., Hansel, A., Dommen, J., Donahue, N. M., Worsnop, D. R., Baltensperger, U., Kulmala, M., Carslaw, K. S., and Curtius, J., Ion-induced nucleation of pure biogenic particles: Nature, 533, 521-526, doi:10.1038/nature17953, 2016.

Kojima, T., Buseck, P. R., Wilson, J. C., Reeves, J. M., and Mahoney, M. J., Aerosol particles from tropical convective systems: Cloud tops and cirrus anvils: J. Geophys. Res., 109, D12201, 2004.

Koren, I., Martins, J. V., Remer, L. A., and Afargan, H., Smoke invigoration versus inhibition of clouds over the Amazon: Science 321, 946-949, 2008.

2030 Koren, I., Remer, L. A., Altaratz, O., Martins, J. V., and Davidi, A., Aerosol-induced changes of
2031 convective cloud anvils produce strong climate warming: Atmos. Chem. Phys., 10, 5001-
2032 5010, doi:10.5194/acp-10-5001-2010, 2010.

2033 Kottayil, A., and Satheesan, K., Enhancement in the upper tropospheric humidity associated with
2034 aerosol loading over tropical Pacific: Atmospheric Environment, 122, 148-153,
2035 doi:10.1016/j.atmosenv.2015.09.043, 2015.

2036 Krejci, R., Strom, J., de Reus, M., Hoor, P., Williams, J., Fischer, H., and Hansson, H. C.,
2037 Evolution of aerosol properties over the rain forest in Surinam, South America, observed
2038 from aircraft during the LBA-CLAIRE 98 experiment: J. Geophys. Res., 108, 4561,
2039 doi:10.1029/2001JD001375, 2003.

2040 Krüger, M. L., Mertes, S., Klimach, T., Cheng, Y., Su, H., Schneider, J., Andreae, M. O., Pöschl,
2041 U., and Rose, D., Assessment of cloud supersaturation by size-resolved aerosol particle
2042 and cloud condensation nuclei (CCN) measurements: Atmos. Meas. Tech., 7, 2615–2629,
2043 doi:10.5194/amt-7-2615-2014, 2014.

2044 Kulmala, M., Reissell, A., Sipila, M., Bonn, B., Ruuskanen, T. M., Lehtinen, K. E. J., Kerminen,
2045 V.-M., and Strom, J., Deep convective clouds as aerosol production engines: Role of
2046 insoluble organics: J. Geophys. Res., 111, D17202, doi:10.1029/2005jd006963, 2006.

2047 Kulmala, M., and Kerminen, V. M., On the formation and growth of atmospheric nanoparticles:
2048 Atmos. Res., 90, 132-150, doi:10.1016/j.atmosres.2008.01.005, 2008.

2049 Laaksonen, A., Kulmala, M., O'Dowd, C. D., Joutsensaari, J., Vaattovaara, P., Mikkonen, S.,
2050 Lehtinen, K. E. J., Sogacheva, L., Dal Maso, M., Aalto, P., Petaja, T., Sogachev, A.,
2051 Yoon, Y. J., Lihavainen, H., Nilsson, D., Facchini, M. C., Cavalli, F., Fuzzi, S.,
2052 Hoffmann, T., Arnold, F., Hanke, M., Sellegri, K., Umann, B., Junkermann, W., Coe, H.,
2053 Allan, J. D., Alfarra, M. R., Worsnop, D. R., Riekkola, M. L., Hyotylainen, T., and
2054 Viisanen, Y., The role of VOC oxidation products in continental new particle formation:
2055 Atmos. Chem. Phys., 8, 2657-2665, 2008.

2056 Laborde, M., Crippa, M., Tritscher, T., Juranyi, Z., Decarlo, P. F., Temime-Roussel, B.,
2057 Marchand, N., Eckhardt, S., Stohl, A., Baltensperger, U., Prevot, A. S. H., Weingartner,
2058 E., and Gysel, M., Black carbon physical properties and mixing state in the European
2059 megacity Paris: Atmos. Chem. Phys., 13, 5831-5856, doi:10.5194/acp-13-5831-2013,
2060 2013.

2061 Lee, L., Wooldridge, P. J., Gilman, J. B., Warneke, C., de Gouw, J., and Cohen, R. C., Low
2062 temperatures enhance organic nitrate formation: evidence from observations in the 2012
2063 Uintah Basin Winter Ozone Study: Atmos. Chem. Phys., 14, 12,441-12,454,
2064 doi:10.5194/acp-14-12441-2014, 2014.

2065 Lee, S. H., Reeves, J. M., Wilson, J. C., Hunton, D. E., Viggiano, A. A., Miller, T. M.,
2066 Ballenthin, J. O., and Lait, L. R., Particle formation by ion nucleation in the upper
2067 troposphere and lower stratosphere: Science, 301, 1886-1889,
2068 doi:10.1126/science.1087236, 2003.

2069 Lee, S. H., Wilson, J. C., Baumgardner, D., Herman, R. L., Weinstock, E. M., LaFleur, B. G.,
2070 Kok, G., Anderson, B., Lawson, P., Baker, B., Strawa, A., Pittman, J. V., Reeves, J. M.,

and Bui, T. P., New particle formation observed in the tropical/subtropical cirrus clouds: J. Geophys. Res., 109, D20209, doi:10.1029/2004jd005033, 2004.

Machado, L. A. T., Laurent, H., Dessay, N., and Miranda, I., Seasonal and diurnal variability of convection over the Amazonia: A comparison of different vegetation types and large scale forcing: Theoretical and Applied Climatology, 78, 61-77, doi:10.1007/s00704-004-0044-9, 2004.

Martin, S. T., Andreae, M. O., Artaxo, P., Baumgardner, D., Chen, Q., Goldstein, A. H., Guenther, A., Heald, C. L., Mayol-Bracero, O. L., McMurry, P. H., Pauliquevis, T., Pöschl, U., Prather, K. A., Roberts, G. C., Saleska, S. R., Dias, M. A. S., Spracklen, D., Swietlicki, E., and Trebs, I., Sources and properties of Amazonian aerosol particles: Rev. Geophys., 48, RG2002, doi:10.1029/2008RG000280, 2010.

Martin, S. T., Artaxo, P., Machado, L. A. T., Manzi, A. O., Souza, R. A. F., Schumacher, C., Wang, J., Andreae, M. O., Barbosa, H. M. J., Fan, J., Fisch, G., Goldstein, A. H., Guenther, A., Jimenez, J. L., Pöschl, U., Silva Dias, M. A., Smith, J. N., and Wendisch, M., Introduction: Observations and modeling of the Green Ocean Amazon (GoAmazon2014/5): Atmos. Chem. Phys., 16, 4785-4797, doi:10.5194/acp-16-4785-2016, 2016.

Merikanto, J., Spracklen, D. V., Mann, G. W., Pickering, S. J., and Carslaw, K. S., Impact of nucleation on global CCN: Atmos. Chem. Phys., 9, 8601-8616, 2009.

Metzger, A., Verheggen, B., Dommen, J., Duplissy, J., Prevot, A. S. H., Weingartner, E., Riipinen, I., Kulmala, M., Spracklen, D. V., Carslaw, K. S., and Baltensperger, U., Evidence for the role of organics in aerosol particle formation under atmospheric conditions: Proc. Natl. Acad. Sci., doi:10.1073/pnas.0911330107, 2010.

Mirme, S., Mirme, A., Minikin, A., Petzold, A., Horrak, U., Kerminen, V. M., and Kulmala, M., Atmospheric sub-3 nm particles at high altitudes: Atmos. Chem. Phys., 10, 437-451, 2010.

Murphy, B. N., Julin, J., Riipinen, I., and Ekman, A. M. L., Organic aerosol processing in tropical deep convective clouds: Development of a new model (CRM-ORG) and implications for sources of particle number: J. Geophys. Res., 120, 10,441-10,464, doi:10.1002/2015JD023551, 2015.

Newell, R. E., Thouret, V., Cho, J. Y. N., Stoller, P., Marenco, A., and Smit, H. G., Ubiquity of quasi-horizontal layers in the troposphere: Nature, 398, 316-319, 1999.

Ng, N. L., Canagaratna, M. R., Jimenez, J. L., Chhabra, P. S., Seinfeld, J. H., and Worsnop, D. R., Changes in organic aerosol composition with aging inferred from aerosol mass spectra: Atmos. Chem. Phys., 11, 6465-6474, doi:10.5194/acp-11-6465-2011, 2011.

Öström, E., Putian, Z., Schurgers, G., Mishurov, M., Kivekäs, N., Lihavainen, H., Ehn, M., Rissanen, M. P., Kurtén, T., Boy, M., Swietlicki, E., and Roldin, P., Modeling the role of highly oxidized multifunctional organic molecules for the growth of new particles over the boreal forest region: Atmos. Chem. Phys., 17, 8887-8901, doi:10.5194/acp-17-8887-2017, 2017.

Petters, M. D., and Kreidenweis, S. M., A single parameter representation of hygroscopic growth and cloud condensation nucleus activity: Atmos. Chem. Phys., 7, 1961–1971, 2007.

2113 Petzold, A., Marsh, R., Johnson, M., Miller, M., Sevcenco, Y., Delhaye, D., Ibrahim, A.,
2114 Williams, P., Bauer, H., Crayford, A., Bachalo, W. D., and Raper, D., Evaluation of
2115 methods for measuring particulate matter emissions from gas turbines: Environ. Sci.
2116 Technol., 45, 3562-3568, doi:10.1021/es103969v, 2011.

2117 Pöhlker, C., Wiedemann, K., Sinha, B., Shiraiwa, M., Gunthe, S., Smith, M., Su, H., Artaxo, P.,
2118 Chen, Q., Cheng, Y., Elbert, W., Gilles, M. K., Kilcoyne, A. L. D., Moffet, R. C.,
2119 Weigand, M., Martin, S. T., Pöschl, U., and Andreae, M. O., Biogenic potassium salt
2120 particles as seeds for secondary organic aerosol in the Amazon: Science, 337, 1075-1078,
2121 2012.

2122 Pöhlker, M. L., Pöhlker, C., Ditas, F., Klimach, T., Hrabe de Angelis, I., Araújo, A., Brito, J.,
2123 Carbone, S., Cheng, Y., Chi, X., Ditz, R., Gunthe, S. S., Kesselmeier, J., Könemann, T.,
2124 Lavrič, J. V., Martin, S. T., Mikhailov, E., Moran-Zuloaga, D., Rose, D., Saturno, J., Su,
2125 H., Thalman, R., Walter, D., Wang, J., Wolff, S., Barbosa, H. M. J., Artaxo, P., Andreae,
2126 M. O., and Pöschl, U., Long-term observations of cloud condensation nuclei in the
2127 Amazon rain forest – Part 1: Aerosol size distribution, hygroscopicity, and new model
2128 parametrizations for CCN prediction: Atmos. Chem. Phys., 16, 15,709-15,740,
2129 doi:10.5194/acp-16-15709-2016, 2016.

2130 Pöschl, U., Martin, S. T., Sinha, B., Chen, Q., Gunthe, S. S., Huffman, J. A., Borrmann, S.,
2131 Farmer, D. K., Garland, R. M., Helas, G., Jimenez, J. L., King, S. M., Manzi, A.,
2132 Mikhailov, E., Pauliquevis, T., Petters, M. D., Prenni, A. J., Roldin, P., Rose, D.,
2133 Schneider, J., Su, H., Zorn, S. R., Artaxo, P., and Andreae, M. O., Rainforest aerosols as
2134 biogenic nuclei of clouds and precipitation in the Amazon: Science, 329, 1513-1516,
2135 2010.

2136 Raes, F., Entrainment of free tropospheric aerosols as a regulating mechanism for cloud
2137 condensation nuclei in the remote marine boundary layer: J. Geophys. Res., 100, 2893-
2138 2903, 1995.

2139 Randel, W. J., and Jensen, E. J., Physical processes in the tropical tropopause layer and their
2140 roles in a changing climate: Nature Geoscience, 6, 169-176, doi:10.1038/ngeo1733, 2013.

2141 Reddington, C. L., Carslaw, K. S., Stier, P., Schutgens, N., Coe, H., Liu, D., Allan, J., Browse,
2142 J., Pringle, K. J., Lee, L. A., Yoshioka, M., Johnson, J. S., Regayre, L. A., Spracklen, D.
2143 V., Mann, G. W., Clarke, A., Hermann, M., Henning, S., Wex, H., Kristensen, T. B.,
2144 Leaitch, W. R., Pöschl, U., Rose, D., Andreae, M. O., Schmale, J., Kondo, Y., Oshima,
2145 N., Schwarz, J. P., Nenes, A., Anderson, B., Roberts, G. C., Snider, J. R., Leck, C.,
2146 Quinn, P. K., Chi, X., Ding, A., Jimenez, J. L., and Zhang, Q., The Global Aerosol
2147 Synthesis and Science Project (GASSP) - Measurements and modelling to reduce
2148 uncertainty: Bull. Am. Meteorol. Soc., 2016, under review.

2149 Riccobono, F., Schobesberger, S., Scott, C. E., Dommen, J., Ortega, I. K., Rondo, L., Almeida,
2150 J., Amorim, A., Bianchi, F., Breitenlechner, M., David, A., Downard, A., Dunne, E. M.,
2151 Duplissy, J., Ehrhart, S., Flagan, R. C., Franchin, A., Hansel, A., Junninen, H., Kajos, M.,
2152 Keskinen, H., Kupc, A., Kürten, A., Kvashin, A. N., Laaksonen, A., Lehtipalo, K.,
2153 Makhmutov, V., Mathot, S., Nieminen, T., Onnela, A., Petäjä, T., Praplan, A. P., Santos,
2154 F. D., Schallhart, S., Seinfeld, J. H., Sipilä, M., Spracklen, D. V., Stozhkov, Y.,
2155 Stratmann, F., Tomé, A., Tsagkogeorgas, G., Vaattovaara, P., Viisanen, Y., Vrtala, A.,

Wagner, P. E., Weingartner, E., Wex, H., Wimmer, D., Carslaw, K. S., Curtius, J., Donahue, N. M., Kirkby, J., Kulmala, M., Worsnop, D. R., and Baltensperger, U., Oxidation products of biogenic emissions contribute to nucleation of atmospheric particles: Science, 344, 717-721, doi:10.1126/science.1243527, 2014.

Riipinen, I., Pierce, J. R., Yli-Juuti, T., Nieminen, T., Hakkinen, S., Ehn, M., Junninen, H., Lehtipalo, K., Petaja, T., Slowik, J., Chang, R., Shantz, N. C., Abbatt, J., Leaitch, W. R., Kerminen, V. M., Worsnop, D. R., Pandis, S. N., Donahue, N. M., and Kulmala, M., Organic condensation: a vital link connecting aerosol formation to cloud condensation nuclei (CCN) concentrations: Atmos. Chem. Phys., 11, 3865-3878, doi:10.5194/acp-11-3865-2011, 2011.

Riipinen, I., Yli-Juuti, T., Pierce, J. R., Petaja, T., Worsnop, D. R., Kulmala, M., and Donahue, N. M., The contribution of organics to atmospheric nanoparticle growth: Nature Geoscience, 5, 453-458, doi:10.1038/ngeo1499, 2012.

Rissler, J., Vestin, A., Swietlicki, E., Fisch, G., Zhou, J., Artaxo, P., and Andreae, M. O., Size distribution and hygroscopic properties of aerosol particles from dry-season biomass burning in Amazonia: Atmos. Chem. Phys., 6, 471-491, 2006.

Riuttanen, L., Bister, M., Kerminen, V. M., John, V. O., Sundstrom, A. M., Dal Maso, M., Raisanen, J., Sinclair, V. A., Makkonen, R., Xausa, F., de Leeuw, G., and Kulmala, M., Observational evidence for aerosols increasing upper tropospheric humidity: Atmos. Chem. Phys., 16, 14,331-14,342, doi:10.5194/acp-16-14331-2016, 2016.

Rizzo, L. V., Artaxo, P., Müller, T., Wiedensohler, A., Paixão, M., Cirino, G. G., Arana, A., Swietlicki, E., Roldin, P., Fors, E. O., Wiedemann, K. T., Leal, L. S. M., and Kulmala, M., Long term measurements of aerosol optical properties at a primary forest site in Amazonia: Atmos. Chem. Phys., 13, 2391-2413, doi:10.5194/acp-13-2391-2013, 2013.

Roberts, G. C., and Andreae, M. O., Reply to "Comment on Cloud condensation nuclei in the Amazon Basin: "Marine" conditions over a continent?" by P. J. Crutzen et al.: Geophys. Res. Lett., 30, doi:10.1029/2002GL015564, 2003.

Roberts, G. C., and Nenes, A., A continuous-flow streamwise thermal-gradient CCN chamber for atmospheric measurements: Aerosol Sci. Tech., 39, 206-221, 2005.

Robinson, N. H., Hamilton, J. F., Allan, J. D., Langford, B., Oram, D. E., Chen, Q., Docherty, K., Farmer, D. K., Jimenez, J. L., Ward, M. W., Hewitt, C. N., Barley, M. H., Jenkin, M. E., Rickard, A. R., Martin, S. T., McFiggans, G., and Coe, H., Evidence for a significant proportion of Secondary Organic Aerosol from isoprene above a maritime tropical forest: Atmos. Chem. Phys., 11, 1039-1050, 2011.

Rose, C., Sellegri, K., Moreno, I., Velarde, F., Ramonet, M., Weinhold, K., Krejci, R., Andrade, M., Wiedensohler, A., Ginot, P., and Laj, P., CCN production by new particle formation in the free troposphere: Atmos. Chem. Phys., 17, 1529-1541, doi:10.5194/acp-17-1529-2017, 2017.

Rose, D., Gunthe, S. S., Mikhailov, E., Frank, G. P., Dusek, U., Andreae, M. O., and Pöschl, U., Calibration and measurement uncertainties of a continuous-flow cloud condensation nuclei counter (DMT-CCNC): CCN activation of ammonium sulfate and sodium chloride aerosol particles in theory and experiment: Atmos. Chem. Phys., 8, 1153-1179, 2008.

2198 Rosenfeld, D., Lohmann, U., Raga, G. B., O'Dowd, C. D., Kulmala, M., Fuzzi, S., Reissell, A.,
2199 and Andreae, M. O., Flood or drought: How do aerosols affect precipitation?: Science,
2200 321, 1309-1313, 2008.

2201 Rosenfeld, D., Andreae, M. O., Asmi, A., Chin, M., de Leeuw, G., Donovan, D. P., Kahn, R.,
2202 Kinne, S., Kivekäs, N., Kulmala, M., Lau, W., Schmidt, K. S., Suni, T., Wagner, T.,
2203 Wild, M., and Quaas, J., Global observations of aerosol-cloud-precipitation-climate
2204 interactions: Rev. Geophys., 52, 750-808, doi:10.1002/2013RG000441, 2014.

2205 Saha, S., Moorthi, S., Wu, X., Wang, J., Nadiga, S., Tripp, P., Behringer, D., Hou, Y.-T.,
2206 Chuang, H.-y., Iredell, M., Ek, M., Meng, J., Yang, R., Mendez, M. P., Dool, H. v. d.,
2207 Zhang, Q., Wang, W., Chen, M., and Becker, E., NCEP Climate Forecast System Version
2208 2 (CFSv2) 6-hourly Products. Research Data Archive at the National Center for
2209 Atmospheric Research, Computational and Information Systems Laboratory. Accessed
2210 20 March 2017, https://rda.ucar.edu/datasets/ds094.0/ (2017).

2211 Sahu, L. K., and Lal, S., Changes in surface ozone levels due to convective downdrafts over the
2212 Bay of Bengal: Geophys. Res. Lett., 33, L10807, doi:10.1029/2006gl025994, 2006.

2213 Schmale, J., Schneider, J., Jurkat, T., Voigt, C., Kalesse, H., Rautenhaus, M., Lichtenstern, M.,
2214 Schlager, H., Ancellet, G., Arnold, F., Gerding, M., Mattis, I., Wendisch, M., and
2215 Borrmann, S., Aerosol layers from the 2008 eruptions of Mount Okmok and Mount
2216 Kasatochi: In situ upper troposphere and lower stratosphere measurements of sulfate and
2217 organics over Europe: J. Geophys. Res., 115, D00l07, doi:10.1029/2009jd013628, 2010.

2218 Schneider, J., Weimer, S., Drewnick, F., Borrmann, S., Helas, G., Gwaze, P., Schmid, O.,
2219 Andreae, M. O., and Kirchner, U., Mass spectrometric analysis and aerodynamic
2220 properties of various types of combustion-derived aerosol particles: Int. J. Mass Spec.,
2221 258, 37-49, 2006.

2222 Schulz, C., Schneider, J., Weinzierl, B., Sauer, D., Fütterer, D., Ziereis, H., and Borrmann, S.,
2223 Aircraft-based observations of IEPOX-derived isoprene SOA formation in the tropical
2224 upper troposphere in the Amazon region: Atmos. Chem. Phys. Discuss., 2017, in
2225 preparation.

2226 Schwarz, J. P., Gao, R. S., Fahey, D. W., Thomson, D. S., Watts, L. A., Wilson, J. C., Reeves, J.
2227 M., Darbeheshti, M., Baumgardner, D. G., Kok, G. L., Chung, S. H., Schulz, M.,
2228 Hendricks, J., Lauer, A., Karcher, B., Slowik, J. G., Rosenlof, K. H., Thompson, T. L.,
2229 Langford, A. O., Loewenstein, M., and Aikin, K. C., Single-particle measurements of
2230 midlatitude black carbon and light-scattering aerosols from the boundary layer to the
2231 lower stratosphere: J. Geophys. Res., 111, D16207, doi:10.1029/2006JD007076, 2006.

2232 Schwarz, J. P., Weinzierl, B., Samset, B. H., Dollner, M., Heimerl, K., Markovic, M. Z., Perring,
2233 A. E., and Ziemba, L., Aircraft measurements of black carbon vertical profiles show
2234 upper tropospheric variability and stability: Geophys. Res. Lett., 44, 1132-1140,
2235 doi:10.1002/2016GL071241, 2017.

2236 Seibert, P., and Frank, A., Source-receptor matrix calculation with a Lagrangian particle
2237 dispersion model in backward mode: Atmos. Chem. Phys., 4, 51-63, 2004.

2238 Sherwood, S., A microphysical connection among biomass burning, cumulus clouds, and
2239 stratospheric moisture: Science, 295, 1272-1275, 2002.

2240 Spracklen, D. V., Carslaw, K. S., Kulmala, M., Kerminen, V.-M., Mann, G. W., and Sihto, S.-L.,
2241 The contribution of boundary layer nucleation events to total particle concentrations on
2242 regional and global scales: Atmos. Chem. Phys., 6, 5631-5648, 2006.

2243 Stein, A. F., Draxler, R. R., Rolph, G. D., Stunder, B. J. B., Cohen, M. D., and Ngan, F.,
2244 NOAA's HYSPLIT atmospheric transport and dispersion modeling system: Bull. Am.
2245 Meteorol. Soc., 96, 2059-2077, doi:10.1175/BAMS-D-14-00110.1, 2015.

2246 Stephens, M., Turner, N., and Sandberg, J., Particle identification by laser-induced
2247 incandescence in a solid-state laser cavity: Applied Optics, 42, 3726-3736,
2248 doi:10.1364/ao.42.003726, 2003.

2249 Stohl, A., Hittenberger, M., and Wotawa, G., Validation of the Lagrangian particle dispersion
2250 model FLEXPART against large-scale tracer experiment data: Atmospheric
2251 Environment, 32, 4245-4264, doi:10.1016/s1352-2310(98)00184-8, 1998.

2252 Stohl, A., and Thomson, D. J., A density correction for Lagrangian particle dispersion models:
2253 Boundary-Layer Meteorology, 90, 155-167, doi:10.1023/a:1001741110696, 1999.

2254 Stohl, A., Eckhardt, S., Forster, C., James, P., Spichtinger, N., and Seibert, P., A replacement for
2255 simple back trajectory calculations in the interpretation of atmospheric trace substance
2256 measurements: Atmospheric Environment, 36, 4635-4648, doi:10.1016/s1352-
2257 2310(02)00416-8, 2002.

2258 Stohl, A., Forster, C., Frank, A., Seibert, P., and Wotawa, G., Technical note: The Lagrangian
2259 particle dispersion model FLEXPART version 6.2: Atmos. Chem. Phys., 5, 2461-2474,
2260 2005.

2261 Stolz, D. C., Rutledge, S. A., and Pierce, J. R., Simultaneous influences of thermodynamics and
2262 aerosols on deep convection and lightning in the tropics: J. Geophys. Res., 120, 6207-
2263 6231, doi:10.1002/2014jd023033, 2015.

2264 Talbot, R. W., Andreae, M. O., Andreae, T. W., and Harriss, R. C., Regional aerosol chemistry
2265 of the Amazon Basin during the dry season: J. Geophys. Res., 93, 1499-1508, 1988.

2266 Talbot, R. W., Andreae, M. O., Berresheim, H., Artaxo, P., Garstang, M., Harriss, R. C.,
2267 Beecher, K. M., and Li, S. M., Aerosol chemistry during the wet season in Central
2268 Amazonia: The influence of long-range transport: J. Geophys. Res., 95, 16,955-16,969,
2269 1990.

2270 Thalman, R., Thalman, R., de Sá, S. S., Palm, B. B., Barbosa, H. M. J., Pöhlker, M. L.,
2271 Alexander, M. L., Brito, J., Carbone, S., Castillo, P., Day, D. A., Kuang, C., Manzi, A.,
2272 Ng, N. L., Sedlacek III, A. J., Souza, R., Springston, S., Watson, T., Pöhlker, C., Pöschl,
2273 U., Andreae, M. O., Artaxo, P., Jimenez, J. L., Martin, S. T., and Wang, J., CCN activity
2274 and organic hygroscopicity of aerosols downwind of an urban region in central
2275 Amazonia: Seasonal and diel variations and impact of anthropogenic emissions: Atmos.
2276 Chem. Phys. Discuss., doi:10.5194/acp-2017-251, 2017.

2277 Thornberry, T., Froyd, K. D., Murphy, D. M., Thomson, D. S., Anderson, B. E., Thornhill, K. L.,
2278 and Winstead, E. L., Persistence of organic carbon in heated aerosol residuals measured
2279 during Tropical Composition Cloud and Climate Coupling (TC4): J. Geophys. Res., 115,
2280 D00J02, doi:10.1029/2009jd012721, 2010.

2281 Tröstl, J., Chuang, W. K., Gordon, H., Heinritzi, M., Yan, C., Molteni, U., Ahlm, L., Frege, C.,
2282 Bianchi, F., Wagner, R., Simon, M., Lehtipalo, K., Williamson, C., Craven, J. S.,
2283 Duplissy, J., Adamov, A., Almeida, J., Bernhammer, A.-K., Breitenlechner, M., Brilke,
2284 S., Dias, A., Ehrhart, S., Flagan, R. C., Franchin, A., Fuchs, C., Guida, R., Gysel, M.,
2285 Hansel, A., Hoyle, C. R., Jokinen, T., Junninen, H., Kangasluoma, J., Keskinen, H., Kim,
2286 J., Krapf, M., Kürten, A., Laaksonen, A., Lawler, M., Leiminger, M., Mathot, S., Möhler,
2287 O., Nieminen, T., Onnela, A., Petäjä, T., Piel, F. M., Miettinen, P., Rissanen, M. P.,
2288 Rondo, L., Sarnela, N., Schobesberger, S., Sengupta, K., Sipilä, M., Smith, J. N., Steiner,
2289 G., Tomè, A., Virtanen, A., Wagner, A. C., Weingartner, E., Wimmer, D., Winkler, P.
2290 M., Ye, P., Carslaw, K. S., Curtius, J., Dommen, J., Kirkby, J., Kulmala, M., Riipinen, I.,
2291 Worsnop, D. R., Donahue, N. M., and Baltensperger, U., The role of low-volatility
2292 organic compounds in initial particle growth in the atmosphere: Nature, 533, 527-531,
2293 doi:10.1038/nature18271, 2016.

2294 Twohy, C. H., Clement, C. F., Gandrud, B. W., Weinheimer, A. J., Campos, T. L., Baumgardner,
2295 D., Brune, W. H., Faloona, I., Sachse, G. W., Vay, S. A., and Tan, D., Deep convection
2296 as a source of new particles in the midlatitude upper troposphere: J. Geophys. Res., 107,
2297 4560, doi:10.1029/2001JD000323, 2002.

2298 Vestin, A., Rissler, J., Swietlicki, E., Frank, G., and Andreae, M. O., Cloud nucleating properties
2299 of the Amazonian biomass burning aerosol: Cloud condensation nuclei measurements
2300 and modeling: J. Geophys. Res., 112, D14201, doi:10.1029/2006JD008104, 2007.

2301 Virji, H., A preliminary study of summertime tropospheric circulation patterns over South
2302 America estimated from cloud winds: Mon. Weather Rev., 109, 599-610, 1981.

2303 Voigt, C., Schumann, U., Minikin, A., Abdelmonem, A., Afchine, A., Borrmann, S., Boettcher,
2304 M., Bucuchholz, B., Bugliaro, L., Costa, A., Curtius, J., Dollner, M., Doernbrack, A.,
2305 Dreiling, V., Ebert, V., Ehrlich, A., Fix, A., Forster, L., Frank, F., Fuetterer, D., Giez, A.,
2306 Graf, K., Grooss, J.-U., Gross, S., Heimerl, K., Heinold, B., Hueneke, T., Jaervinen, E.,
2307 Jurkat, T., Kaufmann, S., Kenntner, M., Klingebiel, M., Klimach, T., Kohl, R., Kraemer,
2308 M., Krisna, T. C., Luebke, A., Mayer, B., Mertes, S., Molleker, S., Petzold, A.,
2309 Pfeilsticker, K., Port, M., Rapp, M., Reutter, P., Rolf, C., Rose, D., Sauer, D., Schaefer,
2310 A., Schlage, R., Schnaiter, M., Schneider, J., Spelten, N., Spichtinger, P., Stock, P.,
2311 Walser, A., Weigel, R., Weinzierl, B., Wendisch, M., Werner, F., Wernli, H., Wirth, M.,
2312 Zahn, A., Ziereis, H., and Zoger, M., ML-CIRRUS: The airborne experiment on natural
2313 cirrus and contrail cirrus with the high-altitude long-range research aircraft HALO: Bull.
2314 Am. Meteorol. Soc., 98, 271-288, doi:10.1175/bams-d-15-00213.1, 2017.

2315 von der Weiden, S. L., Drewnick, F., and Borrmann, S., Particle Loss Calculator – a new
2316 software tool for the assessment of the performance of aerosol inlet systems: Atmos.
2317 Meas. Tech., 2, 479-494, doi:10.5194/amt-2-479-2009, 2009.

2318 Waddicor, D. A., Vaughan, G., Choularton, T. W., Bower, K. N., Coe, H., Gallagher, M.,
2319 Williams, P. I., Flynn, M., Volz-Thomas, A., Pätz, H. W., Isaac, P., Hacker, J., Arnold,
2320 F., Schlager, H., and Whiteway, J. A., Aerosol observations and growth rates downwind
2321 of the anvil of a deep tropical thunderstorm: Atmos. Chem. Phys., 12, 6157-6172,
2322 doi:10.5194/acp-12-6157-2012, 2012.

2323 Walser, A., Sauer, D., Spanu, A., Gasteiger, J., and Weinzierl, B., On the parametrization of
2324 optical particle counter response including instrument-induced broadening of size spectra
2325 and a self-consistent evaluation of calibration measurements: Atmos. Meas. Tech.
2326 Discuss., 2017, 1-30, doi:10.5194/amt-2017-81, 2017.

2327 Wang, H., and Fu, R., The influence of Amazon rainfall on the Atlantic ITCZ through
2328 convectively coupled Kelvin waves: J. Clim., 20, 1188-1201, doi:10.1175/jcli4061.1,
2329 2007.

2330 Wang, J., Krejci, R., Giangrande, S., Kuang, C., Barbosa, H. M. J., Brito, J., Carbone, S., Chi,
2331 X., Comstock, J., Ditas, F., Lavric, J., Manninen, H. E., Mei, F., Moran-Zuloaga, D.,
2332 Pöhlker, C., Pöhlker, M. L., Saturno, J., Schmid, B., Souza, R. A. F., Springston, S. R.,
2333 Tomlinson, J. M., Toto, T., Walter, D., Wimmer, D., Smith, J. N., Kulmala, M.,
2334 Machado, L. A. T., Artaxo, P., Andreae, M. O., Petäjä, T., and Martin, S. T., Amazon
2335 boundary layer aerosol concentration sustained by vertical transport during rainfall:
2336 Nature, 539, 416-419, doi:10.1038/nature19819, 2016a.

2337 Wang, Q., Saturno, J., Chi, X., Walter, D., Lavric, J. V., Moran-Zuloaga, D., Ditas, F., Pöhlker,
2338 C., Brito, J., Carbone, S., Artaxo, P., and Andreae, M. O., Modeling investigation of
2339 light-absorbing aerosols in the Amazon Basin during the wet season: Atmos. Chem.
2340 Phys., 16, 14,775-14,794, doi:10.5194/acp-16-14775-2016, 2016b.

2341 Watson, C. E., Fishman, J., and Reichle, H. G., The significance of biomass burning as a source
2342 of carbon monoxide and ozone in the Southern Hemisphere tropics: A satellite analysis:
2343 J. Geophys. Res., 95, 14,443-14,450, 1990.

2344 Weigel, R., Borrmann, S., Kazil, J., Minikin, A., Stohl, A., Wilson, J. C., Reeves, J. M., Kunkel,
2345 D., de Reus, M., Frey, W., Lovejoy, E. R., Volk, C. M., Viciani, S., D'Amato, F.,
2346 Schiller, C., Peter, T., Schlager, H., Cairo, F., Law, K. S., Shur, G. N., Belyaev, G. V.,
2347 and Curtius, J., In situ observations of new particle formation in the tropical upper
2348 troposphere: the role of clouds and the nucleation mechanism: Atmos. Chem. Phys., 11,
2349 9983-10,010, doi:10.5194/acp-11-9983-2011, 2011.

2350 Weigel, R., Spichtinger, P., Mahnke, C., Klingebiel, M., Afchine, A., Petzold, A., Krämer, M.,
2351 Costa, A., Molleker, S., Reutter, P., Szakáll, M., Port, M., Grulich, L., Jurkat, T.,
2352 Minikin, A., and Borrmann, S., Thermodynamic correction of particle concentrations
2353 measured by underwing probes on fast-flying aircraft: Atmos. Meas. Tech., 9, 5135-
2354 5162, doi:10.5194/amt-9-5135-2016, 2016.

2355 Weigelt, A., Hermann, M., van Velthoven, P. F. J., Brenninkmeijer, C. A. M., Schlaf, G., Zahn,
2356 A., and Wiedensohler, A., Influence of clouds on aerosol particle number concentrations
2357 in the upper troposphere: J. Geophys. Res., 114, D01204, doi:10.1029/2008jd009805,
2358 2009.

2359 Weinzierl, B., Ansmann, A., Prospero, J. M., Althausen, D., Benker, N., Chouza, F., Dollner, M.,
2360 Farrell, D., Fomba, W. K., Freudenthaler, V., Gasteiger, J., Gross, S., Haarig, M.,
2361 Heinold, B., Kandler, K., Kristensen, T. B., Mayol-Bracero, O. L., Muller, T., Reitebuch,
2362 O., Sauer, D., Schafler, A., Schepanski, K., Spanu, A., Tegen, I., Toledano, C., and
2363 Walser, A., The Saharan Aerosol Long-Range Transport and Aerosol-Cloud-Interaction
2364 Experiment: Overview and Selected Highlights: Bull. Am. Meteorol. Soc., 98, 1427-
2365 1451, doi:10.1175/bams-d-15-00142.1, 2017.

Wendisch, M., Pöschl, U., Andreae, M. O., Machado, L. A. T., Albrecht, R., Schlager, H., Rosenfeld, D., Martin, S. T., Abdelmonem, A., Afchine, A., Araùjo, A. C., Artaxo, P., Aufmhoff, H., Barbosa, H. M. J., Borrmann, S., Braga, R., Buchholz, B., Cecchini, M. A., Costa, A., Curtius, J., Dollner, M., Dorf, M., Dreiling, V., Ebert, V., Ehrlich, A., Ewald, F., Fisch, G., Fix, A., Frank, F., Fütterer, D., Heckl, C., Heidelberg, F., Hüneke, T., Jäkel, E., Järvinen, E., Jurkat, T., Kanter, S., Kästner, U., Kenntner, M., Kesselmeier, J., Klimach, T., Knecht, M., Kohl, R., Kölling, T., Krämer, M., Krüger, M., Krisna, T. C., Lavric, J. V., Longo, K., Mahnke, C., Manzi, A. O., Mayer, B., Mertes, S., Minikin, A., Molleker, S., Münch, S., Nillius, B., Pfeilsticker, K., Pöhlker, C., Roiger, A., Rose, D., Rosenow, D., Sauer, D., Schnaiter, M., Schneider, J., Schulz, C., Souza, R. A. F. d., Spanu, A., Stock, P., Vila, D., Voigt, C., Walser, A., Walter, D., Weigel, R., Weinzierl, B., Werner, F., Yamasoe, M. A., Ziereis, H., Zinner, T., and Zöger, M., ACRIDICON–CHUVA campaign: Studying tropical deep convective clouds and precipitation over Amazonia using the new German research aircraft HALO: Bull. Am. Meteorol. Soc., 97, 1885-1908, doi:10.1175/bams-d-14-00255.1, 2016.

Wiedensohler, A., An approximation of the bipolar charge distribution for particles in the sub-micron size range: J. Aerosol Sci., 19, 387-389, 1988.

Wiedensohler, A., Ma, N., Birmili, W., Heintzenberg, J., Ditas, F., Andreae, M. O., and Panov, A., Rare particle nucleation over remote forests: Nature, 2017, submitted.

Williams, J., de Reus, M., Krejci, R., Fischer, H., and Strom, J., Application of the variability-size relationship to atmospheric aerosol studies: estimating aerosol lifetimes and ages: Atmos. Chem. Phys., 2, 133-145, 2002.

Witte, K., HALO Technical Note: Top Fuselage Aperture Plates - Particle Enrichment. DLR Flight Facility Oberpfaffenhofen, Wessling, Germany, 17 p. (2008).

Yang, Q., Easter, R. C., Campuzano-Jost, P., Jimenez, J. L., Fast, J. D., Ghan, S. J., Wang, H., Berg, L. K., Barth, M. C., Liu, Y., Shrivastava, M. B., Singh, B., Morrison, H., Fan, J., Ziegler, C. L., Bela, M., Apel, E., Diskin, G. S., Mikoviny, T., and Wisthaler, A., Aerosol transport and wet scavenging in deep convective clouds: A case study and model evaluation using a multiple passive tracer analysis approach: J. Geophys. Res., 120, 8448-8468, doi:10.1002/2015JD023647, 2015.

Yin, Y., Carslaw, K. S., and Feingold, G., Vertical transport and processing of aerosols in a mixed-phase convective cloud and the feedback on cloud development: Q. J. R. Meterorol. Soc., 131, 221-245, 2005.

Young, L. H., Benson, D. R., Montanaro, W. M., Lee, S. H., Pan, L. L., Rogers, D. C., Jensen, J., Stith, J. L., Davis, C. A., Campos, T. L., Bowman, K. P., Cooper, W. A., and Lait, L. R., Enhanced new particle formation observed in the northern midlatitude tropopause region: J. Geophys. Res., 112, D10218, doi:10.1029/2006jd008109, 2007.

Yu, F., Wang, Z., Luo, G., and Turco, R., Ion-mediated nucleation as an important global source of tropospheric aerosols: Atmos. Chem. Phys., 8, 2537-2554, 2008.

Yu, F., Luo, G., Nadykto, A. B., and Herb, J., Impact of temperature dependence on the possible contribution of organics to new particle formation in the atmosphere: Atmos. Chem. Phys., 17, 4997-5005, doi:10.5194/acp-17-4997-2017, 2017.

Yu, P. F., Murphy, D. M., Portmann, R. W., Toon, O. B., Froyd, K. D., Rollins, A. W., Gao, R. S., and Rosenlof, K. H., Radiative forcing from anthropogenic sulfur and organic emissions reaching the stratosphere: Geophys. Res. Lett., 43, 9361-9367, doi:10.1002/2016gl070153, 2016.

Zhou, J., Swietlicki, E., Hansson, H.-C., and Artaxo, P., Submicrometer aerosol particle size distribution and hygroscopic growth measured in the Amazon rain forest during the wet season: J. Geophys. Res., 107, 8055, doi:10.129/2000JD000203, 2002.

Zhou, J. C., Swietlicki, E., Berg, O. H., Aalto, P. P., Hameri, K., Nilsson, E. D., and Leck, C., Hygroscopic properties of aerosol particles over the central Arctic Ocean during summer: J. Geophys. Res., 106, 32111-32123, 2001.

Zhou, J. Y., and Lau, K. M., Does a monsoon climate exist over South America?: J. Clim., 11, 1020-1040, 1998.

Zhuang, Y., Fu, R., Marengo, J. A., and Wang, H., Seasonal variation of shallow-to-deep convection transition and its link to the environmental conditions over the Central Amazon: J. Geophys. Res., 122, 2649-2666, doi:10.1002/2016JD025993, 2017.

Ziereis, H., Schlager, H., Schulte, P., van Velthoven, P. F. J., and Slemr, F., Distributions of NO, NO_x, and NO_y in the upper troposphere and lower stratosphere between 28° and 61°N during POLINAT 2: J. Geophys. Res., 105, 3653-3664, doi:10.1029/1999jd900870, 2000.

Zipser, E. J., Mesoscale and convective-scale downdrafts as distinct components of squall-line structure: Mon. Weather Rev., 105, 1568-1589, doi:10.1175/1520-0493(1977)105<1568:macdad>2.0.co;2, 1977.